Chapter 26: Molecular Structure

Is ozone linear or bent?

The formation of the chemical bond is the most central issue in chemistry. Chemical bonding determines the structure and energetics of molecules. Making and breaking chemical bonds is the goal of chemical synthesis. The design and synthesis of chemical compounds is the most direct way that chemists have for solving challenges that we face as a society. Chemical bonding is a subtle balance between the decrease in potential energy and increase in kinetic energy of the electrons, relative to the separated atoms. The Coulomb attractions of the electrons for the nuclei act as the "glue" that hold nuclei together. However, understanding the stability of the chemical bond requires an understanding of electron-electron repulsion, electron exchange, and electron correlation interactions. We begin our discussion with the simplest molecule ion, H_2^+. The hydrogen molecule ion is to bonding theory as the hydrogen atom is to atomic structure. The concept of molecular orbitals emerges from the treatment of H_2^+. In turn, molecular orbitals are used to build the electronic structure of H_2 and more complex multi-electron molecules. The orbital approximation is the basis for our understanding of multi-electron molecules.

26.1 Hydrogen Molecular Ion, H_2^+

Born-Oppenheimer Approximation: The complete Schrödinger equation for a molecule includes the kinetic energy of the nuclei, the kinetic energy of the electrons, the Coulomb attractions of the electrons for the nuclei, the Coulomb repulsions of the electrons for each other, and the Coulomb repulsions of the nuclei. Atoms don't stick together unless the nuclear-nuclear and electron-electron repulsions are exceeded by the Coulomb attraction of the electrons for the nuclei. The solution of the complete molecular Schrödinger equation is difficult. Because the mass of a nucleus is much larger than the mass of an electron, the motion of the electrons is much faster than the motion of the nuclei. The **Born-Oppenheimer** approximation assumes that the electronic structure of the molecule adjusts instantaneously to the vibrational motion of the nuclei. The motion of the nuclei and the electrons are assumed to be independent. In the Born-Oppenheimer approximation, the vibrational motion of the nuclei is solved separately from the electronic degrees of freedom. Accordingly, the kinetic energy term for the nuclei does not appear in the molecular Hamiltonian. The vibrational potential energy is determined by a series of calculations of the electronic energy at fixed bond lengths, Figure 26.1.1a. The equilibrium bond length, R_e, is the distance at minimum electronic energy. The bond dissociation limit is at large bond lengths, $R \to \infty$. The bond dissociation energy, D_e, is the difference of the energy at the bond dissociation limit and the minimum energy.

The hydrogen molecule ion has a single electron, which simplifies our first bonding example. For consistency with multi-electron molecules, we label the electron as electron 1. The coordinates for H_2^+ include the distances of the electron from nuclei A and B, r_{1A} and r_{1B}, and the bond length between the two nuclei, R, Figure 26.1.1b. At fixed bond length R, the Schrödinger equation includes the kinetic energy of the electron, the Coulomb attraction of the electron for both nuclei, and the Coulomb repulsion of the nuclei:

$$-\frac{\hbar^2}{2m}\nabla_1^2\Psi + \frac{e^2}{4\pi\varepsilon_o}\left(-\frac{1}{r_{1A}} - \frac{1}{r_{1B}} + \frac{1}{R}\right)\Psi = E\,\Psi \qquad 26.1.1$$

The curvature for electron 1, ∇_1^2, only operates on the coordinates of electron 1.

(a).   (b).
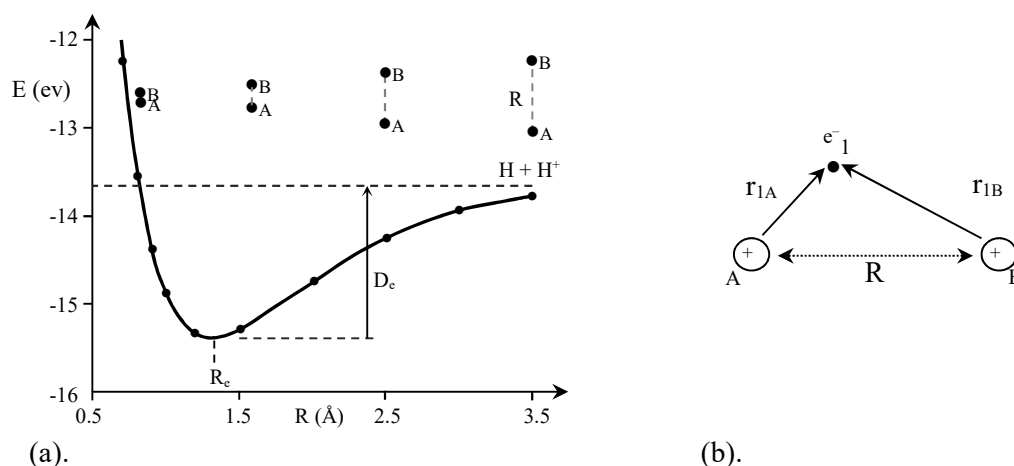
Figure 26.1.1: (a). In the Born-Oppenheimer approximation, the potential energy curve for vibration is determined by a series of electronic structure calculations at fixed bond lengths, R. (b). Coulomb interactions in H_2^+. Nuclei are labeled with letters and electrons with number subscripts. Attractions are shown with solid lines (—) and repulsions with dotted lines (·····).

Example 26.1.1: *Vibrational Potential from the Born-Oppenheimer Approximation*
The total electronic energy of H_2^+ as a function of bond length is given in the following table. The corresponding equilibrium bond length is $R_e = 1.319$ Å. Calculate the bond force constant in the harmonic approximation.

R (Å)	1.1	1.2	1.319	1.4	1.5
E (eV)	-15.1703	-15.3188	-15.3698	-15.3519	-15.2908

Answer: In the harmonic approximation, the potential for vibration is $V(R) = \frac{1}{2}k(R - R_e)^2$, where R is the instantaneous bond length. A table for the bond extension, $R - R_e$, and the electronic energy relative to the lowest energy, $E - E(R_e)$ in joules, is given in the spreadsheet below.
⟦www⟧ A quadratic non-linear curve fit in powers of the extension, $ax^2 + bx + c$, using the "Non-linear Least Squares Curve Fitting" applet on the text Web site and companion CD gives a= k = 54.96 ± 5.32 N/m. The uncertainty results from the anharmonicity in the vibrational potential.

R (Å)	E (eV)	(R - R$_e$) (m)	E-E(R$_e$) (J)
1.1	-15.1703	-2.19E-11	3.197E-20
1.2	-15.3188	-1.19E-11	8.177E-21
1.319	-15.3698	0	6.375E-24
1.4	-15.3519	8.1E-12	2.874E-21
1.5	-15.2908	1.81E-11	1.266E-20

===== Results: Fit $ax^2 + bx + c$ ===
a= 54.96 +- 5.32
b= -2.296e-10 +- 6.6e-11
c= -3.600e-22 +- 1.2e-23
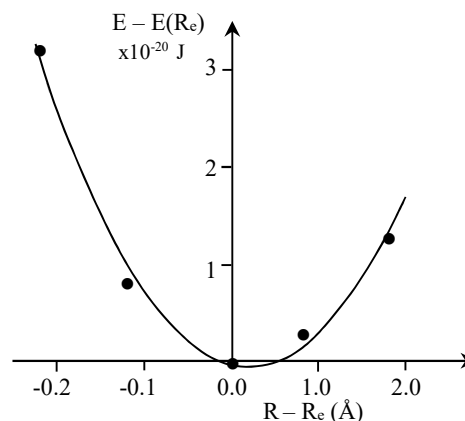
The Molecular Orbitals are Approximated as a Linear Combination of Atomic Orbitals: The Schrödinger equation for H_2^+, Eq. 26.1.1, can be solved exactly, within the Born-Oppenheimer approach. However, exact solutions are only possible for one-electron systems. Instead, we develop an approximation method that is widely applicable to multi-electron molecules and molecular ions. Consider the H_2^+ ion as the bond is stretched. The dissociation limit is a hydrogen atom and a hydrogen ion, $H_2^+ \rightarrow H + H^+$. The wave function upon dissociation is a 1s-atomic orbital on one of the nuclei. However, both nuclei are equally likely to be at the center of the dissociated atom, $H_2^+ \rightarrow H^+ + H$. Accordingly, a possibility for the molecular wave function is the linear combination of an atomic orbital on nucleus A and an atomic orbital on nucleus B:

$$\Psi_{MO} = c_A\Psi_A + c_B\Psi_B \qquad \text{ground state: } \Psi_A = 1s_A, \ \Psi_B = 1s_B \qquad 26.1.2$$

The molecular **orbital coefficients**, c_A and c_B, are constants that are optimized using the Variation Principle. For the ground state of H_2^+, both atomic orbitals are 1s-orbitals, one on each nucleus. Excited states result from the choice of higher energy atomic orbitals in the linear combination. This general approximation is called the linear combination of atomic orbitals-molecular orbital approach, or **LCAO-MO**. LCAO molecular orbitals are the basis for the most commonly used electronic structure programs. The orbital coefficients are chosen to minimize the expectation value of the Hamiltonian, according to the Variation Theorem:

$$E = \frac{\int \Psi_{MO}^* \mathcal{H}\Psi_{MO} \, d\tau}{\int \Psi_{MO}^2 \, d\tau} \qquad 26.1.3$$

The integrals are taken over the position of the electron over all space. Substitution of the LCAO molecular orbital into the integrals gives:

$$E = \frac{\int (c_A\Psi_A + c_B\Psi_B)^* \mathcal{H}(c_A\Psi_A + c_B\Psi_B) \, d\tau}{\int (c_A\Psi_A + c_B\Psi_B)^2 \, d\tau} \qquad 26.1.4$$

$$E = \frac{c_A^2 \int \Psi_A^* \mathcal{H}\Psi_A \, d\tau + c_B^2 \int \Psi_B^* \mathcal{H}\Psi_B \, d\tau + 2\, c_Ac_B \int \Psi_A^* \mathcal{H}\Psi_B \, d\tau}{c_A^2 \int \Psi_A^2 \, d\tau + c_B^2 \int \Psi_B^2 \, d\tau + 2\, c_Ac_B \int \Psi_A\Psi_B \, d\tau} \qquad 26.1.5$$

The expression is simplified using the following definitions:

$$H_{AA} \equiv \int \Psi_A^* \mathcal{H}\Psi_A \, d\tau \qquad \text{Atomic Integral} \approx E_A + \frac{e^2}{4\pi\varepsilon_oR}$$

$$H_{AB} \equiv \int \Psi_A^* \mathcal{H}\Psi_B \, d\tau \qquad \text{Resonance Integral}$$

$$S_{AA} \equiv \int \Psi_A^*\Psi_A \, d\tau \qquad \text{Atomic Normalization}$$

$$S_{AB} \equiv \int \Psi_A^*\Psi_B \, d\tau \qquad \text{Overlap Integral} \qquad 26.1.6$$

The **atomic integral**, H_{AA}, involves only the atomic orbital on atom A. At a coarse level of approximation, H_{AA} is equal to the atomic energy of the electron on atom A, E_A, plus the nuclear-nuclear repulsion. The **resonance integral**, H_{AB}, involves the atomic orbital on both atoms. The resonance integral is largely responsible for the energetic stabilization of the bond, since the electron interacts with both nuclei. S_{AA} is the familiar atomic normalization integral. The overlap integral, S_{AB}, is a measure of the degree to which both atomic orbitals have a significant probability in the bonding region between the nuclei, Figure 26.1.2. The overlap integral has a maximum of 1, or 100% overlap, and a typical range of 0.2–0.7. The overlap integral depends on the atomic orbital extent and the nuclear separation. Corresponding atomic

and normalization integrals centered on atom B are H_{BB} and S_{BB}, respectively. At a coarse, but useful, level of approximation, the resonance integral is roughly proportional to the overlap integral: $H_{AB} = K\,S_{AB}$. The proportionality constant, K, is determined from experimental ionization energies. In short, <u>better overlap gives a stronger bond</u>.
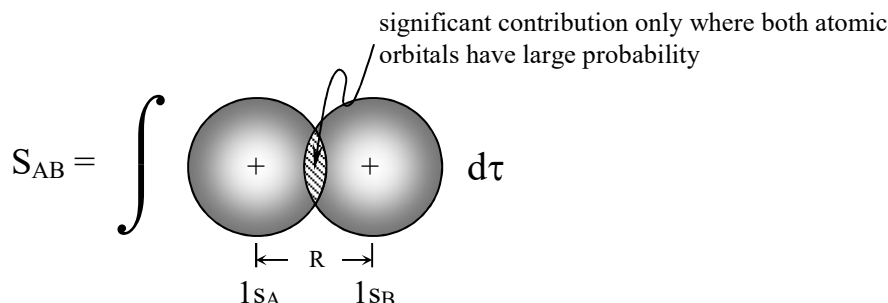
Figure 26.1.2: The overlap integral is determined by the degree of interpenetration of the atomic orbital on each nucleus. Only the region between the two nuclei where both orbitals have a significant probability, the bonding region, contributes significantly to the overlap.

The definitions of the Hamiltonian and overlap integrals, Eqs. 26.1.6, simplify Eq. 26.1.5 to:

$$E = \frac{c_A^2 H_{AA} + c_B^2 H_{BB} + 2\,c_A c_B H_{AB}}{c_A^2 S_{AA} + c_B^2 S_{BB} + 2\,c_A c_B S_{AB}} = \frac{N}{D} \qquad\qquad 26.1.7$$

For convenience, we define the numerator in the previous expression as N and the denominator as D. The lowest energy gives the best possible wave function. The variation parameters are the orbital coefficients, c_A and c_B. To find the minimum energy, we take the derivatives of the energy with respect to c_A and c_B and set the results equal to zero. Using Eq. 1.5.3, the derivative of the ratio N/D to give a minimum is:

$$\left(\frac{\partial(N/D)}{\partial c_A}\right)_{c_B} = \frac{\left(\frac{\partial N}{\partial c_A}\right)_{c_B} D - \left(\frac{\partial D}{\partial c_A}\right)_{c_B} N}{D^2} = 0 \qquad \text{or} \qquad \left(\frac{\partial N}{\partial c_A}\right)_{c_B} D - \left(\frac{\partial D}{\partial c_A}\right)_{c_B} N = 0 \qquad 26.1.8$$

Completing the derivatives gives:

$$\left(\frac{\partial E}{\partial c_A}\right)_{c_B} = 0 = [2c_A H_{AA} + 2c_B H_{AB}]D - [2c_A S_{AA} + 2c_B S_{AB}]N \qquad\qquad 26.1.9$$

Dividing this equation by 2D and noting that E = N/D gives:

$$0 = c_A H_{AA} + c_B H_{AB} - E\,[c_A S_{AA} + c_B S_{AB}] \qquad\qquad 26.1.10$$

In the same manner, the derivative with respect to c_B is:

$$\left(\frac{\partial E}{\partial c_B}\right)_{c_A} = 0 = c_B H_{BB} + c_A H_{AB} - E\,[c_B S_{BB} + AB] \qquad\qquad 26.1.11$$

Collecting terms in c_A and c_B in Eqs. 26.1.10 and 26.1.11 gives a simultaneous set of two equations in three unknowns, which are c_A, c_B, and the electronic energy E:

$$c_A(H_{AA} - ES_{AA}) + c_B(H_{AB} - ES_{AB}) = 0$$
$$c_A(H_{AB} - ES_{AB}) + c_B(H_{BB} - ES_{BB}) = 0 \qquad\qquad 26.1.12$$

These equations are called the **secular equations**. A simultaneous set of homogeneous linear equations has a non-trivial solution only if the determinant of the coefficients vanishes:

$$\begin{vmatrix} H_{AA} - ES_{AA} & H_{AB} - ES_{AB} \\ H_{AB} - ES_{AB} & H_{BB} - ES_{BB} \end{vmatrix} = 0 \qquad\qquad 26.1.13$$

You may be more familiar with the set of homogeneous equations and the determinant written in the generic form:

$$\begin{aligned} Ax + By &= 0 \\ Cx + Dy &= 0 \end{aligned} \qquad \begin{vmatrix} A & B \\ C & D \end{vmatrix} = AD - BC = 0 \qquad\qquad 26.1.14$$

For example, a simple set of equations and the determinant of the coefficients is:

$$\begin{aligned} 4x + 8y &= 0 \\ 2x + 4y &= 0 \end{aligned} \qquad \begin{vmatrix} 4 & 8 \\ 2 & 4 \end{vmatrix} = 4(4) - 2(8) = 0 \qquad\qquad 26.1.15$$

The vanishing determinant shows the set of equations to have an infinite set of solutions with $y = -x/2$. In our case the x and y variables are the coefficients c_A and c_B. Eq. 26.1.13 is called the **secular determinant**. Taking the determinant gives:

$$(H_{AA} - ES_{AA})(H_{BB} - ES_{BB}) - (H_{AB} - ES_{AB})^2 = 0 \qquad\qquad 26.1.16$$

For the ground state of the H_2^+ ion, the orbitals on each nucleus are identical with $H_{AA} = H_{BB}$. In addition, we will assume the atomic orbitals are normalized, $S_{AA} = S_{BB} = 1$. For notational simplicity, we then set $S_{AB} = S$. Solving for the two roots of Eq. 26.1.16 gives:

$$(H_{AA} - E)^2 - (H_{AB} - ES)^2 = 0 \quad \text{or} \quad H_{AA} - E = \pm(H_{AB} - ES) \qquad\qquad 26.1.17$$

Solving for the energy from the two roots gives:

$$E_+ = \frac{H_{AA} + H_{AB}}{1 + S} \qquad\qquad E_- = \frac{H_{AA} - H_{AB}}{1 - S} \qquad\qquad 26.1.18$$

The Hamiltonian integrals H_{AA} and H_{AB} are negative, while the overlap integral between two 1s-orbitals is positive. At long bond lengths, H_{AA} is approximately the atomic orbital energy of the isolated atom, E_A, and the resonance and overlap integrals are negligible. The first root, E_+, is then lower in energy than the isolated atom and corresponds to a bonding molecular orbital. The second root, E_-, is higher in energy and corresponds to an anti-bonding orbital, Figure 26.1.3. The orbital diagram is drawn with the molecular orbitals referenced to the atomic orbital energies at infinite separation. As the bond length decreases, the atomic orbitals overlap, the electron interacts with both nuclei, and the atomic orbitals combine to give a bonding and anti-bonding molecular orbital. For H_2^+, the 1s-orbital reference energy is -13.6 eV. The energetic stabilization of the bonding orbital is given by the resonance integral, H_{AB}. Notice that the anti-bonding orbital is destabilized to a greater extent than the bonding orbital is stabilized, because of the factor (1–S) in the denominator of E_- as opposed to the factor (1+S) in E_+.

   The bonding and anti-bonding roots result algebraically because we combined two atomic orbitals in the LCAO to give a two by two secular determinant, which has two roots. The number of molecular orbitals is equal to the number of atomic orbitals that are combined.
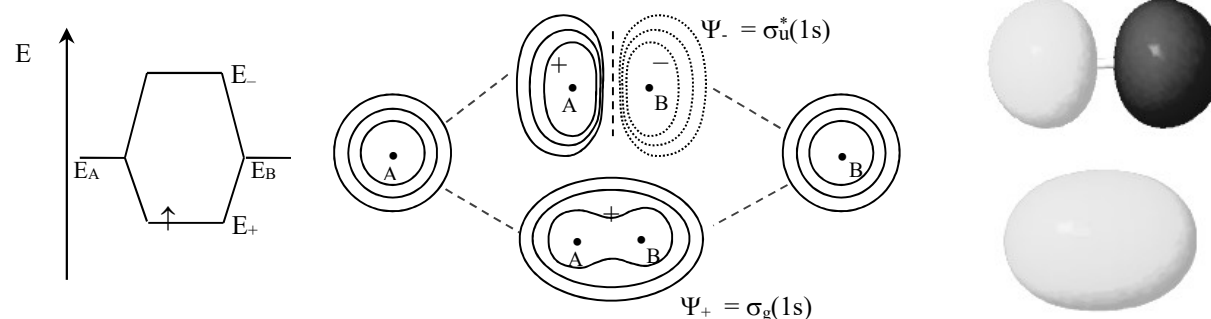
Figure 26.1.3: The hydrogen atomic orbitals combine in-phase to give a bonding orbital and out-of-phase to give an anti-bonding orbital. Computed constant electron density surfaces are plotted at right.

The bonding and anti-bonding energies are substituted separately into the secular equations, Eqs. 26.1.12, to find the molecular orbital coefficients. For the bonding molecular orbital the coefficients are equal and for the anti-bonding orbital the coefficients have opposite signs:

$$c_A = c_B \quad \text{for } E_+ \qquad \text{and} \quad c_A = -c_B \quad \text{for } E_- \qquad\qquad 26.1.19$$

(You will prove these statements in your homework.) For the bonding orbitals, the atomic orbitals combine constructively, in-phase. For the anti-bonding orbitals, the atomic orbitals combine destructively, out-of-phase, Figure 26.1.3. The anti-bonding orbital has a node between the two nuclei. To solve for the numerical values, we apply normalization. First, we rename the coefficients as c_+ for the bonding orbital and $\pm c_-$ for the anti-bonding orbital:

$$
\begin{aligned}
c_A = \ c_B = c_+ \qquad & \Psi_+ = c_+(\Psi_A + \Psi_B) \\
c_A = -c_B = c_- \qquad & \Psi_- = c_-(\Psi_A - \Psi_B)
\end{aligned}
\qquad\qquad 26.1.20
$$

The normalization integral for the bonding orbital gives:

$$\int \Psi_+^2 \, dt = 1 = c_+^2 \left[\int \Psi_A^2 \, d\tau + 2 \int \Psi_A \Psi_B \, d\tau + \int \Psi_B^2 \, d\tau \right] \qquad\qquad 26.1.21$$
$$1 = c_+^2 \left[\quad 1 \quad + \quad 2\,S \quad + \quad 1 \quad \right]$$

The first integral is the atomic normalization on nucleus A. We assume the atomic orbitals to be normalized. The second integral is the overlap integral, S. The third integral is the atomic normalization on nucleus B. Solving for the normalization constants gives:

$$c_+ = \frac{1}{\sqrt{2+2S}} \qquad\qquad c_- = \frac{1}{\sqrt{2-2S}} \qquad\qquad 26.1.22$$

The normalized bonding and anti-bonding orbitals are:

$$\Psi_+ = \frac{1}{\sqrt{2+2S}}(1s_A + 1s_B) \qquad\qquad \Psi_- = \frac{1}{\sqrt{2-2S}}(1s_A - 1s_B) \qquad\qquad 26.1.23$$

Molecular orbitals are depicted in several ways. In electron density contour plots, the contours trace regions with equal values of Ψ. The Ψ contours in Figure 26.1.3 are plotted at increasing factors of four. The closer the contours are to each other, the more rapid the increase in electron density. The isodensity surfaces on the right of the figure correspond to the 3D-surfaces

constructed at just one of the contour levels. An isodensity surface at low electron density is comparable to a 90% contour surface. Isodensity surfaces are useful in depicting the spatial extent of molecular orbitals. The conventional symbol for the Ψ_+ bonding orbital is $\sigma_g(1s)$. Sigma orbitals are cylindrically symmetrical about the internuclear axis. Anti-bonding orbitals are symbolized with a * superscript, giving the name of the Ψ_- anti-bonding orbital as $\sigma_u^*(1s)$. The g and u subscripts will be explained below. The strength of the chemical bond is determined by the degree of interaction of the electron with the two nuclei.

Bonding and Anti-Bonding Orbitals: The bonding and anti-bonding molecular orbitals for $H_2{}^+$ are plotted as a function of the distance along the internuclear axis in Figure 26.1.4. The z-axis is chosen as the internuclear axis. Nucleus A is placed at the origin. The experimental bond length is 1.06Å, which gives the placement of nucleus B. The 1s-atomic orbital wave functions are shown as dotted lines. The atomic orbitals give the electron distribution that would result from two non-interacting atoms. For the bonding molecular orbital, Ψ_+, electron density increases between the nuclei through the constructive interference of the atomic orbitals. The electron in the **bonding region**, along the internuclear axis between the two nuclei, interacts with both nuclei giving a favorable decrease in Coulomb potential energy. For comparison, the electron density for non-interacting atoms is given by the superposition of the atomic electron densities:

$$\Psi^2{}_{\text{noninteracting}} = \tfrac{1}{2}\,(\Psi_A^2 + \Psi_B^2) \qquad\qquad 26.1.24$$

The electron density of the bonding molecular orbital is:

$$\Psi_+^2 = \frac{1}{2+2S}\,(\Psi_A + \Psi_B)^2 = \frac{1}{2+2S}\,(\Psi_A^2 + \Psi_B^2 + 2\Psi_A\Psi_B) \qquad\qquad 26.1.25$$

Comparing Eqs. 26.1.24 and 26.1.25, the extra term for the molecular orbital interaction shows the increase in electron density in the bonding region caused by the constructive interference of the atomic orbitals. The anti-bonding orbital has a node in the bonding region, perpendicular to the internuclear axis. The node decreases the electron density between the two nuclei. The decrease in electron density destabilizes the anti-bonding orbital:

$$\Psi_-^2 = \frac{1}{2-2S}\,(\Psi_A - \Psi_B)^2 = \frac{1}{2-2S}\,(\Psi_A^2 + \Psi_B^2 - 2\Psi_A\Psi_B) \qquad\qquad 26.1.26$$
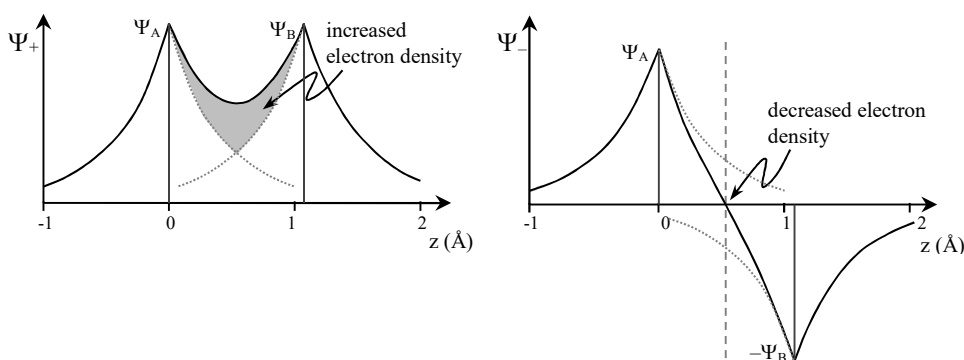
Figure 26.1.4: The bonding molecular orbital, Ψ_+, increases the electron density in the bonding region. The anti-bonding molecular orbital, Ψ_-, decreases the electron density in the bonding region, giving a node. Nucleus A is placed at the origin and B at the experimental bond length 1.06 Å.

The quantitative agreement with experiment is poor. At this initial low level of approximation, the calculated dissociation energy has a 37% error with experiment, Table 26.2.1. However, the general approach is widely applicable to complex molecules. The molecular orbitals for H_2^+ can now be used to model the electronic structure of the H_2 molecule.

26.2 The Hydrogen Molecule

In the H_2 molecule, the Coulomb interactions of the two electrons, 1 and 2, include the four electron-nuclear attractions and the electron-electron repulsion, which varies with the distance between the two electrons, r_{12}. The nuclear-nuclear repulsion is a function of the bond length, R, which is held fixed in accordance with the Born-Oppenheimer approximation, Figure 26.2.1.
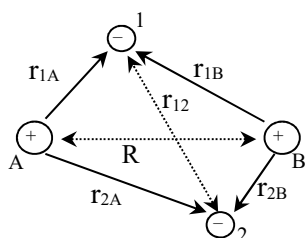
Figure 26.2.1: Coulomb interactions in the H_2 molecule Attractions are shown with solid lines (—) and repulsions are shown with dotted lines (⋯⋯).

The Schrödinger equation for H_2 is:

$$-\frac{\hbar^2}{2m}[\,\nabla_1^2 + \nabla_2^2\,]\,\Psi + \frac{e^2}{4\pi\varepsilon_o}\left(-\frac{2}{r_{1A}} - \frac{2}{r_{1B}} + \frac{1}{r_{12}} + \frac{1}{R}\right)\Psi = E\,\Psi \qquad 26.2.1$$

The H_2 molecular orbital wave function is a function of the coordinates of electron 1 and electron 2, which is schematically written as $\Psi(r_1,r_2)$. The electron-nuclear attractions stabilize the atom and the electron-electron and nuclear-nuclear repulsions destabilize the atom. The electron-electron repulsion term correlates the motion of the two electrons; the motion of electron 1 influences the motion of electron 2. The Schrödinger equation for H_2 cannot be solved exactly, because of electron-electron repulsion. As a consequence we must use approximation techniques to find the molecular orbitals. A first approach is to consider the independent electron approximation, just as we did for the He atom. The H_2^+ bonding molecular orbital is a good starting point for building the molecular orbitals of the H_2 molecule.

Molecular Orbitals are Approximated as the Products of One-Electron Orbitals: In the independent electron model, the overall molecule orbital for the H_2 molecule is the product of one-electron molecular orbitals. Using the LCAO approach, the overall electronic state for the ground state of H_2 is a product of one-electron molecular orbitals of the form of Eq. 26.1.23:

$$\Psi_{MO}(r_1,r_2) = \Psi_+(r_1)\,\Psi_+(r_2) = \frac{1}{2+2S}\,[1s_A(r_1) + 1s_B(r_1)]\,[1s_A(r_2) + 1s_B(r_2)] \qquad 26.2.2$$

If electron-electron repulsion is included, the product wave function is no longer exact. The wave function, at this point, has no adjustable parameters. The electronic energy is given by the

expectation value of the exact Hamiltonian. Based on this simple LCAO approach, the dissociation energy is much too small, at 2.68 eV, and the bond length is too long, at 0.850 Å, Table 26.2.1. Even though the quantitative agreement is poor, the general approach is promising, especially as we consider larger molecules. However, we need to seek better approximations within the LCAO method.

Table 26.2.1: Equilibrium bond lengths and dissociation energies, D_e, for H_2^+ and H_2, with a LCAO basis constructed from hydrogen-like 1s-orbitals, Eq. 26.1.23.

	Source	Z_{eff}	R_e	D_e (eV)	D_e (kJ mol^{-1})
H_2^+	LCAO	1	1.319 Å	1.763 ev	170.2 kJ mol^{-1}
	experimental		1.06 Å	2.78 ev	268.2 kJ mol^{-1}
H_2	LCAO	1	0.850 Å	2.68 eV	258.6 kJ mol^{-1}
	LCAO	1.197	0.732 Å	3.495 eV	334.7 kJ mol^{-1}
	experimental		0.741 Å	4.748 eV	458.1 kJ mol^{-1}

The Variation Method Allows the Calculation of the Effective Nuclear Charge: Taking our inspiration from the Variation treatment of the He-atom, we replace the real nuclear charge on each H-atom, $Z = 1$, with an effective nuclear charge. The minimized energy gives an effective nuclear charge of 1.197, which is greater than Z, Table 26.2.1. The effective nuclear charge felt by the electrons is greater than the real nuclear charge, because the electrons interact with two nuclei instead of one. The increase in effective nuclear charge causes a contraction of the molecular orbitals. The bonding molecular orbital, which is the linear combination of 1s-orbitals on each atom with $Z_{eff} = 1.197$, is smaller than the superposition of two non-interacting 1s-atomic orbitals with $Z = 1$. This contraction causes an increase in kinetic energy of the electrons, which is unfavorable. The increase in kinetic energy can be understood with reference to the particle in a box. Remember that as the box length decreases, the kinetic energy of the particle increases. For stable bond formation the decrease in potential energy must be greater than the increase in kinetic energy.

Accounting for Electron-Electron Repulsion–Polarization Functions: The LCAO molecular orbitals using only 1s-orbitals on each H-atom corresponds to a **minimum basis set**. In a minimum basis set calculation, the atomic orbitals are only the valence orbitals on each atom. For H and He only s-orbitals are included. For main-group elements only s and p-orbitals are included. The quantitative agreement of the LCAO molecular orbitals using only 1s-orbitals on each H-atom is improved by adding in $2p_z$-orbitals on each H-atom. The presence of extra nodes in the added $2p_z$-orbitals allows the electron density to rearrange to increase electron density in the bonding region and to decrease electron-electron repulsion. Adding in atomic orbitals with higher angular momentum than the valence orbitals gives an **extended basis set**. The added orbitals are called **polarization functions,** Table 26.2.2. For moderately sized basis sets, the polarization functions on H and He are p-orbitals, for the main group elements polarization functions are d-orbitals, and for transition elements polarization functions are f-orbitals. Polarization functions are listed in parentheses after the orbital designation, with the designation for H-atoms listed last. Commonly used basis sets with polarization functions on both main group elements and H are 3-21G(d,p) and 6-311G(d,p). Some programs signify polarization functions for main group elements with a "*" and on both main group and hydrogen as "**"; for

example 3-21G(d) is 3-21G* and 3-21G(d,p) is 3-21G**. Adding in $2p_z$ character for the H_2 molecule using the 6-311G(d,p) basis set gives better agreement with experiment than the minimum basis set, Figure 26.2.2:

$$\Psi(\sigma_g) = 0.186 \ 1s_A(\text{inner}) + 0.288 \ 1s_A(\text{middle}) + 0.133 \ 1s_A(\text{outer}) + 0.023 \ 2p_{ZA}$$
$$+ 0.186 \ 1s_B(\text{inner}) + 0.288 \ 1s_B(\text{middle}) + 0.133 \ 1s_B(\text{outer}) - 0.023 \ 2p_{ZB} \qquad 26.2.3$$
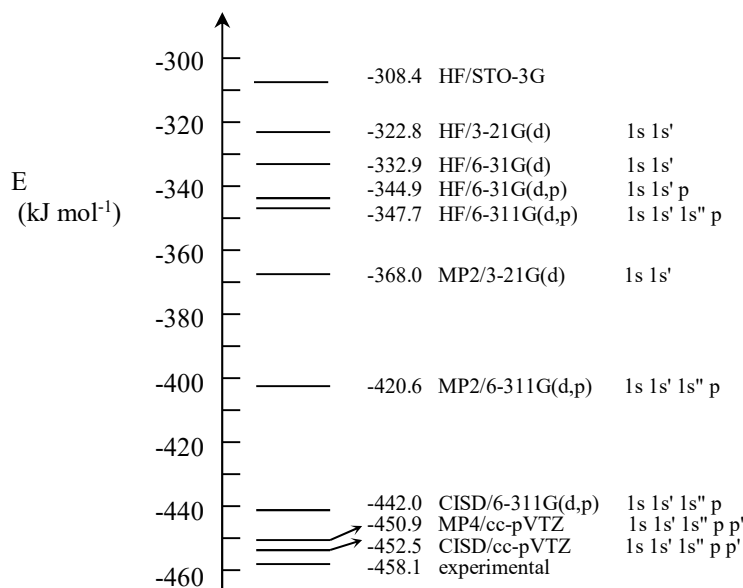
Figure 26.2.2: Electronic energy of the H_2 molecule relative to the dissociated atoms using increasingly complete basis sets and electron correlation.

Table 26.2.2: Atomic Orbital Terms in Gaussian Basis Sets (number of Gaussian primitives).

Atoms:	Hydrogen				2nd and 3rd period[1]						2nd	3rd
Orbital:	1s	1s'	1s"	2p	s	s'	s"	p	p'	p"	3d	3d
STO-3G	3				3			3				
3-21G(*)	2	1			2	1		2	1			1
3-21G*	2	1			2	1		2	1		1	1
6-31G*	3	1			3	1		3	1		1	1
6-31G**	3	1		1	3	1		3	1		1	1
6-311G**	3	1	1	1	3	1	1	3	1	1	1	1
cc-pVTZ	7	1	1	2p1d	7	1	1	3	1	1	2d1f	2d1f

(1). cc-pVTZ gaussian coefficients (α) different for valence s(7-711) and p(7-311) orbitals.

Polarization functions are represented by one primitive in the Gaussian type orbitals, e.g. 6-31G* and 6-31G**. A 6-31G* or 6-31G** orbital on a main-group element uses 6 total primitives for a core orbital and 5 total primitives for the valence orbitals. Adding polarization functions is necessary for accurate calculations. However, the results in Figure 26.2.2 show that considerable error still remains at HF/6-311G(d,p). Electron correlation must be taken into account.

The Motion of the Electrons is Correlated–Configuration Interaction: When one electron moves in a molecule, the positions of the other electrons adjust to decrease electron-electron repulsion. The motions of the electrons are not independent; the motion of the electrons is correlated. The current best method for adjusting the molecular wave functions for electron correlation is **configuration interaction**, CI. CI calculations allow the ground state to mix with excited states of the molecule. The advantage of mixing in excited state character to the ground state is that excited states have nodes between the nuclei, which help the electrons avoid each other and minimize electron-electron repulsion. For example for the H_2 molecule, the ground state configuration and several excited states are diagrammed in Figure 26.2.3.

Ground State
$\sigma_g(1s)^2$

Single Excitation
$\sigma_g(1s)^1\sigma_u^*(1s)^1$

Double Excitation
$\sigma_u^*(1s)^2$
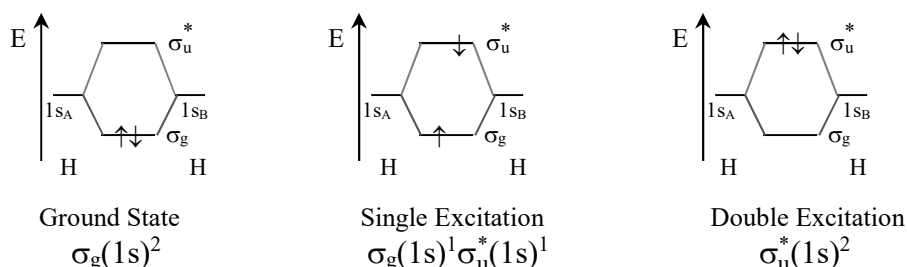
Figure 26.2.3: The configurations of the ground state and two low-lying excited states of H_2.

The mixing of the ground state wave function and excited state wave functions can be done variationally. The mixing coefficients for each excited configuration are adjusted to give the minimum ground state energy during the SCF process. However, the predominant character remains the ground state configuration. This variational-SCF approach leads to techniques called CISD or CISDT. CISD includes single and double excitations. CISDT includes single, double, and triple excitations. For H_2, the single excitation makes a strong contribution in CISD calculations, Figure 26.2.2.

   An easier approach is to use perturbation theory. The Møller-Plesset, MP2, method uses second order perturbation theory to calculate the mixing of the configurations. The MP2 calculation is based on Eq. 25.3.20. That is, the new ground state wave function is mixed in combination with all the excited state wave functions that have the proper symmetry. The wave functions that are closest in energy to the ground state are most important. For the H_2 molecule, MP2 mixes in a small contribution from the $\sigma_u^*(1s)^2$ doubly excited configuration:

$$\Psi_{gs} = 0.9987*\ \ \ \ \ + 0.0518*\ \ \ \ \ \ \ \ \ \ \ \ \text{(MP2) 26.2.4}$$
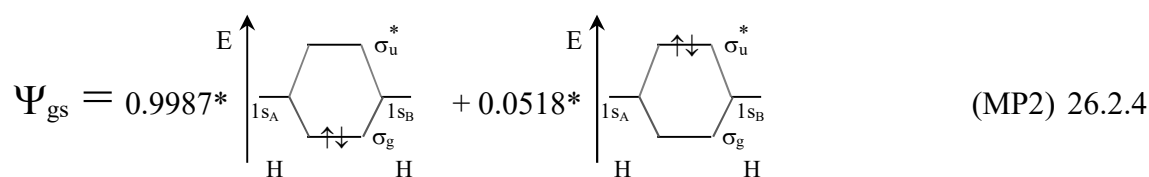
In MP2 calculations, single excitations don't contribute; only double and higher excitations contribute. Of course, for H_2 only single and double excitations are allowed since H_2 has only two electrons. The correlated MP2 and CISD results provide significant improvement in quantitative accuracy. The accuracy of correlated molecular structure calculations is sufficient to explore the contributing factors that determine the strength of the chemical bond.

Why Do Atoms Stick Together? The total electronic energy, the average kinetic energy, and the average potential energy for the H_2 molecule are plotted as a function of bond length in Figure 26.2.4a. The total electronic energy of the molecule is a balance of large opposing kinetic and potential energy contributions. The bond strength is a small fraction of the total potential and kinetic energies of the molecule.

To highlight changes in energy, the three energy curves are replotted relative to the energy of the separated atoms in Figure 26.2.4b. Consider two non-interacting H-atoms at large R. As the bond length decreases the kinetic energy first decreases. This initial decrease in kinetic energy results from delocalization, the ability of the electrons to occupy atomic orbitals on both atoms. The effective "box length" is larger than a single atom, giving a decrease in kinetic energy. However, as the bond length is further decreased, the effective nuclear charge increases as the electrons interact with both nuclei. The orbitals contract giving less room for the electrons, increasing the kinetic energy. Now consider the potential energy. As the two atoms approach each other, the first effect is an increase in electron-electron repulsion. As the bond length decreases further, the electrons interact with both nuclei, increasing the electron density in the bonding region, increasing the effective nuclear charge. The increase in effective nuclear charge decreases the potential energy, which is favorable. However, the contraction also increases electron-electron repulsion, which is unfavorable. At the equilibrium bond length, the electron-nuclear attraction exceeds the electron-electron repulsion and the nuclear-nuclear repulsion.
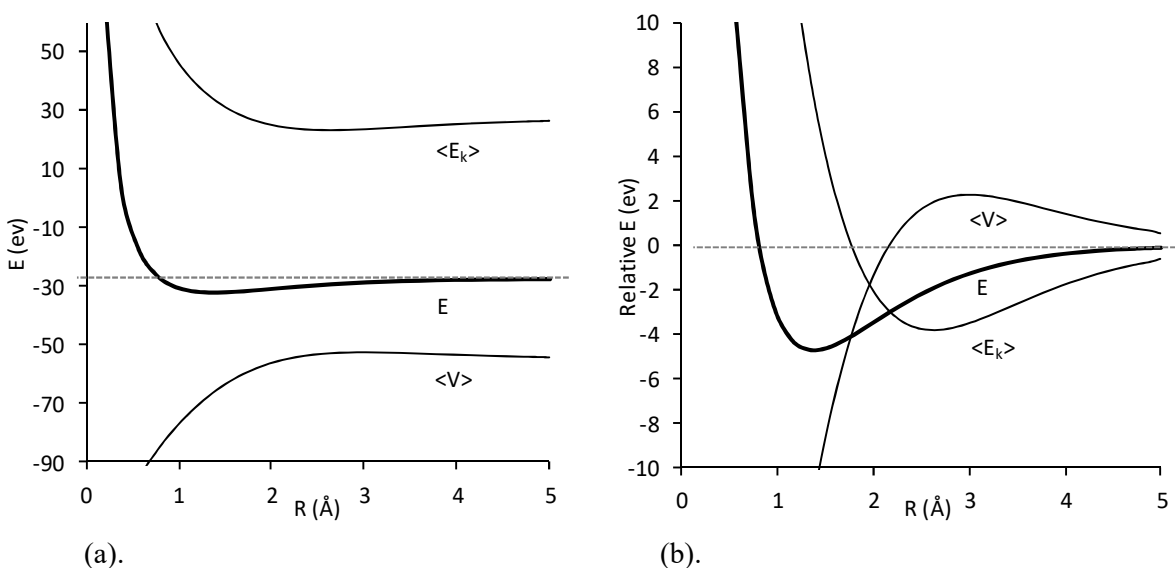
Figure 26.2.4: (a). Electronic energy, E, average kinetic energy, $<E_k>$, and average potential energy, $<V>$, as a function of bond length for H_2. The electronic energy is a balance of large opposing kinetic and potential energy contributions. (b). The same data plotted relative to the separated atoms to highlight changes in energy.

The electron-nuclear attractions are favored by the increase of electron density in the bonding region between the nuclei. However, as electron density is increased in the bonding region, electron density is necessarily decreased in areas remote to the internuclear region. The density changes in the bonding and remote regions counter each other. The density must rearrange to increase the favorable interactions while decreasing the unfavorable effects that are remote to the

internuclear region. One important contribution is that the increase in electron-electron repulsion in the bonding region is countered by a decrease in electron-electron repulsion elsewhere.

The attraction of the electrons for more than one nucleus stabilizes the chemical bond. In addition, correlation effects and the exchange interaction are important for bond stability by decreasing electron-electron repulsion. Calculated bond strengths are too small without inclusion of electron correlation and exchange interactions. The influence of electron correlation and exchange makes the interpretation of the bond strength based only on the Coulomb attraction of the electrons for the nuclei incomplete and oversimplified. The statement that the electrons are "the glue that holds the nuclei together" is a gross oversimplification. An alternative statement is: the chemical bond is favored by the moderation of the increase in kinetic energy and electron-electron repulsion that result from the contraction of the molecular orbitals.

The delicate balance of subtle factors is chemically significant. Were the chemical bond more energetically favorable, then bond breaking processes would be more difficult. Chemical synthesis would be possible only at significantly higher energies. The ease of breaking and making chemical bonds near ambient temperatures is an important requirement of chemical synthesis and the development of life.

26.3 Heteronuclear Diatomic Molecules

Wanted: Good Orbital Overlap and Energy Matching! In homonuclear diatomics, the atomic orbitals on each atom are equivalent. What changes need to be made to consider heteronuclear diatomics? Assume that the atomic orbital on atom B is higher in energy than the atomic orbital on atom A giving $H_{BB} > H_{AA}$. Combining the orbital on atom A and the orbital on atom B gives the secular determinant with differing H_{AA} and H_{BB}, Eq. 26.1.16:

$$(H_{AA} - E)(H_{BB} - E) - (H_{AB} - ES)^2 = 0 \tag{26.1.16}$$

$$(1 - S^2)E^2 - (H_{AA} + H_{BB} - 2H_{AB}S)E + (H_{AA} H_{BB} - H_{AB}^2) = 0 \tag{26.3.1}$$

Neglecting the factor of S^2 compared to 1, using the quadratic formula, and using the approximation $\sqrt{1+x} = 1 + \frac{x}{2}$ gives the bonding and anti-bonding energies as:

$$E_+ = H_{AA} - \frac{(H_{AB} - H_{AA}S)^2}{H_{BB} - H_{AA}} \qquad E_- = H_{BB} + \frac{(H_{AB} - H_{BB}S)^2}{H_{BB} - H_{AA}} \tag{26.3.2}$$

The atomic integrals are roughly approximated by the separated atom energies, $H_{AA} \approx E_A$ and $H_{BB} \approx E_B$, especially at large R. In this approximation, the molecular orbital energies are referenced to the separated atom energies:

$$E_+ \approx E_A - \frac{(H_{AB} - E_A S)^2}{E_B - E_A} \qquad E_- \approx E_B + \frac{(H_{AB} - E_B S)^2}{E_B - E_A} \qquad (R \rightarrow \infty) \tag{26.3.3}$$

The degree of interaction is scaled by the atomic orbital energy difference in the denominators of these expressions. Atomic orbitals with similar energies interact more strongly than atomic orbitals with dissimilar energies, Figure 26.3.1a. Orbital overlap continues to play an important role. The resonance integral is approximately proportional to the overlap integral. The bonding orbital is stabilized and the anti-bonding orbital is destabilized by the resonance interaction. We can summarize the two dependencies as:

| Strong bonds require good atomic overlap and energy matching. |
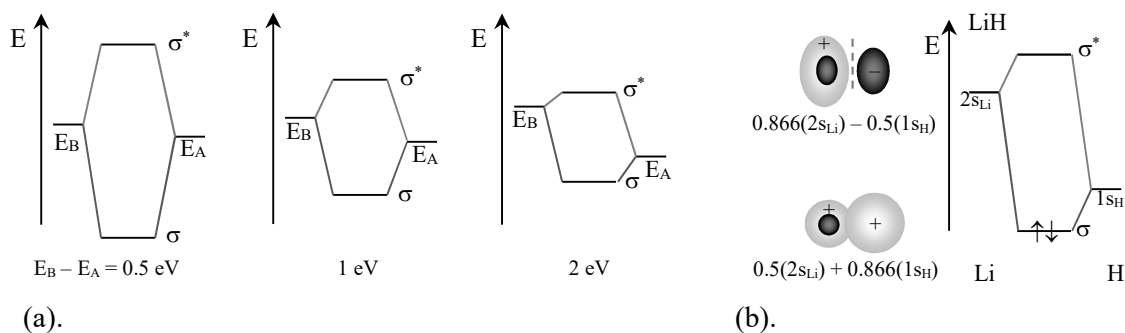
Figure 26.3.1: (a). Energetic stabilization is greatest for interaction of atomic orbitals with similar energy. (b). Molecular orbital model for LiH. The atomic orbital drawings are scaled relative to the contribution of the orbital (bigger MO coefficient-bigger orbital).

In the resulting bonding molecular orbital, the MO coefficient for the lower energy A-orbital is larger than for the B-orbital: $\Psi_{MO} = C_A\Psi_A + c_B\Psi_B$, with $C_A > c_B$. The bonding molecular orbital has a larger component from the lower energy atomic orbital in the LCAO. The energy of the bonding MO is similar to the atomic orbital on A. Conversely, in the anti-bonding molecular orbital, the MO coefficient for the higher energy B-orbital is larger than for the A-orbital; $\Psi_{MO}^* = c_A\Psi_A + C_B\Psi_B$, with $C_B > c_A$. The energy of the anti-bonding MO is similar to the atomic orbital on B. The resulting asymmetry gives partial ionic character to the bond. The fraction ionic character of the bond between atoms A and B is calculated from the MO coefficients:

$$\text{fraction ionic} = \frac{\sum(\text{A coefficients})^2 - \sum(\text{B coefficients})^2}{\sum(\text{A coefficients})^2 + \sum(\text{B coefficients})^2} \qquad 26.3.4$$

The sums extend over all filled molecular orbitals on the given atom.

The simplest stable diatomic is LiH. We first develop a qualitative, diagrammatic model to build our intuition on chemical bonding. The 1s-orbital on Li is much lower in energy than the 1s on H. The energy mismatch is too large for a significant interaction with the H-atom. The 1s-orbital of Li is a non-interacting core orbital. Given the 2s-electron on Li has a principle quantum number of 2, the 2s-orbital on Li is higher in energy than the 1s-orbital on H. The outer radial lobe of the 2s-orbital forms a bonding and anti-bonding pair of molecular orbitals in combination with the H(1s)-orbital, Figure 26.3.1b. The single valence electron on Li and the single electron on H combine to fill the bonding σ-orbital. We don't know the degree of ionic character for LiH, however we can anticipate that the bonding MO has greater H(1s) character, while the anti-bonding orbital has greater Li(2s) character. We can express the result as a combination of two resonance structures, Li–H for the covalent contribution and Li^+H^- for the ionic contribution. As an initial rough guess, assume that the normalized bonding MO is $\sigma = 0.5(2s_{Li}) + 0.866(1s_H)$. Applying Eq. 26.3.4 to the one filled molecular orbital gives the ionic character of the bond as:

$$\text{fraction ionic} = \frac{(0.866)^2 - (0.5)^2}{(0.866)^2 + (0.5)^2} = \frac{0.75 - 0.25}{0.75 + 0.25} = 0.50 \qquad 26.3.5$$

Our rough guess gives a 50% ionic interaction. We now turn to a molecular structure calculation for LiH to verify and amplify our qualitative model.

Lithium Hydride has Partial Ionic Character: The molecular structure calculation is at the CNDO semi-empirical level of approximation. CNDO is a low level of approximation. However, the format of the CNDO output is essentially the same as more sophisticated methods. [www]   The CNDO program is available as a Web applet on the text Web site. The input to a molecular structure calculation is simply the overall charge, multiplicity, and x,y,z coordinates and atomic number of each atom. No information on the bonding is given; the purpose of the calculation is to determine the distribution and strength of the bonds. In this calculation, the Li and H atoms are specified to lie on the x-axis. The output at the CNDO level is given in Figure 26.3.2. The details of CNDO calculations are discussed in Section 26.5. CNDO calculations are semi-empirical calculations, which only consider valence electrons. As in our diagrammatic model, the 1s-orbital on Li is a non-interacting core orbital. The first output section lists the distance between each pair of atoms and the contributions to the nuclear-nuclear repulsion. The units are atomic units; the distances are in multiples of the Bohr radius, a_o = 0.529 Å, and energies are in hartrees, 1 au = 1 H = 27.211 eV. Next follows the overlap matrix. Off-diagonal matrix elements list the overlap integral for each pair of orbitals. The overlap of the $Li(2p_x)$ – $H(1s)$ orbitals is greater than the $Li(2s)$ – $H(1s)$ overlap, because the $2p_x$ orbital is directed along the internuclear axis, Figure 26.3.3. The $Li(2p_z)$ and $Li(2p_y)$-orbitals, which are perpendicular to the internuclear axis, give no net overlap with the 1s-orbital. The next output matrix lists the molecular orbital coefficients, which are the eigenvectors of the Hamiltonian. The molecular orbitals are listed in columns. We are combining five atomic orbitals, so five molecular orbitals are generated. The energy of the MO is listed at the top of each column. For example, the two lowest energy molecular orbitals, which are cylindrically symmetric σ-orbitals, are:

$$\sigma_1 = 0.424 \ 2s(Li) + 0.429 \ 2p_x(Li) + 0.798 \ 1s(H) \qquad E_1 = \text{-0.4818 H}$$
$$\sigma_2 = 0.823 \ 2s(Li) - 0.551 \ 2p_x(Li) - 0.141 \ 1s(H) \qquad E_2 = \ 0.0322 \text{ H} \qquad\qquad 26.3.6$$

The lowest energy orbital, which is anticipated in Figure 26.3.1, also has significant $Li(2p_x)$-character. Even though the energy match between the $Li(2p_x)$ and the $H(1s)$ is not as good as the $Li(2s)$-$H(1s)$, the large overlap between the $Li(2p_x)$ and $H(1s)$-orbitals results in a large contribution to the molecular orbital. The second MO also results from the overlap of the $Li(2s)$ and $Li(2p_x)$ orbitals with the $H(1s)$. The energy is very close to the energy of an isolated $Li(2p)$-orbital, giving a net non-bonding orbital, Figure 26.3.4. The net non-bonding character results because the $Li(2s)$-$H(1s)$ interaction is anti-bonding (opposite signs on the s-coefficients) while the $Li(2p_x)$-$H(1s)$ interaction is bonding. The next two orbitals are the non-bonding atomic $Li(2p_y)$ and $Li(2p_z)$. These orbitals are perpendicular to the internuclear axis giving no net overlap with the $H(1s)$; no interaction is possible by symmetry. The highest energy molecular orbital, σ_5^*, is the anti-bonding complement to σ_1 for the $Li(2p_x)$ – $H(1s)$ interaction.

   In summary, given that the $Li(2p_y)$ and $Li(2p_z)$ are non-interacting; only three atomic orbitals remain to form molecular orbitals: the $Li(2s)$, $Li(2p_x)$ and $H(1s)$. These three orbitals combine to give a bonding, non-bonding, and anti-bonding set. Combining an odd number of atomic orbitals to give a bonding, non-bonding, and anti-bonding set is a commonly observed pattern. Given a total of two valence electrons, only the lowest energy orbital is filled, Figure 26.3.4. Applying Eq. 26.3.4 to the single filled molecular orbital gives the ionic character of the bond as:

$$\text{fraction ionic} = \frac{(0.798)^2 - (0.424)^2 - (0.429)^2}{(0.798)^2 + (0.424)^2 + (0.429)^2} = 0.272 \qquad\qquad 26.3.7$$

The CNDO calculation gives 27.2% ionic character from the Li^+H^- resonance form.

Coulombic repulsion integrals (bottom triangle)(a.u.)
_____ and internuclear distances (top triangle)(a.u.)_____

Atoms: 1 Li   2 H
1 Li 0.2361 3.0425   *R = 3.043*0.529Å = 1.61Å*
2 H   0.254   0.75

_____Overlap Matrix_____

	1 Li2s	1 Li2px	1 Li2py	1 Li2pz	2 H1s
1 Li2s	1.0	0.0	0.0	0.0	0.392
1 Li2px	0.0	1.0	0.0	0.0	0.505
1 Li2py	0.0	0.0	1.0	0.0	0.0
1 Li2pz	0.0	0.0	0.0	1.0	0.0
2 H1s	0.392	0.505	0.0	0.0	1.0

SCF eigenvalues (a.u.) and eigenvectors
_____(eigenvectors listed in columns)_____

E(i)	-0.4818	0.0322	0.0767	0.0767	0.2186
vector	1	2	3	4	5
1 Li2s	0.424	0.823	0.0	0.0	0.379
1 Li2px	0.429	-0.551	0.0	0.0	0.716
1 Li2py	0.0	0.0	0.0	1.000	0.0
1 Li2pz	0.0	0.0	1.000	0.0	0. 0
2 H1s	0.798	-0.141	0.0	0.0	-0.587

_____SCF Population matrix_____

	1 Li2s	1 Li2px	1 Li2py	1 Li2pz	2 H1s
1 Li2s	0.360	0.364	0.0	0.0	0.676
1 Li2px	0.364	0.368	0.0	0.0	0.684
1 Li2py	0.0	0.0	0.0	0.0	0.0
1 Li2pz	0.0	0.0	0.0	0.0	0.0
2 H1s	0.676	0.684	0.0	0.0	1.272

1 Li2s	*1 Li2px*	*1 Li2py 1 Li2pz 2 H1s*
$2c_{Li2s}^2$	$2c_{Li2s}\,c_{Li2px}$	$2c_{Li2s}\,c_{H1s}$
$2c_{Li2px}\,c_{Li2s}$	$2c_{Li2px}^2$	$2c_{Li2px}\,c_{H1s}$
$2c_{H1s}\,c_{Li2s}$	$2c_{H1s}\,c_{Li2px}$	$2c_{H1s}^2$

_____Total Bond Order (Mulliken overlap population)_____

Atoms: 1 Li
2 H   1.221

Electronic energy =   -1.4162 a.u.   *in Hartrees*
Total energy =   -1.0875 a.u.   *in Hartrees with nuclear repulsion*
            = -29.5923 eV
            = -2855.203 kJ/mol
 (the total energy includes nuclear-nuclear repulsion)
Total bond dissociation energy, Do = 9.0279 eV = 871.059 kJ/mol

__Total atom electron densities and atomic charges__

atom	density	charge
1 Li	0.728	0.272
2 H	1.272	-0.272

sum of diagonal entries in bond order matrix:
electron density = $2(c_{Li2s}^2 + c_{Li2px}^2)$
electron density = $c_{1s,H}^2*2$
net negative charge on H on –0.272

Dipole from atom densities

x	y	z
-2.11	0.0	0.0

Complete dipole (including atomic polarization)

x	y	z
-6.21	0.0	0.0

Figure 26.3.2: Molecular structure output for LiH: CNDO level at 1.61 Å bond length.
Annotations in italics are not part of the original output.
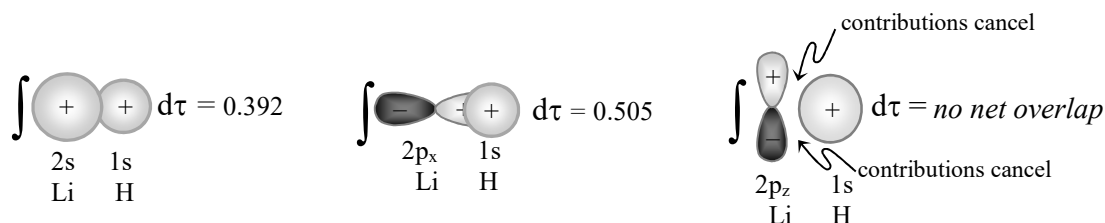
Figure 26.3.3: The overlap of the Li($2p_x$) – H(1s) orbitals is greater than the Li(2s) – H(1s) overlap, because the $2p_x$ orbital is directed along the internuclear axis. The Li($2p_z$) and Li($2p_y$)-orbitals, which are perpendicular to the internuclear axis, give no net overlap with the 1s-orbital.
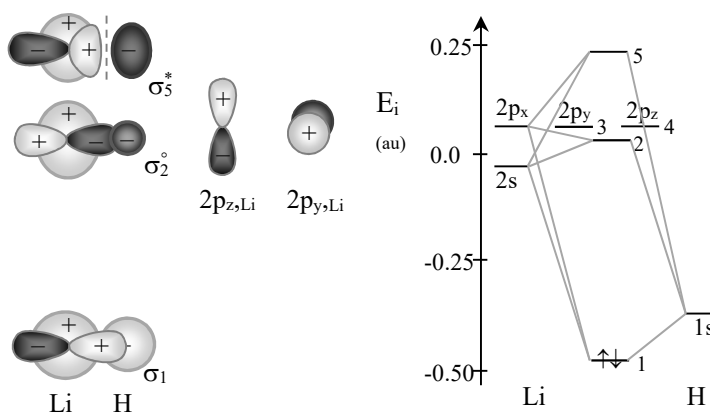
Figure 26.3.4: Molecular orbitals and energy level diagram for LiH. The atomic orbital sizes are scaled to show the relative contribution to the MO. Non-bonding molecular orbitals are labeled with a "°" superscript.

Population Analysis Determines the Atomic Electron Density and Bond Order: The calculation of the ionic character of the Li–H bond is an example of **population analysis**. The analysis is based on the molecular orbital coefficients. The coefficient c_{ij} is for molecular orbital i and atomic orbital j. For example, from the list of eigenvectors for molecular orbital 1, the coefficient for atomic orbital 2, Li($2p_x$), is $c_{12} = 0.429$. The electron density resulting from the overlap of two atomic orbitals is $n_i(c_{ia} \Psi_a + c_{ib} \Psi_b)^2 = n_i(c_{ia}^2\Psi_a^2 + 2c_{ia}c_{ib} \Psi_a\Psi_b + c_{ib}^2\Psi_b^2)$. The first and third terms give the atom electron densities, while the cross-term gives the overlap population between atoms A and B in molecular orbital i. The "SCF Population matrix" has entries, p_{jk}:

$$p_{jk} = \sum_{i=1}^{m} n_i\, c_{ij}\, c_{ik} \qquad\qquad 26.3.8$$

The sum is over all molecular orbitals i with atomic orbitals j and k. The population matrix is also called the **density matrix**. The population matrix shows the atomic orbital terms that contribute to the atom density and overlap population calculations. The **atom electron density** for atom-a is calculated as the sum over all atomic orbitals j on atom-a and the sum over all molecular orbitals i:

$$d_a = \sum_{j\text{ on }a}\sum_{i=1}^{m} n_i c_{ij}^2 = \sum_{j\text{ on }a} p_{jj}^2 \qquad\qquad j = \text{all atomic orbitals on atom a} \qquad 26.3.9$$

The number of electrons in MO-i is called the **occupancy** of the molecular orbital, n_i. There are m atomic and correspondingly m molecular orbitals. The atom electron density on Li is 0.728, Figure 26.3.2. Since Li has one valence electron, the net charge on Li is $1 - 0.728 = +0.272$. The atom electron density on H is 1.272, giving the net charge on H as $1 - 1.272 = -0.272$. The net negative charge agrees with the ionic character of 27.2%, Eq. 26.3.7.

The bond order between atom-a and -b is approximated by the **Mulliken overlap population**, P_{ab}. The overlap population is the sum over all atomic orbitals j on atom-a and atomic orbitals k on atom-b and the sum over all molecular orbitals i with occupancy n_i:[1]

$$P_{ab} = \sum_{j \text{ on } a} \sum_{k \text{ on } b} \sum_{i=1}^{m} n_i \, 2 \, c_{ij} \, c_{ik} \, S_{jk} \qquad \text{for atoms a and b and MO i with } n_i \text{ electrons}$$

$$j = \text{all atomic orbitals on atom-a} \qquad 26.3.10$$
$$k = \text{all atomic orbitals on atom-b}$$

Unoccupied orbitals are called **virtual** orbitals. Because n_i is zero for any virtual orbital, the population sums are effectively over all occupied molecular orbitals. The calculated bond order is 1.221, Figure 26.3.2.

The final section of the output estimates the molecular dipole moment, based on the nuclear charges and the atom electron densities. The **dipole moment operator** for the electrons is:

$$\hat{\vec{\mu}} = -\sum_{i=1}^{n} e \, \hat{\vec{r}}_i \qquad 26.3.11$$

where the sum is taken over the coordinates of each electron, $\vec{r}_i$. The operator is a measure of the skewing of the electron density that results from the formation of polar bonds. In linear molecules the dipole is directed along the internuclear axis, so the dipole moment has only one component, which is along the internuclear axis. The internuclear axis is the x-axis for this calculation. The electronic contribution to the molecular dipole moment is the expectation value of the dipole moment operator. For a linear molecule, the contribution to the dipole moment of the electrons is:

$$<\mu_x> = -\sum_{i=1}^{n} e \int \Psi_{MO}^* \, x_i \, \Psi_{MO} \, d\tau \qquad \text{(linear along x-axis)} \quad 26.3.12$$

The SI units are C m; however for historical reasons the dipole is usually given in **debyes** with:

$$1 \text{ D} = 3.336 \times 10^{-30} \text{ C m} \qquad 26.3.13$$

The CNDO level dipole moment is 6.21 D, but the experimental value is 5.56 D. The discrepancy suggests that the CNDO calculation may overestimate the ionic character of LiH.

Example 26.3.1: *Population Analysis*
Calculate the atom electron density on Li and the bond order in LiH at the CNDO level.

Answer: The atomic orbitals on Li in MO 1 are the 2s and $2p_x$. Using Eq. 26.3.8, the orbital coefficients in Figure 26.3.2, and noting that there is only one occupied molecular orbital gives:

$$d_{Li} = \sum_{j \text{ on Li}} n_1 c_{1j}^2 = 2(0.424)^2 + 2(0.429)^2 = 0.728$$

$$\underbrace{n_1 \, (c_{1,Li(2s)})^2}_{} + \underbrace{n_1 \, (c_{1,Li(2px)})^2}_{}$$

Alternately, the atom electron density on Li is the sum of the diagonal population matrix elements for Li: $d_{Li} = 0.360 + 0.368 = 0.728$.

The overlap population is given by Eq. 26.3.10:

$$P_{LiH} = \sum_{j \text{ on Li}} \sum_{k \text{ on H}} n_1 \, 2c_{1j} \, c_{1k} \, S_{jk} = 4(0.424)(0.798) \, S_{Li(2s)H(1s)} + 4(0.429)(0.798) \, S_{Li(2px)H(1s)}$$

$$\uparrow \quad \uparrow \qquad \uparrow \qquad\qquad\qquad \uparrow \quad \uparrow \qquad \uparrow$$
$$2\,n_1\, c_{1,Li(2s)}\, c_{1,H1(1s)} \quad + \quad 2\,n_1\, c_{1,Li(2px)}\, c_{1,H(1s)}$$

$$= 1.3534(0.392) + 1.3694(0.505) = 1.221$$

Alternately, multiplying the off-diagonal elements of the population matrix in the column for H(1s) with the corresponding $2S_{jk}$ and summing the results also gives the last equation.

Electronegativity Differences Cause Deviations from Equal Sharing: The ionic character of LiH results because the electrons are not shared equally. The H(1s)-orbital is lower in energy than the Li(2s) giving larger H(1s)-character in the bonding orbital. Conversely, in homonuclear molecules, the electrons are equally shared between the two atoms. The deviation from equal sharing is the basis for the definition of the **electronegativity** of the elements. The purpose of the electronegativity scale is to predict the ionic character of chemical bonds. Linus Pauling defined the difference in electronegativity between two elements A and B using the bond dissociation energy of the heteronuclear molecule, $D_o(A–B)$, in comparison with the bond dissociation energies of the homonuclear molecules, $D_o(A–A)$ and $D_o(B–B)$. Pauling's definition predicts that the bond dissociation energy for A–B, assuming equal sharing, is the geometric mean of the homonuclear dissociation energies: $[D_o(A–A) \, D_o(B–B)]^{1/2}$. The deviation of the experimental bond energy from the equal-sharing prediction reflects the difference of the electronegativities:

$$(\chi_A - \chi_B)^2 = D_o(A–B) – [D_o(A–A) \, D_o(B–B)]^{1/2} \qquad\qquad 26.3.14$$

where χ_A and χ_B are the Pauling electronegativities of the two elements, with the bond energies in eV.[5] Pauling chose the value of 4.0 for F to give an overall range of 0–4, Table 26.3.1.

An alternative definition of the electronegativity by Robert Mulliken is based on the element's first ionization potential, I_1, and electron affinity, EA. At large separation, the energy to form the ions $A + B \rightarrow A^+ + B^-$ is $I_{1A} + EA_B$. The energy to form the ions $A + B \rightarrow A^- + B^+$ is $EA_A + I_{1B}$. If the electrons are shared equally, then the energies to form the alternate ion pairs are equal:

$$I_{1A} + EA_B = EA_A + I_{1B} \qquad \text{or rearranging:} \qquad I_{1A} – EA_A = I_{1B} – EA_B \qquad 26.3.15$$

For equal sharing, the electronegativites of the two elements must be equal. Defining the Mulliken electronegativity, x_A, as the arithmetic average of the first ionization potential and the negative of the electron affinity satisfies the requirements applied to equal sharing in Eq. 26.3.14:

$$x_A = \frac{I_{1A} + (-EA_A)}{2} \qquad \text{The two scales are related by: } \chi_A = 0.336(x_A – 0.615) \qquad 26.3.16$$
$$\textit{Pauling} \qquad \textit{Mulliken}$$

The electron affinity is a negative value for most elements. For agreement with the Pauling scale, the ionization energy and electron affinity must be for the valence state of the atom when

participating in the chemical bond. For example for C in methane, the valence state is ^5S with the configuration $2s^1 2p^3$ instead of the ^3P ground state with the configuration $2s^2 2p^2$. Both definitions give similar values for the electronegativity of the elements after the scaling in Eq. 26.3.15. The electronegativity of an atom is useful for predicting the relative valence orbital energies of the atoms in drawing qualitative molecular orbital diagrams. The electronegativity of H is greater than Li, so the H(1s) orbitals are drawn lower in energy than the Li-orbitals, Figure 26.3.1b. We have developed a firm foundation for our understanding of the chemical bond. We can now apply these insights to more complex systems.

Table 26.3.1: Revised values of the Pauling Electronegativities of the Elements.[2,3]

H 2.2							He
Li 0.98	Be 1.57	B 2.04	C 2.55	N 3.04	O 3.44	F 3.98	Ne
Na 0.93	Mg 1.31	Al 1.61	Si 1.90	P 2.19	S 2.58	Cl 3.16	Ar
K 0.82	Ca 1.00	Ga 1.81	Ge 2.01	As 2.18	Se 2.55	Br 2.96	Kr 3.0
Rb 0.82	Sr 0.95	In 1.78	Sn 1.96	Sb 2.05	Te 2.10	I 2.66	Xe 2.6
Cs 0.79	Ba 0.89	Tl 2.04	Pb 2.33	Bi 2.02			

Example 26.3.2: *Electronegativity*
Determine the Pauling electronegativity of Cl. The experimental bond dissociation energies are D_o(H–H) = 4.75 eV, D_o(Cl–Cl) = 2.48 eV, and D_o(H–Cl) = 4.43 eV. The electronegativity of the H-atom is 2.2.

Answer: Using Eq. 26.3.14 gives: $(\chi_{Cl} - \chi_H)^2 = \left(4.43 - [(4.75)(2.48)]^{\frac{1}{2}}\right)$ eV = 1.00

Solving for the electronegativity of Cl, using the positive root: $\chi_{Cl} = 2.2 + \sqrt{1.00} = 3.2$
The positive root is chosen based on the direction of the dipole moment in HCl and the position of the elements in the periodic table.

26.4 Second-Period Homonuclear Diatomic Molecules

   The bonding in the second-period homonuclear diatomics provides a useful series of examples to build upon the principles that we have established. Our goal is to develop a diagrammatic method for predicting the shape and energetics of molecular orbitals. At the same time we use careful molecular structure calculations. The qualitative, diagrammatic development builds our insight into bonding and the careful calculations validate our qualitative ideas.

   The low energy atomic orbitals for Li_2 are the 1s and 2s-orbitals on each atom. The large difference in energy between the 1s and 2s orbitals on Li minimizes the interaction between the 1s on nucleus A and the 2s on nucleus B. The overlap of the 1s-orbitals gives a bonding and anti-bonding $\sigma(1s)$ pair and the overlap of the 2s orbitals on each atom gives a bonding and anti-bonding $\sigma(2s)$ pair, Figure 26.4.1. With six total electrons, the HOMO for Li_2 is the $\sigma_g(2s)$ orbital. An approximate measure of the bond strength is obtained by defining the qualitative bond order, BO:

        BO = ½ (bonding electrons – anti-bonding electrons)   26.4.1

The qualitative bond order of Li_2 is one.
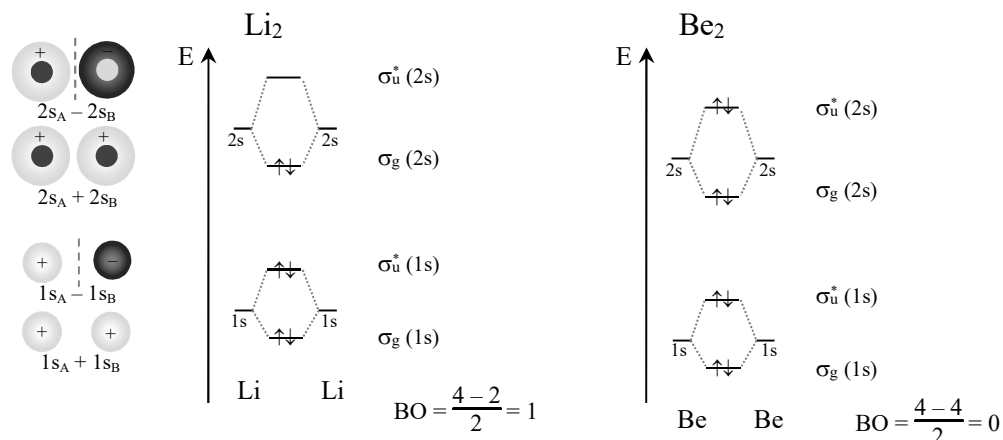
Figure 26.4.1: Molecular orbital diagrams for Li_2 and Be_2. Be_2 is predicted to be unstable, since the qualitative bond order is zero. The g and u subscripts are described in the next section.

The bond order calculated using population analysis is more accurate and useful, but the qualitative bond order is a good first estimate. The same molecular orbital diagram applies to Be_2. Be_2 has two additional electrons giving the qualitative bond order of zero. Be_2 is predicted to be unstable, which is experimentally observed.
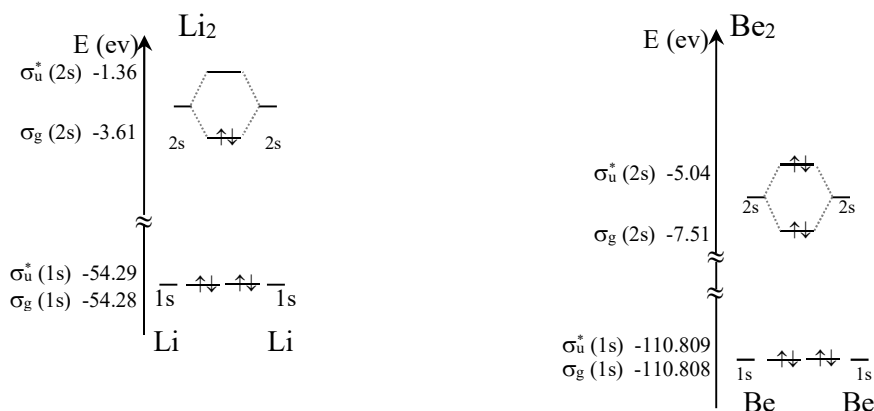
Figure 26.4.2: Quantitative molecular orbital diagrams for Li_2 and Be_2. The splitting between σ_g (1s) and σ_u^*(1s) is small; the 1s-orbitals are weakly interacting. The bond length in Li_2 is 2.67 Å, giving poor overlap of the 1s-orbitals. The broken axes represent large energy gaps.

   Molecular structure calculations agree with our simple diagrammatic approach and provide some additional useful information. Calculated molecular orbital energies are included in Figure 26.4.2. First, the 1s-atomic and σ(1s) molecular orbitals are much lower in energy than the 2s-atomic and σ(2s) molecular orbitals. This difference in energy is so large that it is difficult to accurately draw the energy axes with sufficiently small scale to show the energy gap between the bonding and anti-bonding orbitals. In addition, notice in Figure 26.4.2 that the difference in energy between the σ_g(1s) and σ_u^*(1s) bonding-anti-bonding pair is quite small. The bond length

in H_2, where the 1s-orbitals interact significantly, is 0.74 Å. The bond length in Li_2 is 2.67 Å, so that the overlap of the 1s-orbitals is much diminished. In addition, the 1s-orbitals in Li are contracted compared to the H-atom because of the increased nuclear charge. The bond length in Li_2 optimizes the interaction of the 2s-orbitals. Because of decreased overlap, we can consider the MOs derived from the 1s-orbitals as essentially non-bonding core orbitals. In subsequent MO diagrams, we will omit the 1s-orbitals for convenience and focus only on the valence orbitals. The net contribution to the bonding is minimal for the core orbitals. Notice also in the figure that the valence orbitals of Be_2 are significantly lower in energy than Li_2. Be is more electronegative than Li, shifting all the Be-orbitals to lower energy. In MO diagrams, we usually diminish these energy shifts to simplify the visual depiction of the molecular orbital interactions. In addition, for depictions of molecular orbitals based on 2s-overlap, we often omit the opposite-phase inner lobe of the 2s-atomic orbitals. To continue with the remainder of the second-period homonuclear diatomics, we must consider the overlap of 2p-orbitals on each atom. We begin with O_2.

O_2 Molecular Orbitals: The LCAO Approach: There are two types of p-orbitals on an atom, one pointing along the internuclear axis and two perpendicular to the internuclear axis. The choice of the internuclear axis is arbitrary, however, choosing the z-axis as the internuclear axis is common. Consider the overlap of the p_z-orbitals on each atom, Figure 26.4.3. The p_z-orbitals combine to give a bonding and anti-bonding $\sigma(2p_z)$ pair. The $2p_x$-orbitals are perpendicular to the internuclear axis and combine to form a bonding and anti-bonding $\pi(2p_x)$ pair. The interaction of the p_z-orbitals is greater than the $2p_x$-orbitals because the $2p_z$-orbitals are oriented favorably for good overlap. As a consequence, $\sigma(2p)$ orbitals are usually stronger than $\pi(2p)$ orbitals. Better overlap results in stronger bonding. The $2p_y$-orbitals are also perpendicular to the internuclear axis and combine to form a bonding and anti-bonding $\pi(2p_y)$ pair. The $\pi(2p_x)$ and $\pi(2p_y)$ pairs are degenerate and differ only in orientation. For bonding overlap, the $\sigma(2p_z)$-orbital coefficient signs must be opposite, $\sigma_g = \frac{1}{\sqrt{2}}(2p_{z,A} - 2p_{z,B})$, since by convention the positive lobe of a positive p_z orbital points along the positive x-axis. The $\sqrt{2}$ is required to maintain normalization.

$$\sigma_u^* = \frac{1}{\sqrt{2}}(2p_{z,A} + 2p_{z,B})$$

$$\pi_g^* = \frac{1}{\sqrt{2}}(2p_{x,A} - 2p_{x,B})$$

$$\sigma_g = \frac{1}{\sqrt{2}}(2p_{z,A} - 2p_{z,B})$$

$$\pi_u = \frac{1}{\sqrt{2}}(2p_{x,A} + 2p_{x,B})$$
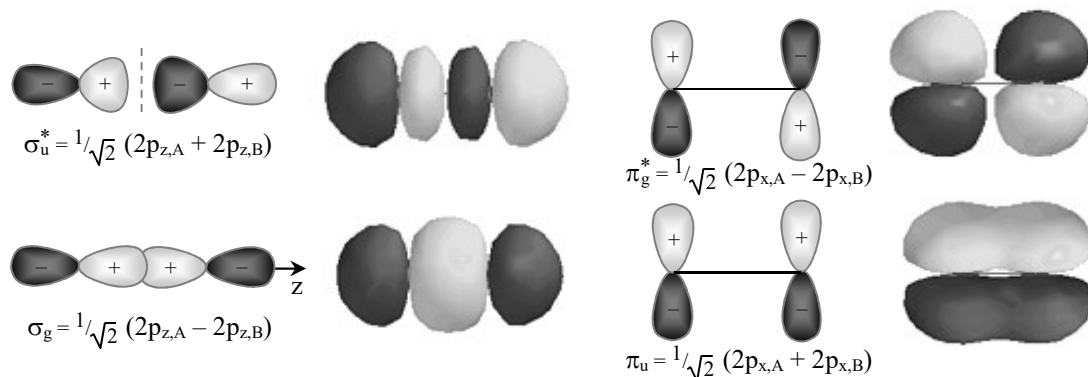
Figure 26.4.3: Interaction of 2p-orbitals give σ type (left) and π-type (right) molecular orbitals in bonding and anti-bonding pairs. The g and u subscripts are explained below.

The complete MO diagram for O_2 consists of the bonding and anti-bonding $\sigma(2s)$ pair and the six MOs constructed from the 2p-orbitals, Figure 26.4.4. The 1s-non-bonding core orbitals are not shown. The total of 12 valence electrons gives half-filled π_g^* orbitals. A singly-occupied highest-

occupied molecular orbital is called a **SOMO** instead of a HOMO. The two parallel electron spins give a triplet ground state. A triplet state is paramagnetic. Paramagnetic substances are attracted into an inhomogeneous magnetic field. Diamagnetic substances are weakly repelled from an inhomogeneous magnetic field. The Lewis dot structure for O_2 is $\ddot{O}=\ddot{O}$, which is all spin-paired and diamagnetic. The correct prediction of the paramagnetism of ground state O_2 was the first convincing accomplishment of molecular orbital theory. Next we need to discuss how each molecular orbital is given a unique identifying symbol to make discussions easier.
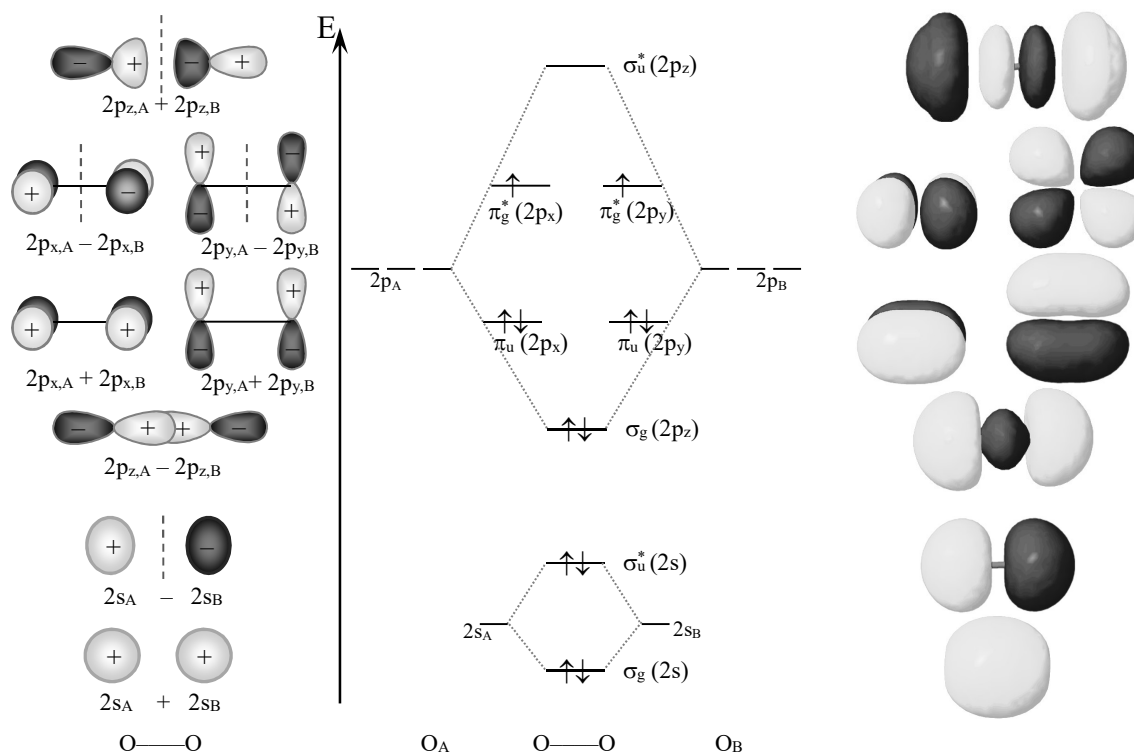
Figure 26.4.4: Molecular orbitals for O_2. Computed isodensity MO plots shown at right.

Molecular Orbitals Are Described by Their Symmetry: The designation of a molecular orbital is determined by its symmetry. The symmetry of a molecular orbital is specified by the symmetry under rotation, reflection, and inversion. The highest symmetry axis for a linear molecule is along the internuclear axis. If rotation around the symmetry axis for a MO leaves the sign of the orbital unchanged for any angle, then the orbital is a σ-orbital. If the sign changes upon rotation by 180°, then the orbital is a π-orbtial. If the sign changes upon rotation by 90°, then the orbital is a δ-orbital (a delta-orbital), Figure 26.4.5. For example, consider the $\sigma_g(2p_z)$-orbital. Upon observation down the internuclear axis, the $\sigma_g(2p_z)$-orbital has the same sign for any rotation. The $\pi_g^*(2p_x)$-orbital on the other hand, changes sign by rotation of 180°; hence the designation as a π-orbital. Consider the overlap of d-orbitals, Figure 26.4.6. The overlap along the z-axis of two d_{z^2} orbitals gives a $\sigma(3d_{z^2})$ bonding orbital. The side-to-side overlap of two d_{yz} orbitals gives a $\pi(3d_{yz})$ orbital. The face-to-face overlap of two d_{xy} orbitals gives a $\delta(3d_{xy})$ orbital.
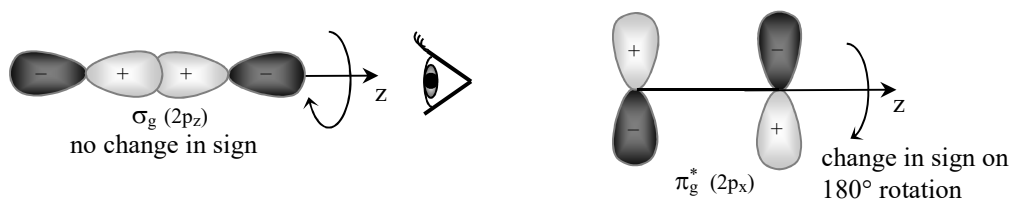
Figure 26.4.5: The symbol assigned to a molecular orbital is determined by the symmetry under rotation, reflection, and inversion. The change in sign upon rotation is observed by looking down the internuclear axis, which is the z-axis in this case.
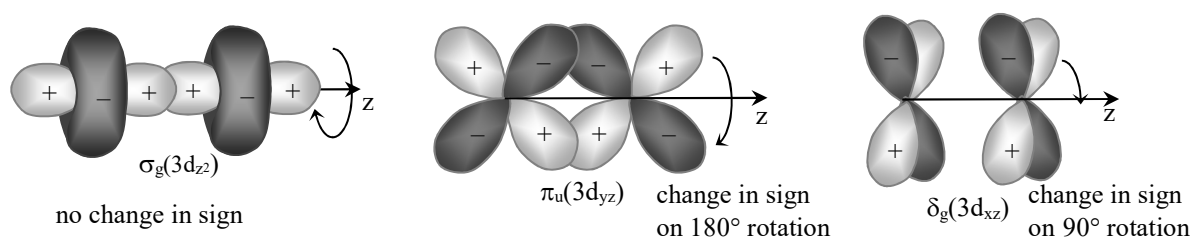
Figure 26.4.6: The overlap of d-orbitals gives σ, π, and δ orbitals (only bonding shown).
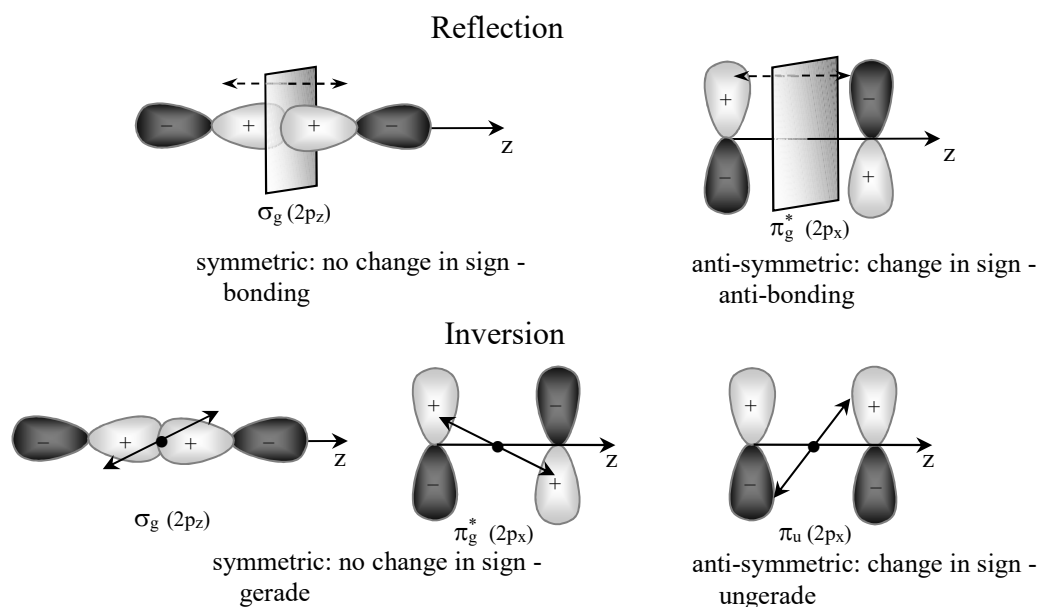
Figure 26.4.7: Bonding orbitals are symmetric with respect to reflection across a plane between the two nuclei, perpendicular to the internuclear axis. Gerade, or even, orbitals are symmetric with respect to inversion through the center of mass. The center of mass (•) is the inversion center.

The second symmetry operation is the reflection across a plane between the nuclei and perpendicular to the internuclear axis. Assuming the internuclear axis is the z-axis, the reflection operation compares a point (x,y,z) with the point $(x,y,-z)$. If the orbital is the same sign, the

orbital is **symmetric with respect to reflection**, giving a bonding orbital, Figure 26.4.7. Anti-symmetric orbitals change sign upon reflection and are anti-bonding.

The third symmetry operation is inversion through the center of mass. The center of mass is the **inversion center**. The inversion operation compares a point (x,y,z) with the point (-x,-y,-z). If the orbital is the same sign, the orbital is **symmetric with respect to inversion**, giving a **gerade** orbital, Figure 26.4.9. Gerade is German for "even." Anti-symmetric orbitals change sign upon inversion and are **ungerade**. The inversion character is called the **parity**. The parity is indicated with a g or u subscript. The symmetry symbols for the diatomic molecular orbitals are listed in Figures 26.4.2-26.4.9. Rotation and reflection symmetry are also applied to orbital phase relationships of heteronuclear diatomic molecules, but inversion does not formally apply. With convenient orbital designations in hand, we can now continue with the second-period diatomics.

N_2 Has the Strongest Bond of the Second-Period Homonuclear Diatomics: The diagram in Figure 26.4.4 also applies to F_2 and Ne_2. However, as we discuss below, the ordering for B_2, C_2, and N_2 has the $\sigma_g(2p_z)$ above the $\pi_u(2p_x)$ and $\pi_u(2p_y)$. The resulting configurations for the second-period homonuclear diatomic molecules are shown in Figure 26.4.8.
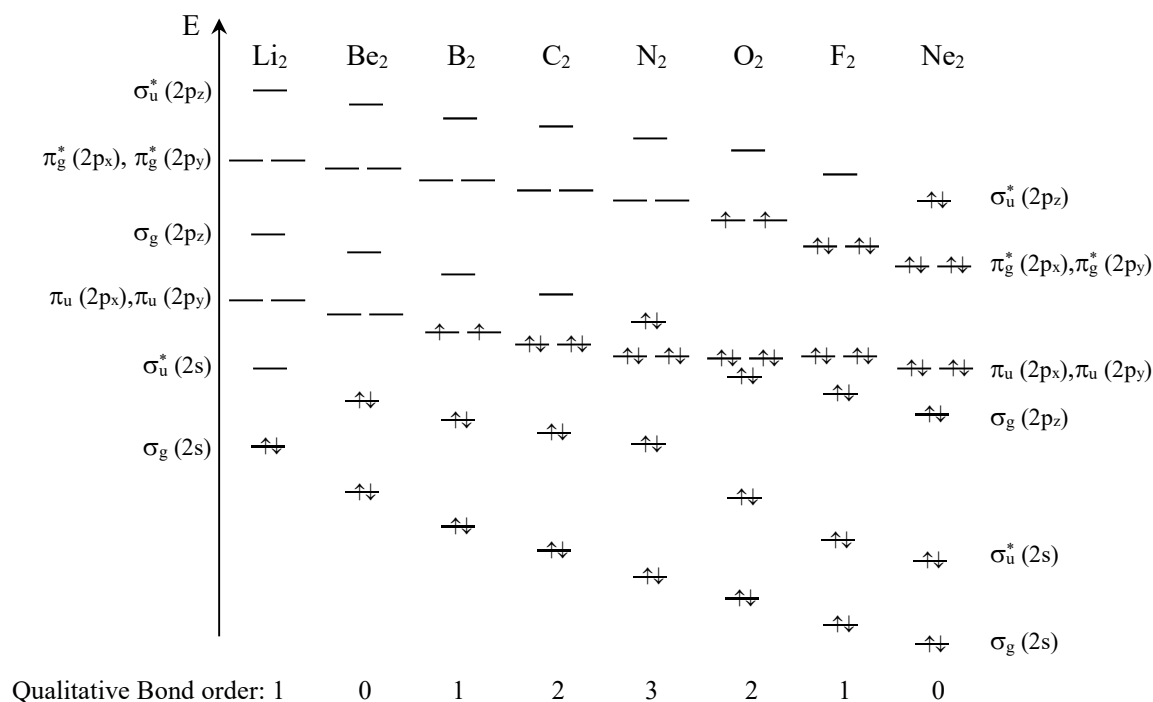
Figure 26.4.8: Predicted configurations of second-period homonuclear diatomic molecules.

Note that molecular orbital theory predicts that B_2 is also paramagnetic, which is experimentally observed. N_2 is predicted to have the strongest bond of the second-period homonuclear diatomics, since the qualitative bond order is 3. The LCAO approach provides an accurate description of the bonding in diatomics. The third-period also follows the same trend, with the MO ordering the same as O_2. The predicted electronic configuration of diatomic molecules is specified by the orbital filling. The core, net non-bonding 1s-orbitals are written either as $\sigma_g(1s)^2\sigma_u^*(1s)^2$ or [KK] in condensed format:

B_2: $[KK]\sigma_g(2s)^2\sigma_u^*(2s)^2\pi_u(2p)^2$

C_2: $[KK]\sigma_g(2s)^2\sigma_u^*(2s)^2\pi_u(2p)^4$

N_2: $[KK]\sigma_g(2s)^2\sigma_u^*(2s)^2\pi_u(2p)^4\sigma_g(2p_z)^2$

O_2: $[KK]\sigma_g(2s)^2\sigma_u^*(2s)^2\sigma_g(2p_z)^2\pi_u(2p)^4\pi_g^*(2p)^2$

F_2: $[KK]\sigma_g(2s)^2\sigma_u^*(2s)^2\sigma_g(2p_z)^2\pi_u(2p)^4\pi_g^*(2p)^4$ 26.4.2
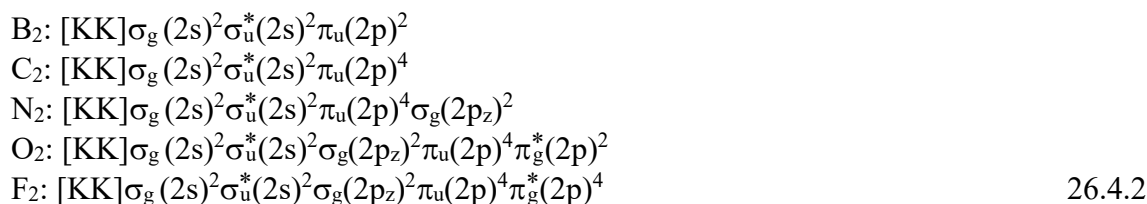
Why is the Orbital Ordering Different for O_2 and N_2? Energy Matching: In building the molecular orbitals from the overlap of p-orbitals, we neglected any interaction between the 2p-orbitals on one atom with the 2s-orbitals on the other. The energy gap between the 2s and 2p-orbitals increases across the period, Figure 26.4.9. For O-atoms and beyond, the 2s-2p gap is large and there is little interaction. However, for B through N, the gap between the 2s and 2p-orbitals is sufficiently small that the 2s and 2p orbitals on opposite atoms interact, Figure 26.4.10a. The result is that the $\sigma_g(2s)$ and $\sigma_u^*(2s)$ are stabilized, while the $\sigma_g(2p_z)$ orbital is destabilized, Figure 26.4.10b. The $\sigma_g(2p_z)$ energy is greater than the $\pi_u(2p)$ orbitals for B_2, C_2, and N_2. Two criteria are important for strong bond formation, <u>good overlap and energy matching</u>. The energy matching is favorable between 2s and 2p-orbitals for B_2, C_2, and N_2.
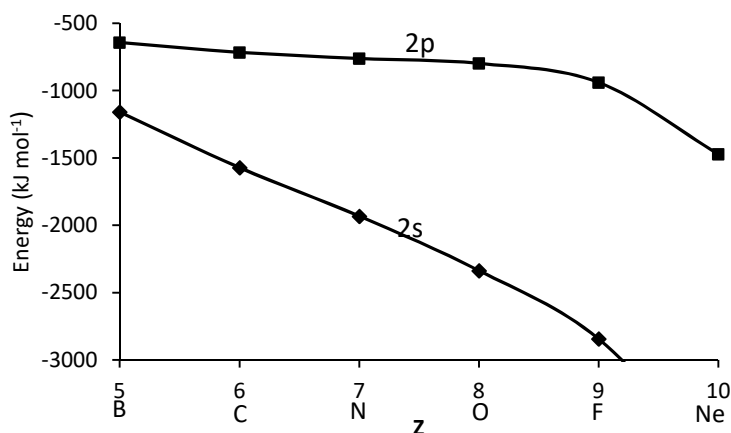
Figure 26.4.9: Valence atomic orbital energies of the second-period elements.
(B3LYP/cc-pVTZ for the neutral hydride, BH_3, CH_4, NH_3, H_2O, HF, Ne, extrapolated to long bond lengths)

The molecular structure calculation output for the N_2 molecule shows significant contribution of the $2p_z$ orbital in the $\sigma_g(2s)$ orbital, Table 26.4.1:

$$\sigma_g(2s) = -0.621(2s_A) - 0.338(2p_{z,A}) - 0.621(2s_{,B}) + 0.338(2p_{z,B})$$ 26.4.3

The relative contribution of the s and p-orbitals to the molecular orbital is depicted by the size of the orbitals in Figure 26.4.10, giving larger 2s and smaller $2p_z$ orbitals. The p-orbital character in the molecular orbital is determined using population analysis on a chosen atom:

$$\% \text{ p character} = \frac{\sum(\text{p coefficients})^2}{(\text{s coefficient})^2 + \sum(\text{p coefficients})^2}$$ 26.4.4

where the sums are taken over the orbital coefficients on the chosen atom, Table 26.4.1. For O_2 and beyond in the periodic table, the $\sigma_g(2s)$ and $\sigma_u^*(2s)$ are primarily s in character, while the $\sigma_g(2p_z)$ is primarily p in character. For N_2, the p-orbital contributes strongly to the $\sigma_g(2s)$ and

$\sigma_u^*(2s)$, leaving less p-character for the $\sigma_g(2p_z)$. The shift in orbital order is also evident in the shape of the molecular orbitals, Figure 26.4.11. The center lobe of the $\sigma_g(2p_z)$ for N_2 is smaller than for O_2, because of the decreased p-character.

(a). (b).
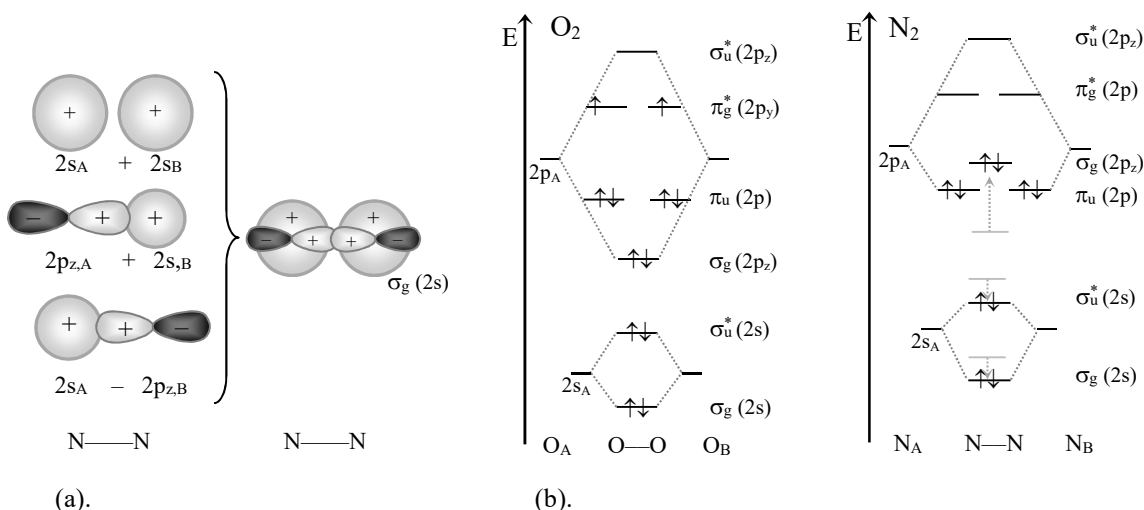
Figure 26.4.10: (a). The interaction of the 2s-orbital on one atom with the $2p_z$-oribtal on the opposite atom is significant for B_2, C_2, and N_2. (b). Compared to O_2, the $\sigma_g(2s)$ and $\sigma_u^*(2s)$ are stabilized, while the $\sigma_g(2p_z)$ orbital is destabilized.

Table 26.4.1: N_2 Occupied Molecular Orbitals. Calculated at the 1.094 Å experimental bond length using the semi-empirical AM1 method. Orbital 1 is the $\sigma_g(2s)$ bonding orbital.

MO:	1	2	3	4	5
Eigenvalues:(eV)	-41.3927	-21.4303	-16.1919	-16.1919	-14.3230
	$\sigma_g(2s)$	$\sigma_u^*(2s)$	$\pi_u(2p_y)$	$\pi_u(2p_x)$	$\sigma_g(2p_z)$
1 N 1 S	-0.6210	-0.6496	0.0000	0.0000	-0.3382
2 N 1 PX	0.0000	0.0000	0.0189	0.7068	0.0000
3 N 1 PY	0.0000	0.0000	0.7068	-0.0189	0.0000
4 N 1 PZ	-0.3382	0.2792	0.0000	0.0000	0.6210
5 N 2 S	-0.6210	0.6496	0.0000	0.0000	-0.3382
6 N 2 PX	0.0000	0.0000	0.0189	0.7068	0.0000
7 N 2 PY	0.0000	0.0000	0.7068	-0.0189	0.0000
8 N 2 PZ	0.3382	0.2792	0.0000	0.0000	-0.6210
% p character	22.8%	15.6%	100%	100%	77.1%

N_2 $\sigma_g(2p_z)$ $\qquad$ O_2 $\sigma_g(2p_z)$
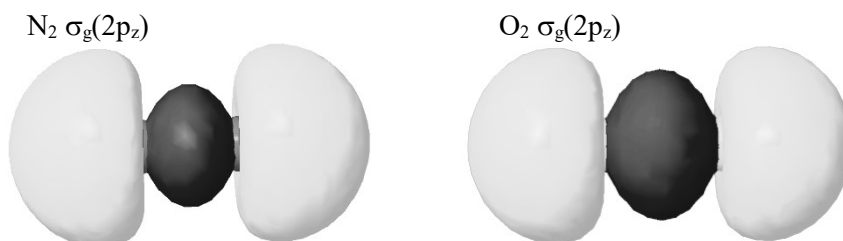
Figure 26.4.11: The decreased $2p_z$ character in the $\sigma_g(2p_z)$ orbital for N_2 results in a smaller central lobe. The calculation is at the HF/6-31G(d) level.

The interaction of the 2s and 2p-orbitals on adjacent atoms in B_2, C_2, and N_2 introduces an important principle. The requirements of good overlap and energy matching are prescriptive and determinative for the interaction of atomic orbitals in a molecular orbital. Orbitals that can overlap, will. In forming a molecular orbital, we must include all possible overlaps between atomic orbitals with similar energy.

Does Molecular Orbital Theory Really Work? Experimental Bond Strength Measures: The molecular orbital theory predictions of the qualitative bond order can be validated using experimental information. The experimental bond dissociation energy, D_o, the experimental bond length, r_o, and the bond force constant, k, are determined using UV-visible, infrared, and vibrational spectroscopy. Strong bonds have large bond dissociation energies, small equilibrium bond lengths, and large force constants. The zero point vibrational energy is $E_o = \frac{1}{2} h\nu_o$, where ν_o is the fundamental vibration frequency. The minimum of the electronic potential curve is at the bond length r_e, Figure 26.1.1. The bond dissociation energy, D_e, is related to the experimental bond dissociation energy after adjusting for the zero point vibrational energy:

$$D_o = D_e - \frac{1}{2} h\nu_o \qquad\qquad 26.4.5$$

The experimental bond length, r_o, is the vibrationally averaged bond length in the zero-point vibrational state. The difference between the experimental r_o and r_e is small. For a harmonic potential the bond force constant, k, is given by the Hooke's Law potential, $V = \frac{1}{2} k(r-r_o)^2$. For anharmonic potentials the bond force constant is determined by the curvature of the electronic potential energy at the equilibrium bond length:

$$k = \left(\frac{\partial^2 V}{\partial r^2}\right)_{r=r_e} \qquad\qquad 26.4.6$$

Experimental bond strength measures for second-period diatomics show an excellent correlation with the qualitative bond order predicted from MO theory, Table 26.4.2 and Figure 26.4.12.[4,5]

Table 26.4.2: Bond Strength Measures for 2nd Period Diatomic Molecules.[4,5]

	H_2	Li_2	LiH	B_2	C_2	N_2	O_2	F_2	CN	CO	NO
D_o (kJ/mol)	435	105	243	289	602	941	494	151	787	1070	632
r_o (Å)	0.76	2.68	1.61	1.59	1.24	1.10	1.21	1.44	1.18	1.13	1.15
k (N/m)	510	25	96	350	930	2240	1140	450	1580	1860	1550
Bond Order	1	1	1	1	2	3	2	1	2½	3	2½

These bond strength correlations and the triplet character of the ground state of oxygen validate the molecular orbital approach. Based on the success of the LCAO-MO method, efficient computational techniques must be developed to extend the approach to larger molecules. The self-consistent field, SCF, method in combination with careful consideration of electron indistinguishability are the basis for a variety of useful computational methods.
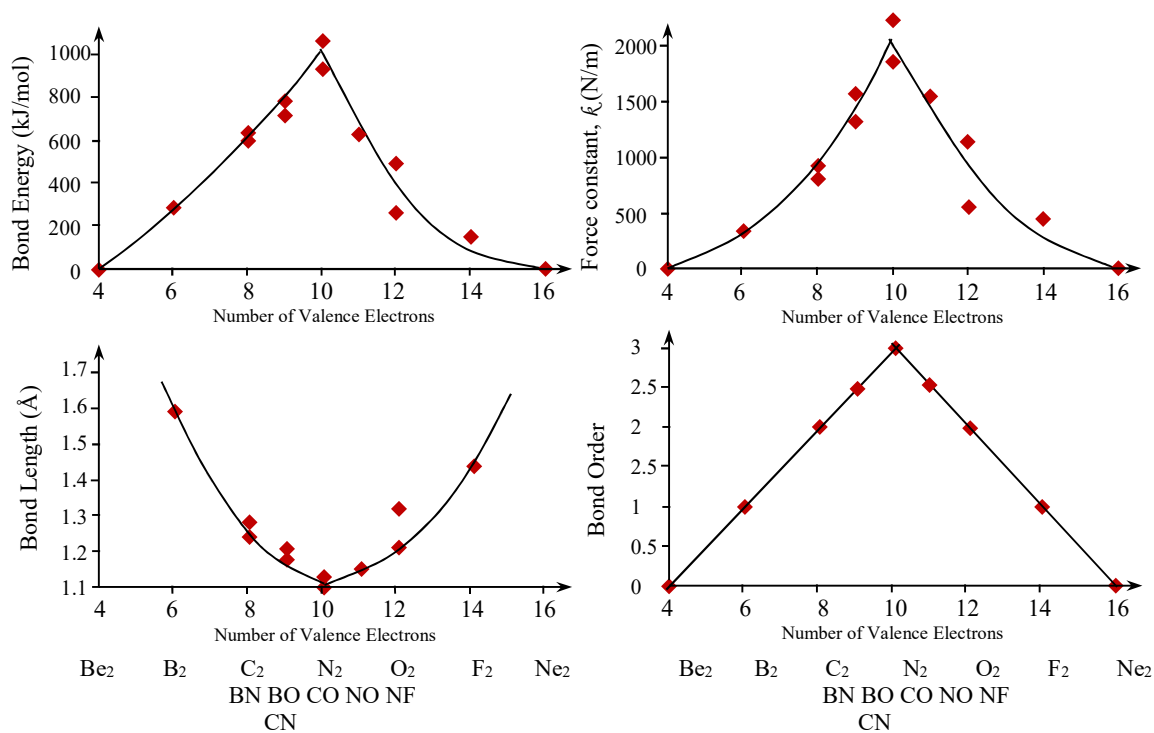
Figure 26.4.12: Experimental measures of bond strength correlate with molecular orbital predictions for the qualitative bond order. The plots are with respect to the total number of valence electrons in the diatomic molecule.[4,5]

26.5 Self-Consistent Field Hartree-Fock Theory

Self-consistent field Hartree-Fock theory is readily applied to molecular structure determination. One common approach is given by the Roothaan equations. We will focus on the results, rather than derive these important equations.

LCAO+Slater Determinants+One-Electron Products = Roothaan Equations: The Roothaan equations are derived under the Born-Oppenheimer and orbital approximations, using the SCF-LCAO approach.[6] A one-electron molecular orbital, Ψ_a, is approximated as the linear combination of atomic orbitals, ϕ_i:

$$\Psi_a = \sum_{i=1}^{N} c_{ia}\, \phi_i \qquad\qquad 26.5.1$$

where the c_{ia} orbital coefficients are optimized as variational parameters. The linear combination extends over the N total atomic orbitals, including all orbitals on each atom in the molecule. The atomic orbitals are usually in Slater or Gaussian form. The one-electron MOs are labeled with subscripts as a, b, c, etc. For example, for a diatomic molecule, Ψ_a is the σ_{1s} orbital, Ψ_b is the σ_{1s}^*, and Ψ_c is σ_{2s}, etc. The complete multi-electron molecular orbital for the molecule is Ψ_{MO}. To be consistent with the Pauli Exclusion Principle, Ψ_{MO}, for n total electrons, is a Slater determinant of the one-electron MOs:

$$\Psi_{MO} = 1/\sqrt{n!} \begin{vmatrix} \Psi_a(1)\alpha(1) & \Psi_a(1)\beta(1) & \Psi_b(1)\alpha(1) & \Psi_b(1)\beta(1) & \dots \\ \Psi_a(2)\alpha(2) & \Psi_a(2)\beta(2) & \Psi_b(2)\alpha(2) & \Psi_b(2)\beta(2) & \dots \\ \Psi_a(3)\alpha(3) & \Psi_a(3)\beta(3) & \Psi_b(3)\alpha(3) & \Psi_b(3)\beta(3) & \dots \\ \vdots & \vdots & \vdots & \vdots & \dots \end{vmatrix} \qquad 26.5.2$$

In the following, the equations are solved for both the α and β spins; σ signifies either α or β: $\sigma(1) = \alpha(1)$ or $\beta(1)$.

The Variation Theorem is used to find the orbital coefficients, c_{ia}. We assume a closed shell molecule with n electrons, which gives paired electrons in $n/2$ filled orbitals. The one-electron molecular orbital energies are determined using the **Hartree-Fock equations**:

$$f_1 \, \Psi_a(1)\sigma(1) = \varepsilon_a \, \Psi_a(1)\sigma(1) \qquad\qquad 26.5.3$$

where ε_a is the one-electron orbital energy for molecular orbital a. Parallel equations are written for molecular orbitals b, c, …. The one-electron **Fock operator** for electron 1, f_1, is given by:

$$f_1 = h_1 + \sum_{j=1}^{n/2} \{2J_j(1) - K_j(1)\} \qquad\qquad \text{(closed shell)} \qquad 26.5.4$$

where the sum extends over all j filled orbitals excluding the orbital that electron 1 occupies. As expressed by the Slater determinant, all electrons in the molecule are equivalent; no one electron belongs to a given MO. Correspondingly, the last equation holds for each electron, 1, 2, 3, …
The **core Hamiltonian**, h_1, is the sum of the kinetic energy of electron 1 and the electron-nuclear attraction of electron 1 with each nucleus k in the molecule:

$$h_1 = -\frac{\hbar^2}{2m} \nabla_1^2 - \sum_{k=1}^{m} \frac{Z_k e^2}{4\pi\varepsilon_o r_{k_1}} \qquad\qquad 26.5.5$$

where the nuclear charge of atom k is Z_k and the distance of electron 1 from nucleus k is r_{k1}, Figure 26.5.1a. The sum is over all m nuclei in the molecule.

(a). Core Hamiltonian, h_1 (b). Coulomb operator, $J_2(1)$
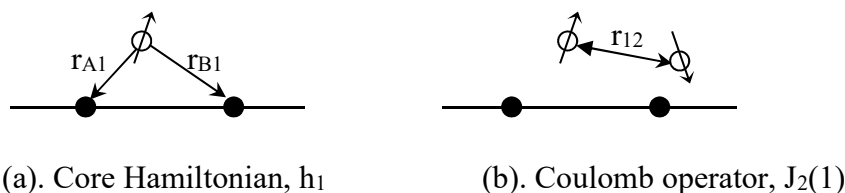
Figure 26.5.1: Interaction terms in the Fock operator: (a) the core Hamiltonian, h_1, includes the electron-nuclear attractions for electron 1. (b). The coulomb operator, $J_2(1)$, determines the average electron-electron repulsion between electron 1 and 2.

Electron-electron repulsion is evaluated using the coulomb and exchange operators. The **coulomb operator** between electron 1 in molecular orbital a and electron 2 in molecular orbital j is, Figure 26.5.1b:

$$J_j(1) \, \Psi_a(1) = \left(\int \Psi_j^*(2) \, \frac{e^2}{4\pi\varepsilon_o r_{12}} \, \Psi_j(2) \, d\tau_2 \right) \Psi_a(1) \qquad\qquad 26.5.6$$

Summed over all one-electron molecular orbitals, this term gives the average effective electron-electron repulsion between electrons 1 and 2, as discussed in Eq. 25.4.1. The **exchange operator** is an exact representation of the cross terms in the Slater determinant necessary to guarantee electron indistinguishablity:

$$K_j(1) \, \Psi_a(1) = \left(\int \Psi_j^*(2) \, \frac{e^2}{4\pi\varepsilon_o r_{12}} \, \Psi_a(2) \, d\tau_2 \right) \Psi_j(1) \qquad\qquad 26.5.7$$

The exchange operator is the source of the quantum mechanical avoidance of parallel electrons that is summarized by Hund's Rule, Sec. 25.4.

The Hartee-Fock equations are recast into matrix form to provide efficient algorithms for molecular structure calculations. For a closed shell molecule, there are no unpaired electrons and the α and β spin-orbitals are equivalent for each MO. Substituting the LCAO sum from Eq. 26.5.1 for $\Psi_a(1)$ in Eq. 26.5.3 and multiplying from the left by atomic orbital $\phi_j(1)$ gives:

$$\sum_{i=1}^{N} c_{ia} \, \phi_j(1) f_1 \phi_i(1) = \varepsilon_a \sum_{i=1}^{N} c_{ia} \, \phi_j(1)\phi_i(1) \qquad\qquad \text{(closed shell)} \quad 26.5.8$$

Integrating both sides of the equation over the coordinates of electron 1 gives:

$$\sum_{i=1}^{N} c_{ia} \int \phi_j(1) f_1 \phi_i(1) \, d\tau_1 = \varepsilon_a \sum_{i=1}^{N} c_{ia} \int \phi_j(1)\phi_i(1) \, d\tau_1 \qquad\qquad \text{(closed shell)} \quad 26.5.9$$

Each integral in each sum is now a constant. The choices for atomic orbitals i and j include all atomic orbitals in the molecule. The complete set of equations with each pair of atomic orbitals in the integrals gives an NxN matrix equation:

$$\underset{\approx}{F} \, \underset{\sim}{c}_a = \varepsilon_a \, \underset{\approx}{S} \, \underset{\sim}{c}_a \qquad\qquad \text{(closed shell)} \quad 26.5.10$$

The eigenvectors of the Fock equation, $\underset{\sim}{c}_a$, are the molecular orbital coefficients. The **Fock matrix elements**, F_{ji}, are the integrals over the Fock operator in Eq. 26.5.9, and the overlap matrix elements, S_{ji}, are the overlap integrals:

$$F_{ji} = \int \phi_j(1) f_1 \phi_i(1) d\tau_1 \qquad\qquad S_{ji} = \int \phi_j(1)\phi_i(1) \, d\tau_1 \qquad\qquad \text{(closed shell)} \quad 26.5.11$$

For example in the matrix equation, Eq. 26.5.10, row j is for atomic orbital j:

$$\sum_{i=1}^{N} c_{ia} F_{ji} = \varepsilon_a \sum_{i=1}^{N} c_{ia} S_{ji} \qquad\qquad \text{(row j, closed shell)} \quad 26.5.12$$

The Roothaan Equations, in matrix form, are the basis of most commonly used molecular structure programs, e.g. CNDO, MOPAC, Spartan, and Gaussian. However, the coulomb and exchange integrals are difficult and time consuming to calculate. For *ab initio* calculations all the integrals in the Fock matrix are calculated for all electrons. Choosing Gaussian basis sets facilitates the determination of the integrals. However, for efficient approximate calculations, some integrals can be neglected.

Semi-Empirical Molecular Orbital Theory: CNDO, MNDO, AM1, PM3:   Semi-empirical molecular orbital methods were developed concurrently with *ab initio* methods to provide very quick approximate calculations for large molecules. Semi-empirical calculations only consider the <u>valence electrons</u>. The core electrons are included in the nuclear core. The basis sets are simplified to include only a <u>minimum basis set</u>. A minimum basis set contains only occupied atomic orbitals with no polarization functions. For example, for carbon only 2s and 2p functions are included. For silicon, phosphorus, sulfur and chlorine, only 3s and 3p atomic orbitals are included; no d-orbitals are used in MNDO, AM1, or PM3 calculations. Semi-empirical methods use <u>Slater-type orbitals</u> or the corresponding Gaussian STO-3G equivalents. Many of the coulomb and exchange integrals are obtained by fitting the results of trial calculations on well characterized molecules to experimental data or *ab initio* calculations. The set of molecules that is used to extract integral parameters is called the **training set**. The dependence on <u>empirical parameters,</u> which are based on a selected training set, gives a training set dependence that limits the applicability of semi-empirical calculations. In addition, many <u>two-electron integrals</u> are neglected. The general form of a coulomb or exchange integral for atomic orbitals i, j, k, and l is:

$$\int \phi_i(1) \ \phi_j(1) \ \frac{e^2}{4\pi\varepsilon_o r_{12}} \ \phi_k(2) \ \phi_l(2) \ d\tau_1 \ d\tau_2 \qquad\qquad 26.5.13$$

where the four orbitals may be on the same atom or different atoms. To help simplify consideration of these integrals, we represent each atomic orbital by a capital letter and each electron by a number:

$$\int A(1) \ B(1) \ \frac{e^2}{4\pi\varepsilon_o r_{12}} \ C(2) \ D(2) \ d\tau_1 \ d\tau_2 \qquad\qquad 26.5.14$$

Semi-empirical methods differ as to the types of integrals that are neglected. The oldest semi-empirical method in common use, and the most approximate is CNDO. CNDO is an acronym for complete neglect of differential overlap. In the CNDO method an integral is assumed to be zero unless orbitals A and B are identical on the first atom and orbitals C and D are identical on the second atom. Such integrals are called **two-center integrals**, Figure 26.5.2a. For example, orbitals A and B can both be 2s orbitals or both can be 2p orbitals on the same atom.

CNDO: integral zero unless:

A=B   C=D

two-center integrals only

MNDO: integral zero unless:

A, B on   C, D on
same atom   same atom
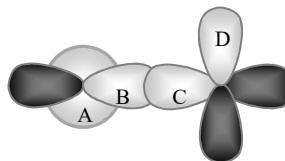
(a). complete neglect of differential overlap   (b). neglect of diatomic differential overlap

Figure 26.5.2: Semi-empirical methods neglect some types of integrals. (a). CNDO includes only integrals with the same orbitals on the first and the same orbitals on the second atom. (b). MNDO methods include integrals with different orbitals on the same atom.

In methods with modified neglect of differential overlap, or MNDO methods, orbitals A and B can be different, but on the first atom, while orbitals C and D can also be different, but on the second atom, Figure 26.5.2b. The AM1 and PM3 methods use MNDO approximations, but the training sets of molecules that are used to determine the parameters are expanded to include a wider diversity. The AM1 training set includes primarily molecules containing C, H, N, and O. The PM3 training set is expanded to include many molecules with Si, P, S, and halogens. PM3 calculations are also useful for calculations involving hydrogen-bonding. ZINDO is parameterized to reproduce electronic spectra of simple organics. No d-orbitals are used unless the method has been specifically expanded, as in MNDO/d, which includes d orbitals for 3rd period representative elements. PM3/TM includes d-orbitals for transition metals.

Semi-empirical calculations on moderate size molecules require at most a few seconds of computer time. However, the training-set dependence and lack of d-orbitals in most semi-empirical methods limits the applicability. Much caution is warranted:

- If your molecule is *similar* to the training set, then the *results may be very good*.
- If your molecule is *significantly different* from the training set, the *results may be very poor*.
- The bonding description can be *useful in aggregate*. Howevernote that:
- Semi-empirical molecular orbital energies can be in the *wrong order*.
- *Results are not useful* for transition states, unstable molecules, and unstable ions.

Semi-empirical methods are not as sensitive to training set bias as molecular mechanics. In general, semi-empirical methods are useful for molecular geometry determinations of stable molecules and ions. However, correlated *ab initio* methods are necessary for excited state, transition state, and thermochemical determinations. Electron-electron correlation plays an important role in the electronic structure of molecules and atoms and is not represented well in semi-empirical calculations.

Density Functional Theory: DFT: The effects of electron correlation are not included in basic Hartree-Fock theory. Configuration interaction approaches are used within the Hartree-Fock framework to include electron correlation (review Section 26.2). However, full CI calculations are time consuming. An alternate approach called **Density Functional Theory**, or **DFT**, has been developed that includes exchange and correlation effects directly.[7] In density functional theory, the electronic energy is given as the sum of the kinetic energy of the electrons, the potential energy of attraction of the electrons for the nuclei, the Coulomb repulsion of the electrons for each other, and finally the exchange-correlation energy:

$$E = E_T + E_V + E_J + E_{xc} \qquad 26.5.15$$

kinetic + e-n *attraction* + *Coulomb* e-e *repulsion* + *exchange-correlation energy*

The kinetic, electron nuclear attraction, and electron-electron repulsion terms are essentially the same as Hartree-Fock theory. In DFT theory, however, the exchange and electron correlation terms are included in the exchange-correlation energy, E_{xc}. In DFT, the one-electron Fock operator is given as:

$$f_1 = h_1 + \sum_{j=1}^{n/2} \{2J_j(1) - V_j^{XC}(1)\} \qquad 26.5.16$$

where $V_j^{XC}(1)$ is the potential energy that results from both the exchange and correlation interactions. In this way, electron correlation is included as an inherent and central part of the molecular orbital energy. E_J, E_{XC}, and $V_j^{XC}(1)$ are taken as a function of the electron density:

$$\rho(r) = 2 \sum_{i=1}^{n/2} |\Psi_i(r)|^2 \qquad 26.5.17$$

The sum is taken over all occupied molecular orbitals. Assuming the functional dependence on the electron density rather than the wave function itself results in some computational simplifications. The electron density is a point-to-point measure of the probability of finding the electron. The electron-nuclear Coulomb interaction is essentially equivalent between Hartree-Fock and DFT methods. Formally, the exchange-correlation potential is the derivative of the exchange-correlation energy with respect to the electron density:

$$V_j^{XC}(1) = \frac{\partial E_{XC}[\rho(r)]}{\partial \, \rho(r)} \qquad 26.5.18$$

The derivative of a function with respect to another function is called a functional derivative. The change in the exchange-correlation energy as the density of the electrons in the molecular orbitals changes gives the exchange-correlation potential energy. The electron density cannot be determined exactly, just as in Hartree-Fock theory. DFT theory is similar to Hartree-Fock theory in many respects. However, the DFT approach gives a different point of departure for approximation methods.

One specific problem that has been treated to a very high level of approximation is the **uniform electron gas** (using quantum Monte Carlo simulations). A uniform electron gas is an infinitely large container filled with electrons that interact with a completely delocalized and uniform equal positive charge. The gas is electrically neutral, but the positive charge is "smeared out" instead of being localized in multiple nuclei. The results describe the response of the electron gas when the electron density is changed at some particular spot, r. For example, if the electron density is decreased at r, then electron-electron repulsions are decreased at that spot and the electron density relaxes about r, Figure 26.5.3. In other words, a change in electron density at one spot causes a correlated motion of all the other electrons as the gas adjusts to the change. One approach to density functional calculations is to "wrap" this correlation around the nuclei of the molecule under study.

change the electron density at one point, r

difference density
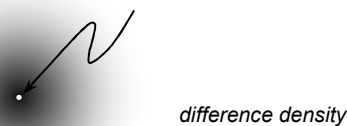
Figure 26.5.3: The response of the electron density of the uniform electron gas as the electron density at a point r is changed. The electron motion is correlated; the change in electron density at one point is reflected in changes in electron density remote to the change.

Using the uniform electron gas as a model for electron correlation results in the "local" density approaches that are the basis for LSDA/VWN level approximations (LSDA is an acronym for local spin density approximation). Many more accurate extensions have also been implemented, Table 26.5.1. In most discrete molecule DFT methods, the initial approximation of the electron density is calculated using a Hartree-Fock calculation. Then the exchange-correlation potential is calculated at some level of approximation and an improved electron density distribution is determined. However, this approach gives an approximation of both the exchange and correlation energies. One advantage of the Hartree-Fock approach is that the exchange energy is exact, assuming that the exact wave function is known. Several "hybrid" methods are commonly used that combine the "exact" exchange energy from the Hartree-Fock calculation with the exchange-correlation energy from the DFT calculation. One of the most commonly used DFT methods is such a **hybrid functional**, **B3LYP**. The B3 results from the use of three empirical parameters that are used to combine the Hartree-Fock exchange term with the DFT exchange-correlation interaction.

Table 26.5.1: Source of the Coulomb, Exchange, and Correlation terms in DFT methods.

Functional	Source of Coulomb and Exchange Energies
"Pure": LSDA/VWN, BP, BLYP, EDF:	HF Coulomb, DFT exchange-correlation
"Hybrid": B3LYP, MO6, APFD:	HF Coulomb and exchange, DFT correlation

The world of molecular structure methods can be a daunting welter of acronyms, however the point is to appreciate the strengths and weaknesses of the general method types. Density functional methods are in general more accurate than Hartree-Fock methods, because DFT methods include electron correlation in addition to exchange. Hartree-Fock methods give exact exchange, assuming the exact wave function is known. Hybrid functionals are commonly used to take the best advantage of a melding of Hartree-Fock exchange with density functional exchange-correlation. However, advanced correlated methods, such as CISD and CISDT, are generally considered to be superior to B3LYP, though slower. **Coupled cluster** methods, CCSD, CCSD(T), and CCSDT, use the same philosophy as the corresponding CI method, but have been optimized for computational efficiency.[6] CCSD(T) is commonly used, which makes a strategic choice of a subset of all possible triple excitations. CCSD(T) is faster than CCSDT. With appropriate computational models in hand, we are now ready to study polyatomic molecules.

26.6 Bonding in Polyatomic Molecules

Linear BeH$_2$, triplet CH$_2$, NH$_2$, and H$_2$O: *An Initial Model*:   The bonding in polyatomics is an extension of the techniques we have discussed so far. A valid set of molecular orbitals is based on the following principles:

  1. LCAO approach
  2. Combination of AOs with good overlap and similar energy (orbitals that can overlap, will)
  3. Number of AOs = number of MOs
  4. MOs must have the same symmetry as the molecule

The second-period triatomic hydrides are a good first example. We begin with the linear geometry, Figure 26.6.1. The linear geometry applies to BeH$_2$, triplet CH$_2$ (methylene triplet

radical), and linear models for NH_2 and H_2O. The 1s-orbital on the central atom is a low energy core orbital and is not shown on the MO diagram. We consider only the valence orbitals on the central atom. Counting the 2s, $2p_x$, $2p_y$, and $2p_z$ on the central atom and the 1s on each H, there are six valence atomic orbitals. We correspondingly need to find six molecular orbitals. We choose the internuclear axis as the x-axis, for convenience. The lowest energy molecular orbital combines the in-phase combination of the s-orbitals on each atom. The MO is cylindrically symmetrical about the internuclear axis, giving a σ-bonding orbital: $\sigma_1 = 1s_H + 2s_A + 1s_H$.
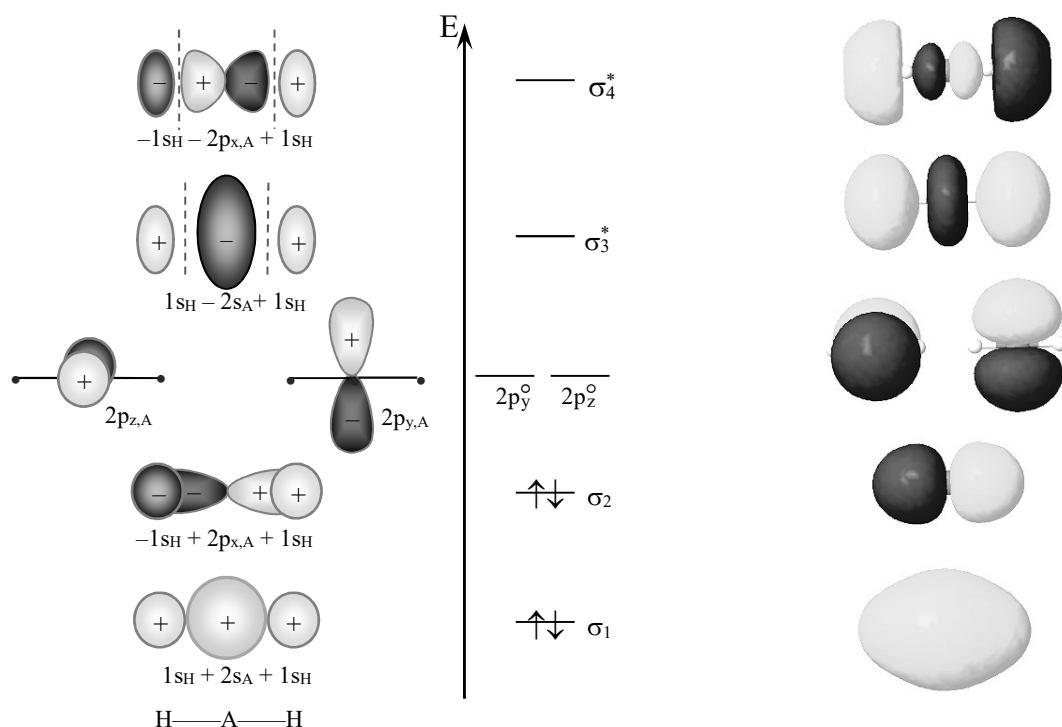
Figure 26.6.1: Linear models for 2nd-period hydrides: BeH_2, triplet CH_2, NH_2, and H_2O. Computed orbital isodensity surfaces are shown on the right. The orbital filling is for BeH_2.

Two procedures are helpful for the diagrammatic development of a complete set of molecular orbitals. The first is to consider changing the sign of the <u>central</u> atomic orbital. The second is to consider changing the sign of one of the <u>outer</u> orbitals. For example, changing the sign of the central 2s-orbital in σ_1 gives the anti-bonding complement, $\sigma_4^* = 1s_H - 2s_A + 1s_H$. Changing the sign of one of the outer 1s-orbitals gives an antisymmetric combination that has the proper phases to combine with a p-orbital on the central atom. By convention, a positive p-orbital has the positive-phase lobe pointing in the positive x-direction, Figure 26.6.2a. The combination of the H-atom 1s-orbitals with a p-orbital on the central atom gives the second σ-bonding orbital: $\sigma_2 = -1s_H + 2p_{x,A} + 1s_H$.

The antisymmetric combination of the outer 1s-orbitals cannot combine with the central 2s-orbital, because the linear combination is anti-bonding on the left and bonding on the right. The second-period hydrides are symmetric, the left and right bonds are equivalent. Therefore, the proper molecular orbitals must also have equivalent character, left and right. A valid molecular orbital must be bonding left and right or anti-bonding left and right, Figure 26.6.2a.
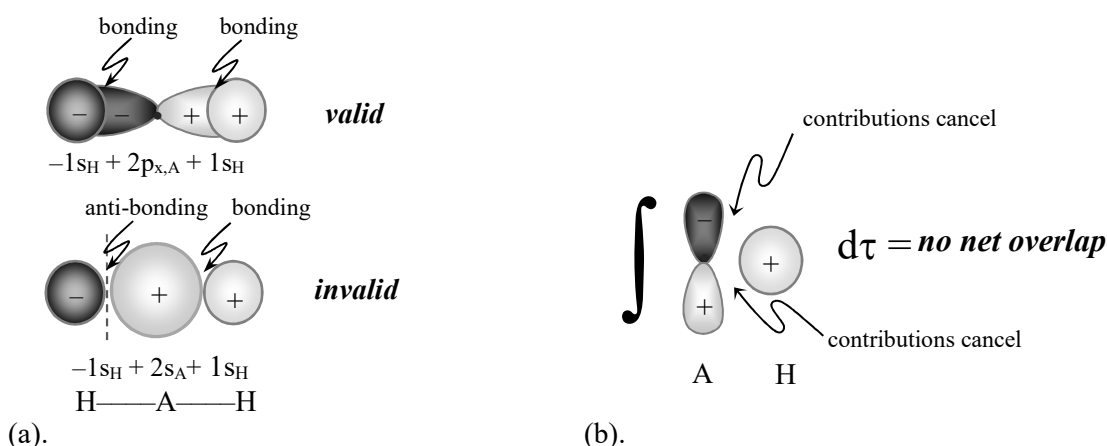
Figure 26.6.2: (a). Molecular orbitals must have the same symmetry as the molecule. Since BeH$_2$ has equivalent bonds, the valid molecular orbitals must have the same character left and right. (b). Out-of-plane p-orbitals give no net overlap with the 1s-orbitals.

For further discussion, it is helpful if the orbitals are given unique symbols, Figure 26.6.3. Rotation and inversion symmetry are applied as for diatomics. However, the bonding and anti-bonding character is specified with respect to the overall number of pairwise bonding and anti-bonding interactions, rather than reflection symmetry. The orbitals are numbered sequentially within each symmetry class, starting with the core orbitals. The lowest energy orbital is the 1s-core orbital on the central atom, which transforms as σ_g. This 1s-core orbital is designated $1\sigma_g$, giving the σ_g-bonding orbital resulting from overlap with the 2s-orbital as $2\sigma_g$. The non-bonding orbitals have π-symmetry because they are perpendicular to the internuclear axis.

With two valence electrons on Be and one each on H, the electron configuration fills $1\sigma_u$. Assuming a linear geometry, the configurations for some additional second-period triatomic hydrides are given in Figure 26.6.3. The total bond order of BeH$_2$, CH$_2$ and H$_2$O is each two, giving an equivalent single-bond on each side of the molecules. The non-bonding electrons don't contribute to the bond order, because they are non-interacting. Methylene, CH$_2$, has two parallel electrons in the singly occupied non-bonding orbitals, which results in triplet spin multiplicity. The experimental structures for BH$_2$, CH$_2$, NH$_2$, and of course H$_2$O are all bent. Our linear models are a good point of comparison with the bent models that we now construct.
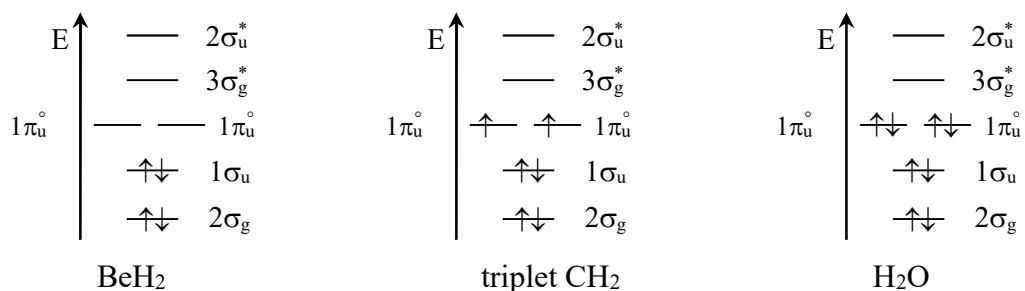
Figure 26.6.3: Linear models for the second period triatomic hydrides. The experimental bond angles are: BeH$_2$ (180°), triplet CH$_2$ (133.84±0.05°), and H$_2$O (104.5°).

Using the same principles that we developed for linear AH_2, the molecular orbitals for a 90°
bond angle are shown on the right in Figure 26.6.4. The molecular orbitals for linear AH_2 are
redrawn on the left for comparison. Each molecular orbital must involve both of the 2p-orbitals
that are in the bonding plane to maintain the symmetry of the molecule; the bonding plane is the
plane of the paper. The molecular orbitals must be three-center orbitals. To have the same
symmetry as the molecule, valid molecular orbitals must be either symmetric or antisymmetric
with respect to each of the symmetries of the molecule.

symmetry	rotate 180°	reflect across σ_v
symmetric	a	1
antisymmetric	b	2
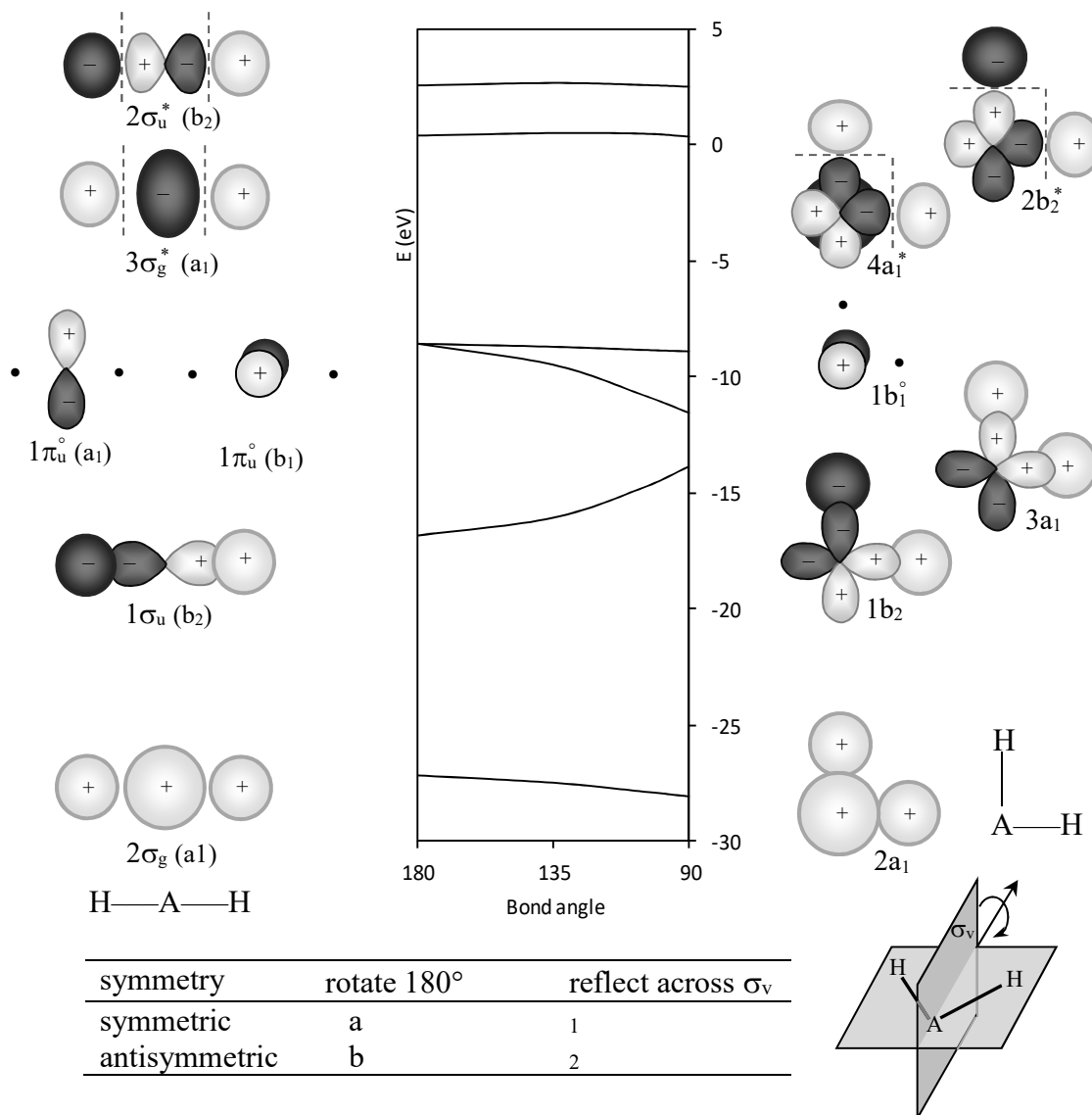
Figure 26.6.4: Walsh diagram for triatomic hydrides. Orbitals of the same symmetry
correlate. The symmetry is determined by rotation about the two-fold axis by 180° and
reflection across the vertical plane that bisects the bond angle, σ_v. (See Figure 26.4.5a.)

The symmetry in bent molecules is determined by rotation about the two-fold axis by 180° and
reflection across the vertical plane, σ_v, that bisects the bond angle. The symmetry axis lies in the
bonding plane and bisects the bond angle, Figure 26.6.4. If the orbital phase is unchanged upon

rotation, then the orbital is symmetric with respect to the rotation and is an "a" orbital. Antisymmetric orbitals with respect to rotation are designated "b". Orbitals that are symmetric with respect to reflection are designated with a "1" subscript. Antisymmetric orbitals with respect to reflection are designated with a "2" subscript. The lowest energy orbital is the 1s-core orbital on the central atom, which transforms as a_1. This 1s-core orbital is $1a_1$, giving the bonding orbital resulting from overlap with the 2s-orbital as $2a_1$.

Walsh Diagrams Predict the Equilibrium Bond Angle: The changes in orbital energies determine the lowest energy structure and the corresponding equilibrium bond angle. Figure 26.6.4 is an example of a **Walsh diagram**.[8] Molecular orbital energies are plotted as a function of bond angle for pairs of correlated orbitals. Correlated orbitals are matched by symmetry. That is, if the linear orbitals are reclassified according to the symmetry operations of the bent molecule, then the orbitals occur in pairs with the same symmetry, Figure 26.6.5a. This reclassification is listed in parentheses in Figure 26.6.4. The energies change smoothly as the bond is bent. Upon bending, orbitals of a_2 or b_2 symmetry have a node that decreases electron density between the H-atoms and destabilizes the orbital. Orbitals with a_1 or b_1 symmetry give constructive overlap that increases the electron density between the H-atoms and stabilizes the orbital, Figure 26.6.5b.

   In establishing the correlated orbital pairs, some ambiguity can result. For example, the $2\sigma_g - 2a_1$ and $1\pi_u^\circ - 3a_1$ pairs have the same a_1 symmetry. How do we know that the correlation is not $2\sigma_g - 3a_1$ and $1\pi_u^\circ - 2a_1$? Calculations at small angle increments allow the energies of the orbitals to be followed in detail, which results in the **non-crossing rule**. Orbital energies of the same symmetry do not cross. This rule allows ambiguities to be resolved. The pairings $2\sigma_g - 3a_1$ and $1\pi_u^\circ - 2a_1$ are not valid because the energy curves cross upon bending. In summary:

   1. Orbital energies vary smoothly with bond angle.
   2. Orbitals of the same symmetry correlate.
   3. Orbital energies of the same symmetry do not cross (non-crossing rule).
   4. Orbitals with a node between the two outer atoms increase in energy upon bending.

| (a). Orbital correlation | (b). Energy changes |
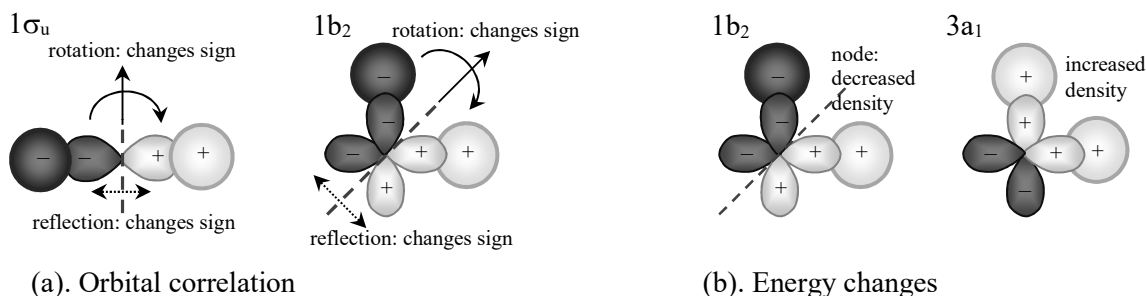
Figure 26.6.5: Orbital correlations for the $1\sigma_u$–$1b_2$ pair. (a). The symmetry of the linear $1\sigma_u$ orbital transforms as b_2 with respect to rotation about the symmetry axis and reflection across the σ_v plane that bisects the bond angle. (b). Upon bending, the energy of a_2 and b_2 orbitals increase, while the energy of a_1 and b_1 orbitals decrease.

   The Walsh diagram allows the equilibrium bond angles of the second-period hydrides to be predicted. With four valence electrons, BeH_2 fills the molecular orbitals up to $1\sigma_u$, Figure 26.6.3. As the bond angle is bent, the $2\sigma_g(a_1)$ orbital drops in energy and the $1\sigma_u(b_2)$ orbital increases in

energy, giving no net energy change. BeH_2 is then predicted to be linear. For methylene, CH_2, the linear model gives a triplet state, Figure 26.6.3. As the bond is bent, the $1\pi_u(b_1)$ orbital remains essentially an atomic 2p-orbital with little change in energy. The $1\pi_u(a_1)$ orbital drops in energy upon bending. The net decrease in energy of the $1\pi_u$–$3a_1$ pair causes the equilibrium bond angle to bend, but not so much that the electrons are forced to spin-pair in the $3a_1$ orbital to give a singlet state, Figure 26.6.6a.

(a). Triplet and singlet CH_2 (b). H_2O
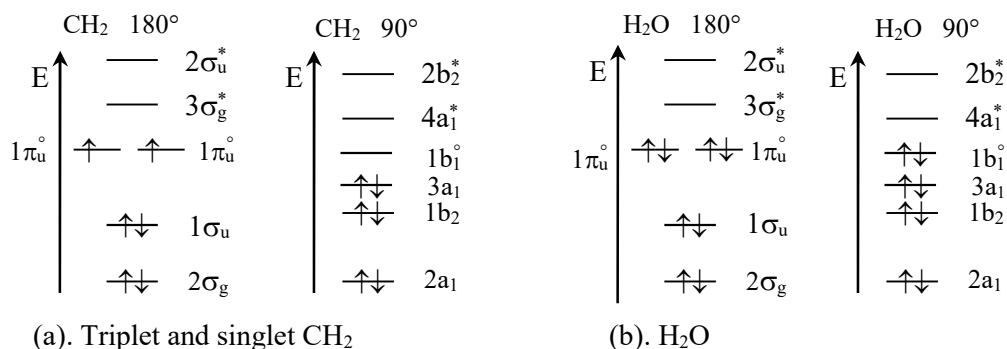
Figure 26.6.6: Comparison of linear and bent models for CH_2 and H_2O. Triplet-CH_2 is stabilized by the exchange interaction, while H_2O is stabilized by bending.

The half-filled orbitals are maintained so that electron-electron repulsion is minimized with a bond angle slightly less than 180°. The experimental bond angle for the triplet state is 133.1°. The minimum energy bond angle is 137.8° at B3LYP/6-311G**. The singlet state is an excited state, and because both electrons are in the $3a_1$ orbital, the bond angle is predicted to be close to 90°. The experimental bond angle for the excited singlet state is 101.5° and the singlet state is 0.42 eV, 41 kJ mol^{-1}, higher in energy than the triplet state.

H_2O is Bent: Water has eight valence electrons, which fill through the non-bonding $1b_1$ state. With no energy penalty for spin pairing, as in triplet-CH_2, the overall energy is decreased by bending the bond to small angles. Three of the occupied orbitals decrease in energy on bending, while only the $1b_2$ energy increases. The HOMO is a non-bonding, essentially atomic 2p orbital. The Lewis dot structure for H_2O suggests two equivalent non-bonding pairs, $H_2\ddot{O}$:. However, the MO diagram shows the non-bonding electrons to be a core 1s-orbital on O and the HOMO, which is an atomic 2p orbital. The MO energy ordering predicted by molecular orbital theory is significantly different than the Lewis dot prediction. Building on the success of the MO description of the triatomic hydrides, we next consider non-hydrogen triatomics.

CO_2 has 3-Center π-Orbitals: The molecular orbitals for CO_2 are built using the same guidelines. The 1s-orbitals on each atom give a low energy set of molecular orbitals: a bonding, non-bonding, and anti-bonding set: $\circ\circ\circ$ ($1\sigma_g$), $\circ-\bullet$ ($1\sigma_u$), and $\circ\bullet\circ$ ($2\sigma_g^*$). In combination, these three orbitals have no net effect on the bonding. As a consequence, the 1s-orbitals are considered to be a filled set of low-energy core orbitals. The 12 valence atomic-orbitals then combine to give 12 molecular orbitals, Figure 26.6.7a. The O(2s) atomic orbitals are much lower in energy than the C(2s) and have minimal interactions. We assign the in-phase $3\sigma_g^\circ$ and out-of-phase $2\sigma_u^\circ$ combinations of the O(2s)-orbitals as core non-bonding orbitals. The x-axis is assigned as the internuclear axis for convenience. The lowest energy bonding orbital in CO_2 is the in-phase combination of the O($2p_x$) orbitals and the central C(2s) orbital, $\Psi_{4\sigma_g} = p_{x,O} + s_C - p_{x,O}$.

Changing the phase of the central orbital gives the anti-bonding complement, $5\sigma_g^*$. The next bonding orbital is the in-phase combination of the $O(2p_x)$ and $C(2p_x)$ orbitals, $\Psi_{3\sigma_u} = -p_{x,O} + p_{x,C} - p_{x,O}$. Changing the phase of the central p_x-orbital gives the anti-bonding complement, $4\sigma_u^*$. We next consider the p-orbitals that are perpendicular to the internuclear axis, which combine to give doubly degenerate bonding and anti-bonding pairs $1\pi_u(2p_y)$, $1\pi_u(2p_z)$, and $2\pi_u^*(2p_y)$, $2\pi_u^*(2p_z)$.
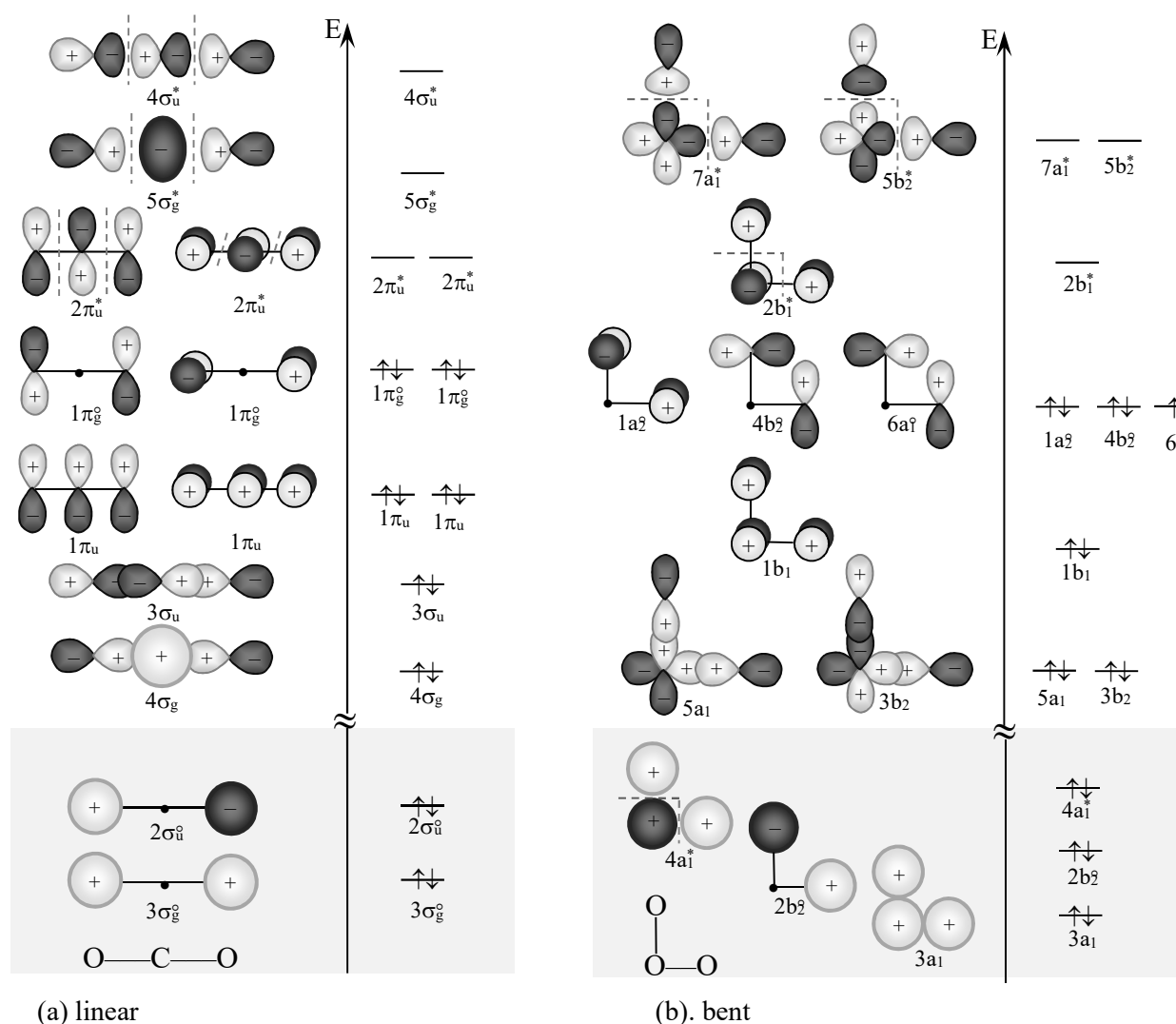
Figure 26.6.7: Molecular orbitals for linear and bent XY_2. The electron filling is shown for linear CO_2 and bent O_3. Net non-bonding core-orbitals are shown on the gray background.

The molecular orbitals are three-center orbitals. Neither the σ nor π-orbitals are localized between only two atoms. At this point, we have found only ten molecular orbitals. The two remaining orbitals are obtained by changing the sign of one of the outer orbitals in the π-set. The result has no possible orbital on the central atom that gives net overlap with a bonding pattern that is symmetrical left and right. These two remaining orbitals are then degenerate non-bonding orbitals with π-symmetry, $1\pi_g^\circ(2p_y)$ and $1\pi_g^\circ(2p_z)$. CO_2 has 16 valence electrons that fill through the non-bonding π-orbitals. The molecular orbital result is consistent with the Lewis dot structure, a net total qualitative bond order of four with four non-bonding pairs, $\cdot\ddot{O}=C=\ddot{O}\cdot$. The

diagram also applies in general to XY_2 triatomics, where X and Y are non-hydrogen elements. Ozone, for example, has two additional valence electrons, which extends the filling to give two unpaired electrons in the degenerate $2\pi_u^*$ anti-bonding levels. Linear ozone is then predicted to have triplet spin multiplicity. We next consider the bent model for XY_2.

Is Ozone Linear or Bent?   Now consider bent ozone. The 2s-orbitals on each O-atom in ozone are, of course, the same energy. Compared to CO_2, the central O(2s) orbital joins the 2s-orbitals on the outer atoms to give a bonding $3a_1$, non-bonding $2b_2^\circ$, anti-bonding $4a_1^*$ set, which together give no net contribution to the bonding. We can consider these three 2s-based molecular orbitals as core orbitals, Figure 26.6.7b. The remaining molecular orbitals are constructed using the same principles as for bent AH_2. The symmetry of the molecular orbitals is also designated using the same labeling rules as for bent AH_2, Figure 26.6.4. Correspondingly, the general trend is for a_1 and b_1 orbitals to decrease in energy upon bending and for a_2 and b_2 orbitals to increase in energy upon bending. We can now consider if O_3 is linear or bent, Figure 26.6.8.
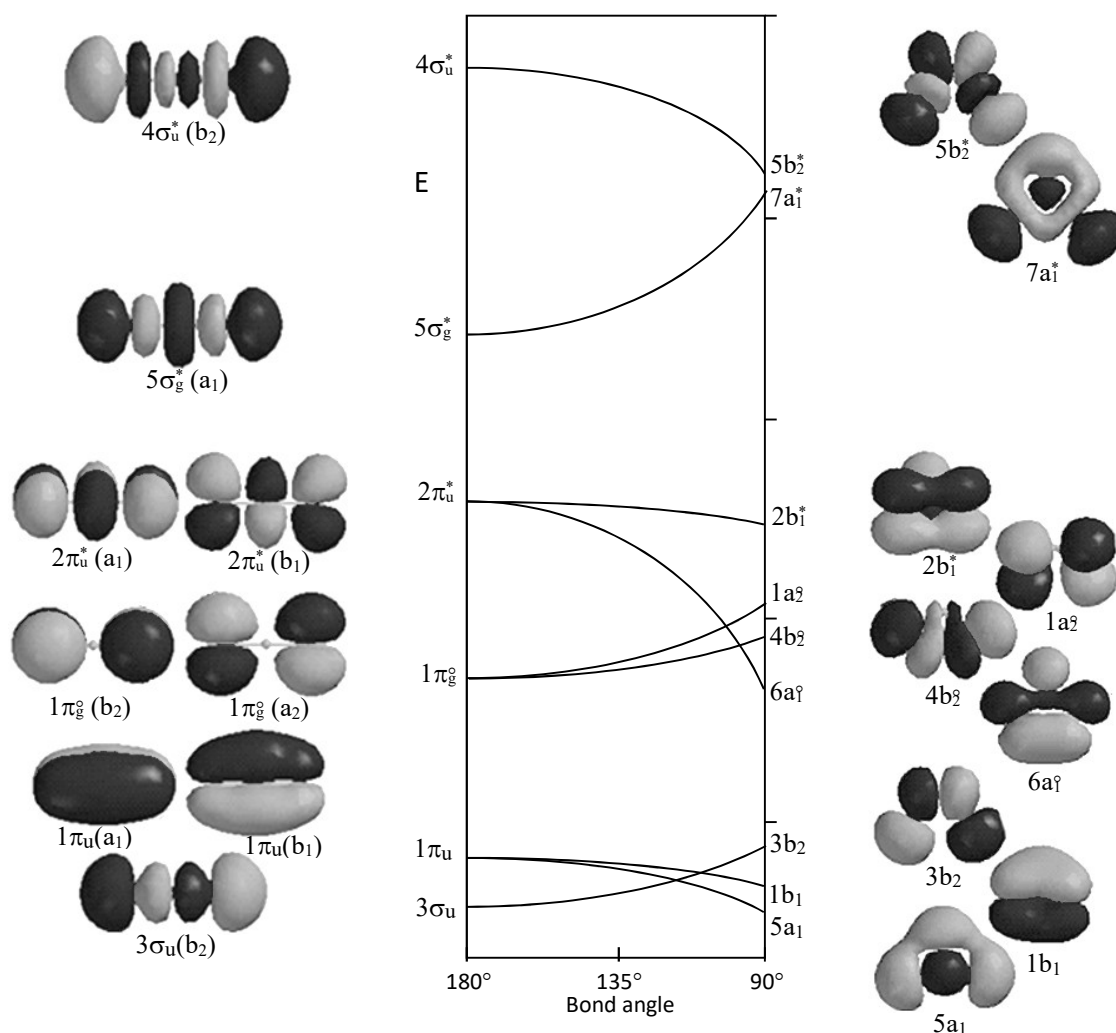
Figure 26.6.8: Walsh diagram for XY_2 molecules. The 2s-based orbitals are not included for simplicity. The symmetry of the linear orbitals, using the symmetry transformations of the bent molecule, are given in parenthesis. For example, the $3\sigma_u$ orbital is antisymmetric with respect to both two-fold rotation and reflection across the σ_v plane, which corresponds to b_2.

The Walsh diagram for linear and bent ozone shows the biggest change in energy for the in-plane $2\pi_u^* - 6a_1^\circ$ correlation.[9] The $6a_1^\circ$ orbital is a σ-non-bonding orbital with all p character. In the extreme 90° structure, the $6a_1^\circ$ orbital has some bonding character that corresponds to the cyclic Lewis resonance structure:

$$26.6.1$$
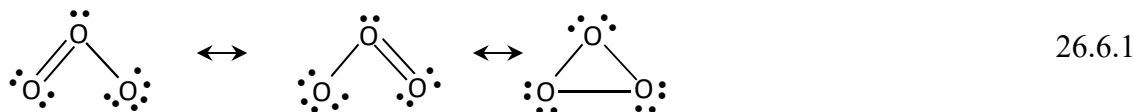
This additional overlap makes the $6a_1^\circ$ orbital the lowest energy non-bonding orbital. Upon bending, four occupied orbitals decrease and three occupied orbitals increase in energy, which favors the bent structure. In addition, the decrease in energy of the $6a_1^\circ$ orbital is so favorable that the electrons pair to give double occupancy of the $6a_1^\circ$ orbital and a corresponding singlet state. A doubly occupied $6a_1^\circ$ favors the bent molecule.

The O_3 Walsh diagram is also applicable to other XY_2 molecules and ions. Predictions for the geometry of the triatomics are summarized by **Walsh's Rules**, which are based on the occupancy of the non-bonding and anti-bonding orbitals in the XY_2 Walsh diagram, Figure 26.6.9

Electrons:	16	17	18	19	20	22
	O=C=O	NO_2	O_3	ClO_2	OF_2	F-Kr-F
		NO_2^-			ClO_2^-	F-Xe-F
		SO_2	BrO_2	BrO_2^-	$[I\text{-}I\text{-}I]^-$
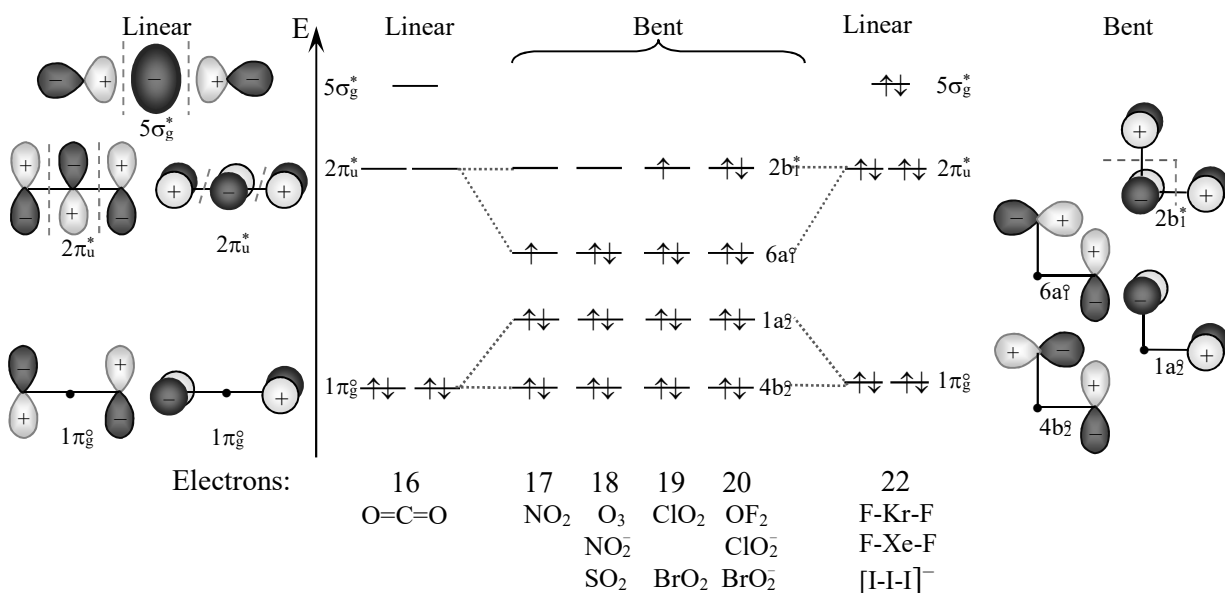
Figure 26.6.9: Walsh's Rule Predictions: The number of valence electrons determines the correlated MO pairs that have the predominant influence. Up to 16 electrons gives a linear molecule. For 17-21 electrons, the $2\pi_u^* - 6a_1^\circ$ pair gives preference for bent molecules. For 22 electrons, the $5\sigma_g^*$ increases rapidly with bending, giving a linear molecule.

The Walsh diagrams that we have presented are schematic. The diagrams seek to generalize the behavior of many different molecules in a single diagram. However, the details differ with spin multiplicity. CH_2 and O_3 are triplets when linear and singlets when bent. For molecules that change multiplicity upon bending, two sets of curves are necessary, one for the triplet state and one for the singlet state. The generalized curves we have presented are averages over both multiplicities. On the other hand, linear and bent H_2O and OF_2 are singlets, giving a single set of curves for each symmetry pair. Careful calculations, including configuration interaction, are

208

necessary to find the equilibrium bond angle of each specific case. However, the generalized Walsh diagrams provide a point of reference for the interpretation of individual cases. The Walsh diagrams also demonstrate the influence of atomic orbital overlap on molecular structure.

26.7 Hybridization

Hybridization Combines Atomic Orbitals to Maximize Overlap: Determining the molecular orbitals of complex molecules is straightforward. However, the σ-bond framework of stable molecules and ions is sufficiently *pro forma* that careful molecular orbital descriptions are often not required. Instead, the concept of hybridization has been developed to provide an adequate description of the bonding in simple systems. The results are sufficiently equivalent to a full MO approach in many regards and are considerably easier to visualize. The concept was developed by Linus Pauling. As a first step, atomic orbitals on each central atom are combined to give a set of **hybrid atomic orbitals** that are equivalent in energy and shape. The hybrid atomic orbitals are geometrically disposed to maximize overlap with adjacent atoms. The overlap of the hybrid atomic orbitals on adjacent atoms creates bonding and anti-bonding pairs of localized molecular orbitals that form the σ-framework of the molecule. The concept is summarized as:

Bonds form in the direction of maximum overlap.

Consider BeH_2 as an example. First focus on the central atom, Be. The low lying orbitals are 2s, $2p_x$, $2p_y$, and $2p_z$. The x-axis is assigned as the internuclear axis. The $2p_x$-orbital is oriented favorably for overlap with the H-atoms. The two hybrid atomic orbitals that combine the 2s and $2p_x$-orbitals with equal weight are called sp-hybrids:

$$\Psi_{sp,a} = {}^1/_{\sqrt{2}} (s + p_x) \qquad\qquad \Psi_{sp,b} = {}^1/_{\sqrt{2}} (s - p_x) \qquad\qquad 26.7.1$$

The positive lobes of the 2s and $2p_x$ orbital add to increase the wave function amplitude to the right for $\Psi_{sp,a}$ and to the left for $\Psi_{sp,b}$, compared to the 2s or $2p_x$ alone, Figure 26.7.1a. The $\sqrt{2}$ maintains normalization.

(a).   (b).
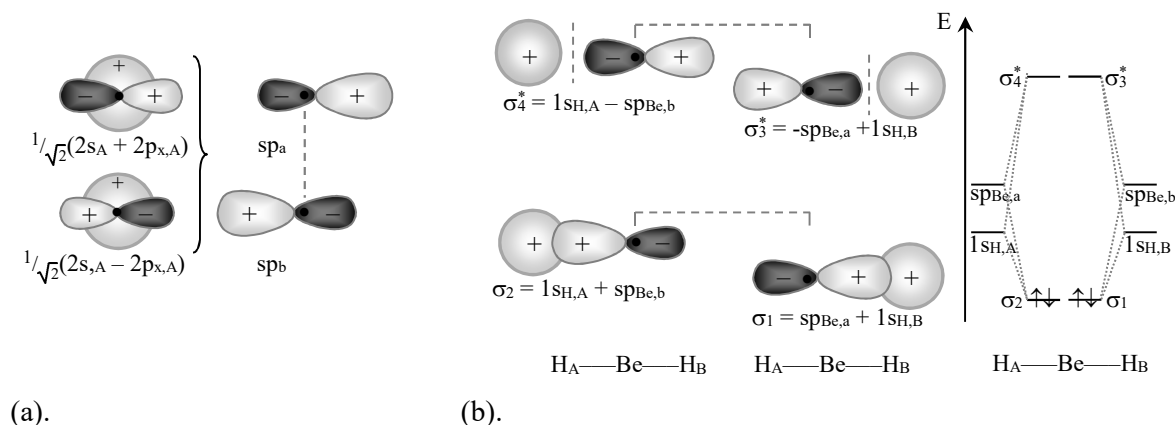
Figure 26.7.1: (a). sp-Hybridized atomic orbitals are linear. (b). The orientation of the hybrids maximizes overlap with adjacent atomic orbitals to form bonding and anti-bonding pairs of localized molecular orbitals. The non-bonding $Be(2p_y)$ and $Be(2p_z)$ are not shown.

The two sp-hybrids are the same size, shape, and energy. The two differ only in orientation, with the hybrids disposed for optimal overlap with a bond angle of 180°. The energy of the hybrids is the average of the 2s and 2p-orbitals. Four localized molecular orbitals are constructed from the in-phase and out-of-phase overlap of the hybrids with 1s-orbitals on the adjacent H-atoms, Figure 26.7.1b. Comparison with the molecular orbital diagram in Figure 26.6.1 shows an equivalent net overlap, bond order, and <u>overall</u> energy. However, the true molecular orbitals are not degenerate. Hybridization is not useful for determining the energetic details of molecular orbitals. In addition, the true σ-bonds in BeH$_2$ are three-center bonds. The σ-electrons are not localized between atom pairs. In summary, the hybridization scheme is deficient in several important respects, but the ease of visualization of the orbitals is a compensating factor.

  The radial portion of an sp-hybrid along the internuclear axis is shown in Figure 26.7.2. The negative lobe is only 25-30% smaller than the positive lobe. General Chemistry texts often overemphasize the difference in extent of the two lobes. Notice also that the nucleus is in the negative lobe; the nucleus is at r = 0. The nucleus does not sit on the node. The hybrid orbitals are atomic orbitals; as such they must be orthogonal and normalized. Taking the square of $\Psi_{sp,a}$, Eq. 26.7.1, and integrating gives the normalization integral as:

$$\int \Psi_{sp,a}^2 \, d\tau = \frac{1}{2} \int (s^2 + 2\, sp_x + p_x^2)\, d\tau = \frac{1}{2}\left[\int s^2\, d\tau + 2 \int sp_x\, d\tau + \int p_x^2\, d\tau \right] = 1 \qquad 26.7.2$$

$$\underset{1}{\uparrow} \qquad \underset{0}{\uparrow} \qquad \underset{1}{\uparrow}$$

The first and last integrals are atomic normalization integrals; the original atomic orbitals are assumed to be normalized. The middle integral is zero because of orthogonality; the s and p$_x$ orbitals are on the same nucleus. The sp-atomic hybrids are normalized. The orthogonality integral between the two sp-hybrids is zero:

$$\int \Psi_a \Psi_b \, d\tau = \frac{1}{2} \int (s + p_x)(s - p_x)\, d\tau = \frac{1}{2} \int (s^2 - p_x^2)\, d\tau = \frac{1}{2}\left[\int s^2\, d\tau - \int p_x^2\, d\tau \right] = 0 \qquad 26.7.3$$

$$\underset{1}{\uparrow} \qquad \underset{1}{\uparrow}$$

given that the s and p$_x$ orbitals are normalized. The sp-hybrids are 50% s-character and 50% p-character, giving linear electron domain geometry, Figure 26.7.3a.
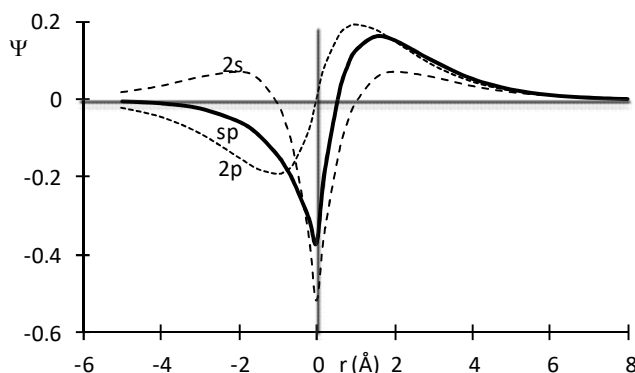
Figure 26.7.2: The radial portion of the sp hybrid, $\Psi_{sp,a} = 1/\sqrt{2}\ (2s + 2p_x)$, along the x-axis. The 2s-orbital is shown with the central lobe with negative phase. (2s-orbital – – –, 2p$_x$ ----, sp-hybrid ——).

Different Hybrids Give Different Bond Angles: Mixing M atomic orbitals gives M orthonormal hybrid atomic orbitals. The sp²-hybrid atomic orbitals have 66.7% p-character. Once the orientation of the first hybrid is chosen, the remaining hybrids are fixed by orthogonality. The first sp²-hybrid is arbitrarily chosen to lie along the x-axis:

$$sp^2: \quad \Psi_{sp2,a} = \frac{1}{\sqrt{3}} s + \frac{\sqrt{2}}{\sqrt{3}} p_x$$

$$\Psi_{sp2,b} = \frac{1}{\sqrt{3}} s - \frac{1}{\sqrt{6}} p_x + \frac{1}{\sqrt{2}} p_y$$

$$\Psi_{sp2,c} = \frac{1}{\sqrt{3}} s - \frac{1}{6} p_x - \frac{1}{\sqrt{2}} p_y \qquad\qquad 26.7.4$$

The squares of the s and p-coefficients give 33.3% s and 66.7% p-character. All three hybrids lie in the x-y plane. The orientation of the hybrids is determined by the coefficients of the p-orbitals, Figure 26.7.3b. The vector representing $\Psi_{sp2,a}$ is of length $\sqrt{2}/\sqrt{3}$ in the x-direction. The vector representing $\Psi_{sp2,b}$ has a component of $-1/\sqrt{6}$, along the x-axis and $1/\sqrt{2}$ along the y-axis. The vector representing $\Psi_{sp2,c}$ has a component of $-1/\sqrt{6}$ along the x-axis and $-1/\sqrt{2}$ along the y-axis. The resulting angle between the hybrids is 120°. Bonding or non-bonding electrons may occupy hybrid atomic orbitals. Ozone may be thought of as sp² hybridized, O=Ö–O ↔ O–Ö=O. Other substances adopting sp² hybridization include BF_3, NO_2, CO_3^{2-}, NO_2^-, and $H_2C{=}O$.

(a). sp-hybrids   (b). sp²-hybrids   (c). sp³-hybrids
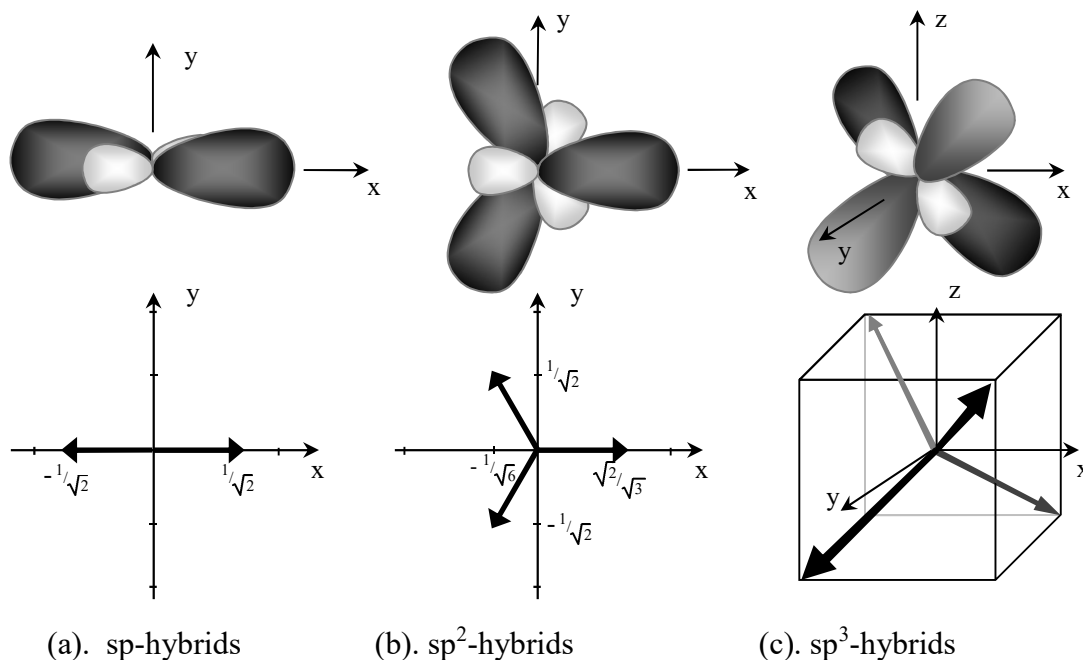
Figure 26.7.3: The orientation of a hybrid is given by the direction-vectors based on the p-orbital coefficients.

The sp³-hybrid atomic orbitals have 75% p-character. The first sp³-hybrid is arbitrarily chosen to point to the corner of a cube at (x,y,z) = (+½, +½, +½):

sp^3: $\Psi_{sp^3,a} = \frac{1}{2}\,(s + p_x + p_y + p_z)$

$\Psi_{sp^3,b} = \frac{1}{2}\,(s - p_x + p_y - p_z)$

$\Psi_{sp^3,c} = \frac{1}{2}\,(s + p_x - p_y - p_z)$

$\Psi_{sp^3,d} = \frac{1}{2}\,(s - p_x - p_y + p_z)$ 26.7.5

The squares of the s and p-coefficients give 25% s and 75% p-character. The direction vectors representing the hybrids point to the corners of the cube shown in Figure 26.7.3c. The resulting shape is a tetrahedron with the well known tetrahedral bond angles of 109.5° (109°28"). Substances adopting sp^3 hybridization include CH_4, NH_3, H_2O, PO_4^{3-}, SO_4^{2-}, ClO_4^{-}.

Hybridization applies primarily to second-period elements, because of small atomic radius. Elements from the third and higher periods are much less likely to hybridize. For example, the bond angles in PH_3 and H_2S are near 90°, Table 26.7.1. The molecule orbitals in PH_3 and H_2S result from the direct overlap of the p_x, p_y, and p_z orbitals on the central atom with $H(1s)$-orbitals. Third period atoms are much bigger than the second period elements, which decreases electron crowding and electron-electron repulsion. The designation p^3 is used to describe bonding that is close to 100% p-character on the central atom. In other words, p^3 indicates that the central atom is not hybridized.

The sp, sp^2, and sp^3 hybrids are idealized. Intermediate hybridizations are routine. **Valence shell electron pair repulsion theory**, VSEPR, predicts that non-bonding pairs of electrons have a larger extent than bonding pairs. For a bonding pair, a positively charged nucleus is situated at each end of the bond. For a non-bonding pair, a nucleus is at only one end of the hybrid atomic orbital. Electrons in bonding orbitals feel a large effective nuclear charge, which contracts the bonding orbital. The larger extent for non-bonding electrons increases electron repulsion with electrons in other hybrid orbitals on the same nucleus. For example, for $:NH_3$ the electron domain geometry is tetrahedral with sp^3 hybridization. However, one of the hybrids is occupied with a non-bonding pair, which forces the resulting bond angle, 107°, to be less than the ideal tetrahedral angle, Table 26.7.1. According to VSEPR, the resulting hybridization on the N-atom has greater p-character than sp^3. The molecular shape is trigonal pyramidal. Water, $H_2\ddot{O}:$, has two non-bonding pairs, which create repulsions that decrease the bond angle even further, to 104.5°. The molecular shape is bent.

Table 26.7.1: Bond Angles in Binary Compounds.

bond angle:	90°	109.5°	120°	180°
hybridization:	p^3	sp^3	sp^2	sp
examples:	PH_3 (93°)	CH_4 (109.5°)	BF_3 (120°)	BeH_2 (180°)
	H_2S (92°)	NH_3 (107°)	CO_3^{2-} (120°)	$HC{\equiv}CH$ (180°)
		H_2O (104.5°) O_3 (116.8°)	$:CH_2$ (137.8°)	

For third and higher period elements, one can also consider mixing in d-character to form hybrid orbitals. For example, sd^3 hybridization is tetrahedral, sp^{3}d hybridization is trigonal bipyramidal, and sp^{3}d^2 hybridization is octahedral. In sp^{3}d^2 hybrids, the $d_{x^2-y^2}$ and d_{z^2}-orbitals, which lie along the x, y, and z-axes, form the hybrids. However, hybrids based on d-orbitals almost always over-estimate the contribution of the d-orbitals. Hybridization is a commonly used, but artificial, construct that is not directly experimentally observable. Equations for

hybridized orbitals can be generated with any arbitrary bond angle by adjusting the amount of p or d-character in the hybrids. However, given the arbitrary nature of the hybridization concept, a better approach is to project from careful molecular orbital calculations the effective hybridization that results for each central atom. Several methods are available to generate these projections, including the sigma-pi decomposition that is available in some semi empirical programs and natural bond order analysis that is available in many *ab initio* packages.

Example 26.7.1: *Hybridization Angles*
Calculate the bond angle in sp^2 hybridization.

Answer: The dot-product of two vectors is related to the angle between the two vectors by: $\vec{u} \cdot \vec{v} = |u|\,|v|\cos\theta$. The direction-vectors representing $\Psi_{sp2,a}$ and $\Psi_{sp2,b}$ are $(\sqrt{2}/\sqrt{3},0,0)$ and $(-1/\sqrt{6},1/\sqrt{2},0)$, respectively. The lengths are equal: $|\sqrt{2}/\sqrt{3},0,0| = |-1/\sqrt{6},1/\sqrt{2},0| = 0.8165$, and the dot-product is:

$$(\sqrt{2}/\sqrt{3},0,0) \cdot (-1/\sqrt{6},1/\sqrt{2},0) = |0.8165|\,|0.8165|\cos\theta$$
$$-0.3333 = 0.6667\cos\theta$$

giving: $\cos\theta = -0.5$ or $120°$.

Hybridization also provides a basis for a simplified approach to delocalized π-systems.

26.8 Hückel Molecular Orbital Theory

Conjugated Double Bonds are Extensively Delocalized: Semi-empirical and *ab initio* molecular orbital calculations require significant computational resources. **Hückel Molecular Orbital** Theory provides an approximate method that can be done using pencil and paper that helps build insight into delocalized π-systems. The Hückel approach also gives a glimpse into the inner workings of more rigorous methods, while allowing us to complete all the calculations ourselves. As a first example, consider ethylene, $H_2C=CH_2$. We assume that the σ-bonding framework is well described using sp^2-hybrid orbitals on each C-atom, in overlap with each other and 1s-orbitals on the H-atoms, Figure 26.8.1a. The ethylene σ-bonds are placed in the x,y-plane. In turn we can then focus on the π-molecular orbitals, which are described as linear combinations of the 2p$_z$-orbitals on the C-atoms, Figure 26.8.1b:

$$\Psi_i = c_{iA}\,p_{zA} + c_{iB}\,p_{zB} \qquad\qquad i = 1, 2 \qquad\qquad 26.8.1$$

We anticipate that the linear combination of two atomic orbitals will give two molecular orbitals, one bonding, Ψ_+, and one anti-bonding, Ψ_-, Figures 26.8.1b and c. The secular equations formed using the ethylene LCAO in Eq. 26.8.1 have the same form as Eq. 26.1.12. One simplification is that the π-system in ethylene is homonuclear, giving $H_{AA} = H_{BB}$. To remind us that we are describing just the π-system, with a σ-bond framework that is handled separately, we denote the atomic integrals H_{AA} and H_{BB} as α and the resonance integral H_{AB} as β:

$$(\alpha - ES_{AA})\, c_{iA} + (\beta - ES_{AB})\, c_{iB} = 0$$
$$(\beta - ES_{AB})\, c_{iA} + (\alpha - ES_{BB})\, c_{iB} = 0 \qquad\qquad 26.8.2$$

$$\alpha = \int p_{zA}^{*}\, \hat{\mathcal{H}}_{eff}\, p_{zA}\, dt \qquad\qquad \text{Coulomb Integral}$$
$$\beta = \int p_{zA}^{*}\, \hat{\mathcal{H}}_{eff}\, p_{zB}\, dt \qquad\qquad \text{Resonance Integral}$$
$$S_{AB} = \int p_{zA}^{*}\, p_{zB}\, dt = 0 \qquad\qquad \text{Overlap Integral}$$

(a). sp^2-framework   (b). LCAO-MO π-orbitals   (c). π-orbital energies
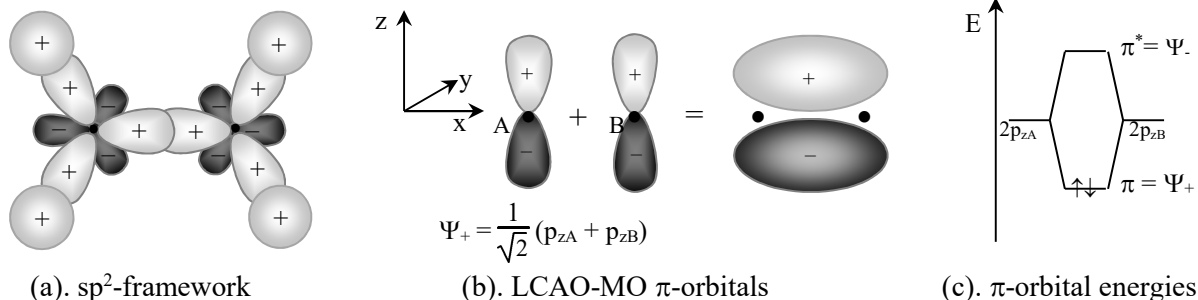
Figure 26.8.1: Hückel approach for ethylene assumes an (a) sp^2-hybridized σ-framework with (b) π-molecular orbitals constructed from a LCAO of the 2p$_z$-orbitals on each C-atom. (c). The π-bonding orbital is filled with two electrons, one for each sp^2-hybridized C-atom.

The effective Hamiltonian, $\hat{\mathcal{H}}_{eff}$, includes the averaged electron-electron repulsion of the core and σ-electrons for the π-electrons. We usually use normalized atomic orbitals; $S_{AA} = S_{BB} = 1$. The overlap integral is small between two p$_z$ orbitals, so that to a rough approximation we set $S_{AB} = 0$ to give the simplified secular equations:

$$\begin{array}{l}(\alpha - E)c_A + \beta c_B = 0 \\ \beta c_A + (\alpha - E)c_B = 0\end{array} \quad \text{or in matrix form:} \quad \begin{pmatrix} \alpha - E & \beta \\ \beta & \alpha - E \end{pmatrix}\begin{pmatrix} c_A \\ c_B \end{pmatrix} = 0 \qquad (S_{AB} \cong 0) \quad 26.8.3$$

Solutions to the secular equations are obtained by setting the determinant of the coefficient matrix equal to zero. Two roots result, one for the bonding and one for the anti-bonding π-orbitals:

$$\begin{vmatrix} \alpha - E & \beta \\ \beta & \alpha - E \end{vmatrix} = 0 \qquad\qquad E_+ = \alpha + \beta \qquad E_- = \alpha - \beta \qquad\qquad 26.8.4$$

The total π-bond energy for ethylene is $E^\pi = 2E_+ = 2\alpha + 2\beta$. The π-molecular orbitals correspond to the molecular orbitals for H_2^+, but constructed with 2p$_z$-atomic orbitals:

$$\Psi_+ = \frac{1}{\sqrt{2}}\,(p_{zA} + p_{zB}) \qquad\qquad \Psi_- = \frac{1}{\sqrt{2}}\,(p_{zA} - p_{zB}) \qquad\qquad 26.8.5$$

The π-bond order is based Eq. 26.3.10; however, we set $2S_{jk}$ to one for this purpose. There is only one p$_z$ orbital on each atom leaving just the sum over each molecular orbital:

$$P_{jk}^{\pi} = \sum_{i=1}^{m} n_i\, c_{ij}\, c_{ik} \qquad\qquad \text{(Hückel)} \qquad 26.8.6$$

The π-bond order in ethylene, with doubly occupied Ψ_+, is $P^\pi_{AB} = 2(1/\sqrt{2})(1/\sqrt{2}) = 1$. Similarly, the π-electron density on atom j from Eq. 26.3.8 simplifies to:

$$d^\pi_j = \sum_{i=1}^{m} n_i c_{ij}^2 \qquad \text{(Hückel)} \qquad 26.8.7$$

The π-density on each C-atom is one. Now consider 1,3-butadiene, which has the Lewis dot structure with two isolated double bonds: $H_2C=CH–CH=CH_2$. We assume that the σ-bonding framework is well described using sp^2-hybrid orbitals on each C-atom, Figure 26.8.2a. The ethylene σ-bonds are placed in the x,y-plane. The π-molecular orbitals are described as linear combinations of the $2p_z$-orbitals on the C-atoms, Figure 26.8.2b:

$$\Psi_i = c_{iA}\, p_{zA} + c_{iB}\, p_{zB} + c_{iC}\, p_{zC} + c_{iD}\, p_{zD} \qquad i = 1 \ldots 4 \qquad 26.8.8$$

(a). sp^2-framework　　　(b). LCAO-MO π-orbitals　　　(c). π-orbital energies
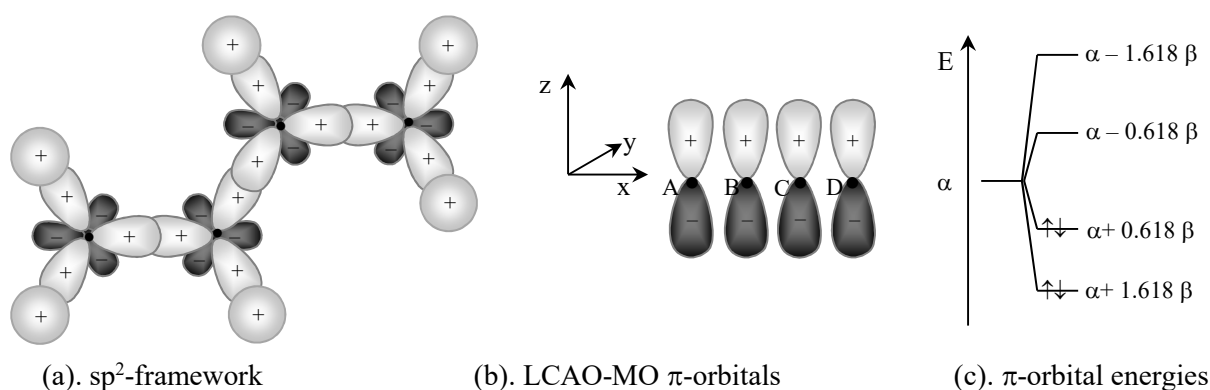
Figure 26.8.2: Hückel approach for butadiene assumes an (a) sp^2-hybridized σ-framework with (b) π-molecular orbitals constructed from a LCAO of the $2p_z$-orbitals on each C-atom. (c). The π-bonding orbitals are filled with four electrons, one for each sp^2-hybridized C-atom.

We anticipate that the linear combination of four atomic orbitals will give four molecular orbitals, two net bonding and two net anti-bonding, Figures 26.8.1b and c. The most bonding π-orbital results from the constructive all-in-phase overlap of the p_z orbitals, ⚇⚇⚇⚇. The most anti-bonding π-orbital results from alternating phases of the p_z orbitals, ⚇⬤⚇⬤. The secular equations are constructed analogously to the ethylene case using the approximations:

Hückel Approximations:
1. All atomic integrals, α, are equal.
2. All resonance integrals for adjacent atoms, β, are equal.
3. All resonance integrals for non-adjacent atoms are zero.
4. All overlap integrals in the secular equations are set to zero.

These approximations are extreme, but result in algebraically tractable expressions. The Hückel secular equations and determinant are easy to construct, by simply noting adjacent atoms. For butadiene, A and B are adjacent, B and C are adjacent, but A and C are not adjacent:

$$\begin{pmatrix} \alpha - E_i & \beta & 0 & 0 \\ \beta & \alpha - E_i & \beta & 0 \\ 0 & \beta & \alpha - E_i & \beta \\ 0 & 0 & \beta & \alpha - E_i \end{pmatrix} \begin{pmatrix} c_{iA} \\ c_{iB} \\ c_{iC} \\ c_{iD} \end{pmatrix} = 0 \qquad \begin{vmatrix} \alpha - E_i & \beta & 0 & 0 \\ \beta & \alpha - E_i & \beta & 0 \\ 0 & \beta & \alpha - E_i & \beta \\ 0 & 0 & \beta & \alpha - E_i \end{vmatrix} = 0 \qquad 26.8.9$$

To simplify these expressions to allow for "back of the envelope" calculations, we divide each term by β:

$$\begin{pmatrix} \dfrac{\alpha - E_i}{\beta} & 1 & 0 & 0 \\ 1 & \dfrac{\alpha - E_i}{\beta} & 1 & 0 \\ 0 & 1 & \dfrac{\alpha - E_i}{\beta} & 1 \\ 0 & 0 & 1 & \dfrac{\alpha - E_i}{\beta} \end{pmatrix} \begin{pmatrix} c_{iA} \\ c_{iB} \\ c_{iC} \\ c_{iD} \end{pmatrix} = 0 \quad \text{or} \quad \begin{vmatrix} \dfrac{\alpha - E_i}{\beta} & 1 & 0 & 0 \\ 1 & \dfrac{\alpha - E_i}{\beta} & 1 & 0 \\ 0 & 1 & \dfrac{\alpha - E_i}{\beta} & 1 \\ 0 & 0 & 1 & \dfrac{\alpha - E_i}{\beta} \end{vmatrix} = 0 \qquad 26.8.10$$

We simplify the diagonal elements by defining x_i as:

$$x_i = \frac{E_i - \alpha}{\beta} \qquad \text{which gives the energy as} \qquad E_i = \alpha + x_i \beta \qquad 26.8.11$$

Substituting x_i into the diagonal elements gives:

$$\begin{pmatrix} -x_i & 1 & 0 & 0 \\ 1 & -x_i & 1 & 0 \\ 0 & 1 & -x_i & 1 \\ 0 & 0 & 1 & -x_i \end{pmatrix} \begin{pmatrix} c_{iA} \\ c_{iB} \\ c_{iC} \\ c_{iD} \end{pmatrix} = 0 \qquad \text{or} \qquad \begin{vmatrix} -x & 1 & 0 & 0 \\ 1 & -x & 1 & 0 \\ 0 & 1 & -x & 1 \\ 0 & 0 & 1 & -x \end{vmatrix} = 0 \qquad 26.8.12$$

The calculation of determinants is introduced in the Addendum, Chapter 2.8. The 4x4 secular determinant for butadiene gives the fourth-order polynomial:

$$x^4 - 3x^2 + 1 = 0 \qquad\qquad 26.8.13$$

This polynomial is in "bi-quadratic" form, which is simplified by defining $y = x^2$ so that the resulting polynomial can be solved using the quadratic formula:

$$y^2 - 3y + 1 = 0 \qquad \text{with} \quad y = \frac{3 \pm \sqrt{9 - 4}}{2} = 2.618, \, 0.382 \qquad 26.8.14$$

Solving for x gives four roots, $x_i = \sqrt{y} = \pm 1.618, \pm 0.618$, which when substituted into the formula for the orbital energies in Eqs. 26.8.11 gives the four π-orbital energies as:

$$E_i = \alpha + x_i \beta = \alpha \pm 1.618 \, \beta \quad \text{or} \quad \alpha \pm 0.618 \, \beta \qquad 26.8.15$$

These π-orbital energies are used to generate the energy level diagram, Figure 26.8.2c. The Hamiltonian integrals α and β are both negative, so that $E_1 = \alpha + 1.618 \, \beta$ is the lowest energy, most bonding orbital, and $E_4 = \alpha - 1.618 \, \beta$ is the most anti-bonding orbital. With four total π-electrons, the lowest two orbitals are filled. These results, although a bit tedious, can be easily completed with paper and pencil. The corresponding molecular orbital coefficients can also be generated on the "back of an envelope" using Kramer's rules. However, if you allow the use of a

short, simple general purpose Web applet, MatLab, or Mathematica program, the π-molecular orbital energies and coefficients are easily generated.

The Hückel secular equations can be converted to an eigenvalue equation. Adding the diagonal elements to both sides of Eqs. 26.8.12 gives:

$$\begin{pmatrix} 0 & 1 & 0 & 0 \\ 1 & 0 & 1 & 0 \\ 0 & 1 & 0 & 1 \\ 0 & 0 & 1 & 0 \end{pmatrix} \begin{pmatrix} c_{iA} \\ c_{iB} \\ c_{iC} \\ c_{iD} \end{pmatrix} = x_i \begin{pmatrix} c_{iA} \\ c_{iB} \\ c_{iC} \\ c_{iD} \end{pmatrix} \qquad E_i = \alpha + x_i\,\beta \qquad\qquad 26.8.16$$

The x_i values are the eigenvalues and the molecular orbital coefficients are the eigenvectors of the Hückel matrix, which has zeros set for the diagonal elements. The eigenvalues for butadiene are identical to Eq. 26.8.15. The corresponding eigenvectors give the π-orbitals, Figure 26.8.3. Our initial qualitative expectations are realized. The most bonding orbital is the all-in-phase linear combination and the most anti-bonding orbital has alternating phases.

$$E_4 = \alpha - 1.618\,\beta \qquad \Psi_4 = 0.372 p_A - 0.602 p_B + 0.602 p_C - 0.372 p_D$$

$$E_3 = \alpha - 0.618\,\beta \qquad \Psi_3 = 0.602 p_A - 0.372 p_B - 0.372 p_C + 0.602 p_D$$

$$E_2 = \alpha + 0.618\,\beta \qquad \Psi_2 = 0.602 p_A + 0.372 p_B - 0.372 p_C - 0.602 p_D$$

$$E_1 = \alpha + 1.618\,\beta \qquad \Psi_1 = 0.372 p_A + 0.602 p_B + 0.602 p_C + 0.372 p_D$$
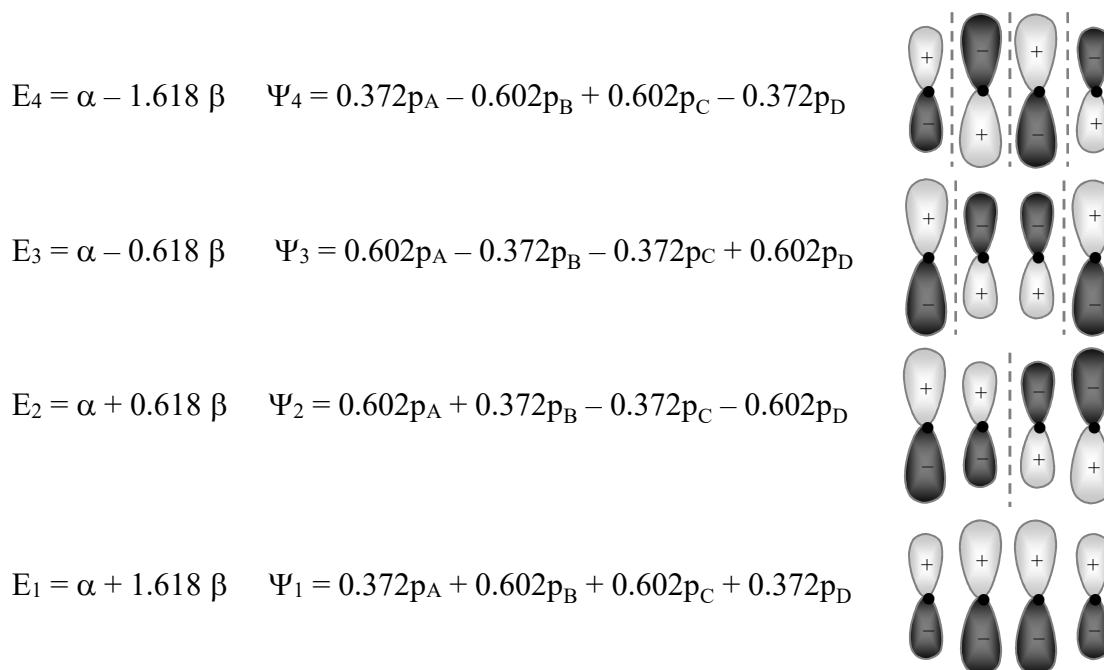
Figure 26.8.3: π-molecular orbitals for butadiene. Higher energy requires higher curvature, which requires more nodes.

The π-orbitals are four-center orbitals. The electrons are delocalized across all four C-atoms. The extra stability resulting from the delocalization is quantitatively determined by the π-delocalization energy, which is the difference between the total π-bond energy of the molecule and the equivalent number of localized double bonds. The equivalent number of localized double bonds is given by the Lewis dot structure. For butadiene, the comparison is to the π-energy of two isolated ethylenes:

$$E^\pi = 4\,\alpha + 4.472\,\beta$$
$$-\{\, 2\, E^\pi_{\text{ethylene}} = 4\,\alpha + 4\,\beta \,\}$$

$$\pi\text{-delocalization energy} = 0.472\,\beta \qquad\qquad 26.8.17$$

The π-bond order of each bond is given by Eq. 26.8.6. Consider the π-bond between A and B. The first term in the sum is for molecular orbital $i = 1$ which has an occupation of two electrons giving $n_i = 2$. The molecular orbital coefficients for atoms A and B in molecular orbital 1 match up as follows:

$$P_{AB}^\pi = \Sigma\; n_i\; \underset{\uparrow}{c_{iA}}\quad \underset{\uparrow}{c_{iB}}$$
$$\Psi_1 = \;\; c_{1A}\; p_A + c_{1B}\; p_B + c_{1C}\; p_C + c_{1D}\; p_D$$
$$\Psi_1 = 0.372\; p_A + 0.602\; p_B + 0.602\; p_C + 0.372\; p_D \qquad \text{(first term)} \quad 26.8.18$$

Completing the sums over all the molecular orbitals gives the π-bond order between atom pairs A-B and B-C as:

$$P_{AB}^\pi = 2(0.372)(0.602) + 2(0.602)(0.372) = 0.89$$
$$P_{BC}^\pi = 2(0.602)(0.602) + 2(0.372)(-0.372) = 0.45 \qquad\qquad 26.8.19$$

P_{BC}^π shows the effect of delocalization. $P_{AB}^\pi = P_{CD}^\pi$ by symmetry. The total π-bond order for butadiene is then $0.89 + 0.45 + 0.89 = 2.23$, which is 0.23 larger than expected from the Lewis dot structure. The molecular orbitals of benzene are also extensively delocalized.

Example 26.8.1: π-*Molecular Orbitals for Benzene*
Use the Hückel molecular orbital approach to find the π-bond order and π-delocalization energy of benzene.

Answer: The secular matrix for the atom lettering shown is given below, Figure 26.8.4.
$\boxed{www}$ The "eigen" applet on the text Web site or companion CD is a general matrix diagonalization application, which finds the eigenvectors and eigenvalues of a real symmetric matrix. The secular matrix is entered into the "eigen" applet as shown at right, below:

	A	B	C	D	E	F
A	-x	1	0	0	0	1
B	1	-x	1	0	0	0
C	0	1	-x	1	0	0
D	0	0	1	-x	1	0
E	0	0	0	1	-x	1
F	1	0	0	0	1	-x

(a). atom lettering   (b) Hückel secular matrix   (c) "eigen" applet input
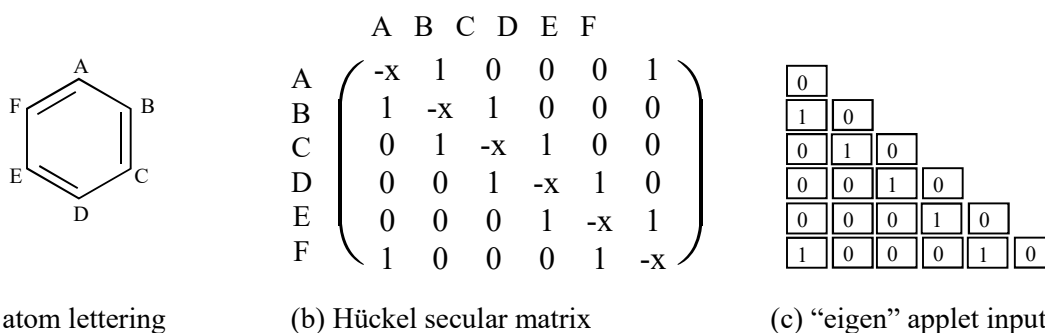
Figure 26.8.4: Hückel molecular orbital input matrix for benzene. (a). The atom lettering is arbitrary. (b). The secular matrix with $E_i = \alpha + x_i\,\beta$. (c). "eigen" Web applet input.

Only the lower triangular portion of the matrix need be input, since the matrix is symmetric. Zeros are entered along the diagonal, as required by Eq. 26.8.16. The output is given in Figure 26.8.5 with depictions of the π-orbitals as viewed from above the plane of the molecule.

Eigenvector 1: Eigenvalue=2
0.408248
0.408248
0.408248
0.408248
0.408248
0.408248   0 nodes

Eigenvector 2: Eigenvalue=1
-0.577282
-0.28095
0.296332
0.577282
0.28095
-0.296332   1 node

E Eigenvector 3: Eigenvalue=1
-0.00888074
-0.504381
-0.4955
0.00888074
0.504381
0.4955   1 node

Eigenvector 4: Eigenvalue=-1
-0.00752905
-0.496193
0.503722
-0.00752905
-0.496193
0.503722   2 nodes

Eigenvector 5: Eigenvalue=-1
0.577301
-0.295171
-0.28213
0.577301
-0.295171
-0.28213   2 nodes

Eigenvector 6: Eigenvalue=-2
-0.408248
0.408248
-0.408248
0.408248
-0.408248
0.408248   3 nodes

E

$\alpha - 2\beta$

$\alpha - \beta$

α

$\alpha + \beta$

$\alpha + 2\beta$

Figure 26.8.5: Hückel π-orbitals for benzene and the molecular orbital energy diagram.

The orbital energies are calculated using Eq. 26.8.11. The molecular orbital energy diagram is filled with six electrons, one for each sp^2-hybridized C. The small coefficients in eigenvectors 3 and 4 are zero to within the accuracy of the applet. If the coefficient is zero at an atom, the atom sits on a nodal plane. The degenerate pairs of orbitals have the same number of nodal planes.

   Each bond in benzene is equivalent, so we need only calculate the bond order of one atom pair. The π-bond order between atoms A and B is given by Eq. 26.8.6, with three doubly occupied orbitals:

$$P_{AB} = 2(0.408248)(0.408248) + 2(-0.577282)(-0.28095) + 2(0)(-0.504381)$$
$$= 0.66 = {}^2/_3$$

The average qualitative π-bond order predicted by the Lewis dot representation is ½, which shows that delocalization results in stronger bonding than isolated double bonds. The π-delocalization energy is obtained by comparison with three isolated double bonds, the equivalent of three isolated ethylenes:

$$\pi\text{-DE} = [2(\alpha + 2\beta) + 4(\alpha + \beta)] - [3(2\alpha + 2\beta)] = 2\beta$$
$$\textit{benzene} \qquad - \quad \textit{3(ethylene)}$$

The π-system in benzene is significantly lower in energy than three isolated double bonds.

   The enthalpy of hydrogenation of benzene is used to determine the experimental π-delocalization energy of benzene. A good comparison to benzene for a localized double bond is cyclohexene. At the time of the development of Hückel theory, the enthalpies of hydrogenation of benzene and cyclohexene were reported to be -206.0 kJ mol^{-1} and -118.4 kJ mol^{-1}, respectively

(for the current values, see the Problems). The π-delocalization energy of benzene is given by comparison to the hydrogenation of three moles of cyclohexene:

$$\pi\text{-DE} = [-206.0 \text{ kJ mol}^{-1}] - [3(-118.4 \text{ kJ mol}^{-1})] = 149.2 \text{ kJ mol}^{-1} = |2\beta| \qquad 26.8.20$$
$$\text{\textit{benzene}} \qquad - \text{ \textit{3(cyclohexene)}}$$

Setting the experimental π-delocalization energy equal to the magnitude of 2β gives an estimate of the resonance integral of $\beta \cong -75 \text{ kJ mol}^{-1}$.

The approximations used in the Hückel approach are extreme and are justified only by the computational simplicity. **Extended Hückel theory** is an intermediate approach between Hückel and *ab initio* methods that maintains ease of use, while removing some of the most drastic approximations. The extended Hückel approach has been supplanted by AM1 and PM3 semi-empirical techniques for moderate sized molecules. However, the extended Hückel method introduces important concepts used in more rigorous electronic structure methods.

The Extended Hückel Method Accommodates All Elements and Orbital Overlap: Extended Hückel theory is applicable to both σ- and π-molecular orbitals and easily incorporates all the atoms in the periodic table. While not as rigorous as MNDO, AM1, PM3 or *ab initio* methods, extended Hückel calculations are useful as a rough approximation for polymers, large macrocyclic systems, solids, and surfaces.[10] The first step is to note that the atomic integrals in the secular equations, H_{ii}, are approximately given by valence atomic orbital ionization energies, VOIEs, Table 26.8.1. These values are the configuration averaged energy necessary to remove an electron from a specific atomic orbital in a given atom. For example, the VOIE for the 2p-orbital of carbon is the ionization energy for the gas phase process:

$$C(1s^2 2s^2 2p^2) \rightarrow C^+(1s^2 2s^2 2p^1) + 1 \text{ e}^-$$
$$\text{VOIE} = E^+(1s^2 2s^2 2p^1)_{\text{averaged}} - E(1s^2 2s^2 2p^2)_{\text{averaged}} \qquad 26.8.21$$
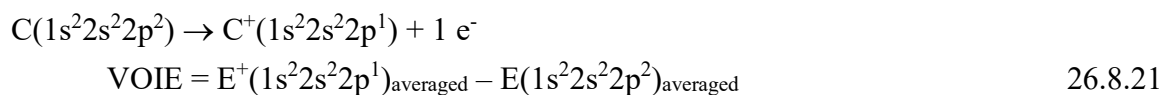
The energies of the atom and the cation are averaged over all electronic terms with the same configuration. For the neutral C-atom, the configurations are ^3P_o, $^3P_1$, $^3P_2$, $^1D_2$, ^1S_o. The averages are weighted by the degeneracy of each term, $g_J = 2J + 1$.

Table 26.8.1$^{(DS)}$: Valence Atomic Orbital Ionization Energies (eV).[11,12]

Atom	1s	2s	2p
H	13.60		
He	24.5		
Li		5.45	3.50
Be		9.30	6.00
B		14.0	8.30
C		19.5	10.7
N		25.5	13.1
O		32.3	15.9
F		40.4	18.7

(DS) Additional values listed in the Appendix Data Section

The resonance integral is expected to be proportional to the degree of atomic orbital overlap, S_{ij}. A rough approximation for the resonance integral between atoms i and j is:

$$H_{ij} = KS_{ij}\frac{(H_{ii} + H_{jj})}{2} \qquad\qquad 26.8.22$$

where K is often approximated as 1.75. Using VOIEs to approximate the atomic and resonance integrals then allows the extended method to be applied to all elements. Another problem with the Hückel method is that we had to set the overlap integrals to zero in the secular matrix.

The matrix form of the LCAO secular equations with two orbitals, from Eq. 26.1.12 is:

$$\begin{pmatrix} H_{AA} - E_iS_{AA} & H_{AB} - E_iS_{AB} \\ H_{AB} - E_iS_{AB} & H_{BB} - E_iS_{BB} \end{pmatrix}\begin{pmatrix} c_{iA} \\ c_{iB} \end{pmatrix} = 0 \qquad 26.8.23$$

This equation can be factored and rearranged to give:

$$\begin{pmatrix} H_{AA} & H_{AB} \\ H_{AB} & H_{BB} \end{pmatrix}\begin{pmatrix} c_{iA} \\ c_{iB} \end{pmatrix} - E_i\begin{pmatrix} S_{AA} & S_{AB} \\ S_{AB} & S_{BB} \end{pmatrix}\begin{pmatrix} c_{iA} \\ c_{iB} \end{pmatrix} = 0$$

$$\text{and} \quad \begin{pmatrix} H_{AA} & H_{AB} \\ H_{AB} & H_{BB} \end{pmatrix}\begin{pmatrix} c_{iA} \\ c_{iB} \end{pmatrix} = E_i\begin{pmatrix} S_{AA} & S_{AB} \\ S_{AB} & S_{BB} \end{pmatrix}\begin{pmatrix} c_{iA} \\ c_{iB} \end{pmatrix} \qquad 26.8.24$$

If we let $\underset{\approx}{H}$ be the matrix of the Hamiltonian integrals, $\underset{\approx}{S}$ the overlap matrix, and $\underset{\sim}{c_i}$ be the vector of molecular orbital coefficients for eigenstate i, this matrix equation becomes:

$$\underset{\approx}{H}\,\underset{\sim}{c_i} = E_i\,\underset{\approx}{S}\,\underset{\sim}{c_i} \qquad\qquad 26.8.25$$

which is the same form as the Roothaan equations, Eq. 26.5.9. Multiplying from the left by the inverse of the overlap matrix and using $\underset{\approx}{S^{-1}}\underset{\approx}{S} = 1$, gives:

$$(\underset{\approx}{S^{-1}}\underset{\approx}{H})\,\underset{\sim}{c_i} = E_i\,\underset{\sim}{c_i} \qquad\qquad 26.8.26$$

The molecular orbitals and energies are then the eigenvectors and eigenvalues of the matrix $(\underset{\approx}{S^{-1}}\underset{\approx}{H})$. Eq. 26.8.26 is easily solved using general matrix methods. Unfortunately, a weakness of the method is that the extended Hückel approach does not include the effects of electron spin, so electron exchange and correlation interactions are not included.

Example 26.8.2: *Extended Hückel Calculation*
Calculate the bond order for LiH. Assume the molecule is oriented along the x-axis. For a bond length of 1.61 Å, the H(1s)- Li(2s) overlap integral is 0.392 and the H(1s)- Li(2p$_x$) overlap is 0.505 (see Figure 26.3.2).

Answer: The valence orbital ionization energies are listed in Table 26.8.1. At this low level of approximation, the energies of the Li(2p$_y$) and Li(2p$_z$) are unaffected by the electrons in the σ-molecular orbitals. Because the 2p$_y$ and 2p$_z$ are non-interacting, we don't need to include them in the secular equations. The resonance integrals are given using Eq. 26.8.22 and K = 1.75 as:

$$\text{H(1s)- Li(2s):} \quad H_{1s,2s} = KS_{ij}\frac{(H_{ii} + H_{jj})}{2} = 1.75(0.392)\frac{(-5.45 + (-13.6))}{2}\text{ eV} = -6.53\text{ eV}$$

H(1s)- Li(2p$_x$): $H_{1s,2px} = 1.75(0.505) \dfrac{(-3.50 + (-13.6))}{2}$ eV = -7.56 eV

$\boxed{www}$ The "Secular" applet available on the text Web site or companion CD was used to solve the secular equations, Eq. 26.8.25, with the input set-up as:
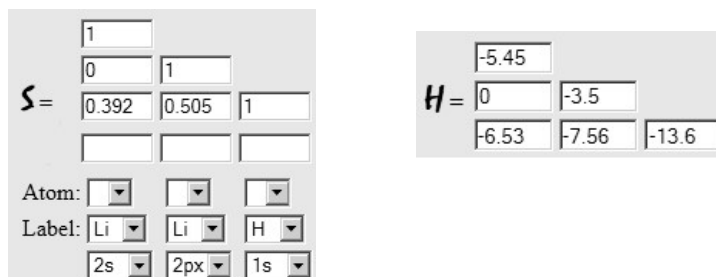
$$S = \begin{matrix} 1 & & \\ 0 & 1 & \\ 0.392 & 0.505 & 1 \\ & & \end{matrix}$$

Atom: [▼] [▼] [▼]
Label: [Li ▼] [Li ▼] [H ▼]
       [2s ▼] [2px ▼] [1s ▼]

$$H = \begin{matrix} -5.45 & & \\ 0 & -3.5 & \\ -6.53 & -7.56 & -13.6 \end{matrix}$$

The labels are optional; in this case they are simply used to label the orbitals in the output for easier reading. The output of the applet is:

```
        Eigenvalues and eigenvectors
    (eigenvectors listed in columns)
E(i)    -13.7867    -4.7341     5.2162
vector      1           2          3
atom:
   Li2s    0.1336     0.8348     0.4630
   Li2px   0.0575    -0.5355     0.6737
    H1s    0.9894    -0.1279    -0.5760
```

With two valence electrons, only the lowest energy orbital is filled. The Mulliken bond order is given by Eq. 26.3.10:

$$P_{LiH} = \sum_{j \text{ on Li}} \sum_{k \text{ on H}} \sum_{i=1}^{m} n_i \, 2c_{ij} \, c_{ik} \, S_{jk} = 4 \, c_{1,2sLi} \, c_{1,1sH} \, S_{2sLi,1sH} + 4 \, c_{1,2pxLi} \, c_{1,1sH} \, S_{2pxLi,1sH}$$
$$= 4(0.1336)(0.9894)(0.392) + 4(0.0575)(0.9894)(0.505) = 0.322$$

The extended Hückel bond order of 0.322 is significantly smaller than the CNDO bond order of 1.22. The CNDO bond order is more realistic, but the extended Hückel result is easy to calculate and applicable to elements that are not available in common semi-empirical methods (see the Appendix Data section Table 26.8.1). In general, Hückel bond orders are often too small. Note that clicking the "Generate H" button in the applet automatically sets up the Hamiltonian matrix, based on the atom labels chosen and the corresponding VOIEs. The secular equation is also easily solved using MatLab.

26.9 Summary – Looking Ahead

The formation of a chemical bond is a delicate balance of the increase in electron kinetic energy, a decrease in the electron-nuclear Coulomb potential energy, and the increase in the Coulomb repulsions of the electrons. The strength of the chemical bond is enhanced by the decrease in electron-electron repulsion that results from quantum mechanical avoidance, as determined by the exchange energy. The correlation of the motion of the electrons, as determined by the correlation energy, is a major contributor to the strength of the chemical bond. Chemical bonding is a small perturbation on the overall energy of the atoms in the molecule, because balancing of large increases in kinetic energy by large decreases in the Coulomb potential energy result in a

bond dissociation energy that is small in comparison with the total atomic energy. *Ab initio* methods are readily available that accurately reflect the delicate balance of the energetics, including exchange and correlation interactions. *Ab initio* methods use no information from experimental data on atomic or molecular systems. Semi empirical calculations simplify the calculation of molecular orbitals by using experimental values to estimate important integrals and by assuming some multi-center integrals are negligible. Semi empirical methods apply only to valence electrons. Hückel and extended Hückel methods are important stepping stones in the historical development of practical molecular structure methods. Hückel and extended Hückel methods are useful as guides to chemical intuition and are still useful for very large systems, such as extended solid surfaces. A final molecular orbital example is useful as a summary.

Consider the formation of the hydrogen bond between the F^- ion and HF molecule. On the basis of Lewis dot rules, no strong interaction is expected since F^- and HF are both closed shell. Experimentally, however, the [F–H–F]$^-$ ion has the strongest hydrogen bond known. The bonding is symmetrical on either side of the H-atom. The F(1s) and F(2s) orbitals are much lower in energy than the H(1s); the F s-orbitals form a non-bonding core set. Combining six 2p-orbitals and one H(1s) gives seven final MOs. However, only the $2p_x$ orbitals and the 1s are oriented to give favorable overlap. Molecular orbitals are constructed using the overlap of the F($2p_x$) orbitals and the H(1s), Figure 26.9.1.[4,5] The orbitals are formed that optimize overlap and follow the symmetry of the molecule. In other words, the bonding and anti-bonding character must be symmetrical with respect to the plane passing through the H-atom that is perpendicular to the internuclear axis.
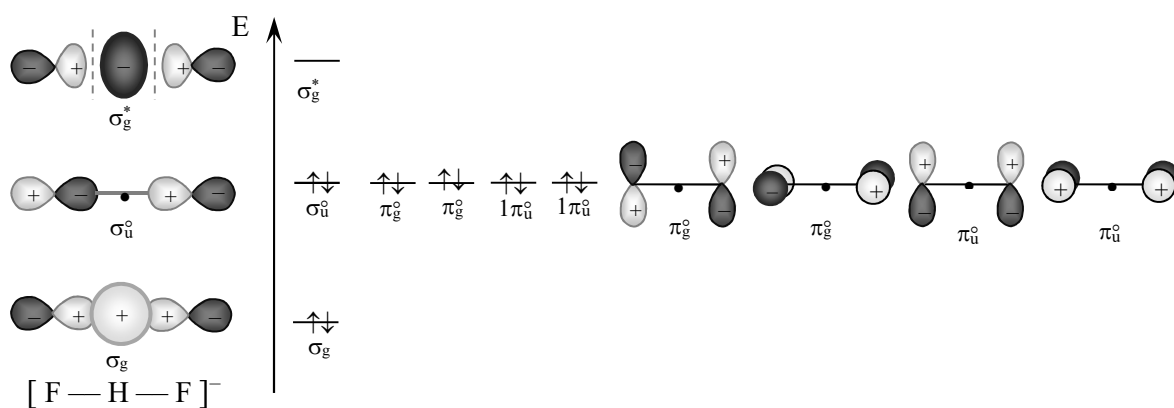
Figure 26.9.1: Molecular orbitals for the [F–H–F]$^-$ hydrogen bonded ion. The σ-orbitals are in a bonding, non-bonding, anti-bonding trio, which are filled through the non-bonding orbital. The overall qualitative bond order is one, or ½-order on each side.

The overall bond order is one, giving a ½-order bond on each side of the H-atom. This ion is considered an <u>electron excess</u> species, because the F^- and HF are closed shell. No additional sharing of electrons is necessary for stable configurations. The hydrogen bonded ion is stable because the excess pair is in a non-bonding orbital. The non-bonding electrons neither help nor hinder bonding. If the σ_u° did not form, then a pair of electrons would be forced into an anti-bonding orbital and the hydrogen bond would not be stable. Similar molecular orbital schemes can be constructed for the unsymmetrical hydrogen bonds in other systems, such as water. The

molecular orbital approach provides useful insight into strong inter-molecular interactions as well as covalent bonding.

The molecular orbital approach is central to our understanding of all chemical phenomena. Our next step is to discuss the experimental methods that are used to determine molecular structure and energetics. Then the energetics determined through quantum mechanical calculations or directly from experiment are used to predict important thermodynamic properties, including equilibrium constants.

Chapter Summary

1. The Schrödinger equation for H_2^+ includes the kinetic energy of the electron, the Coulomb attraction of the electron for both nuclei, and the Coulomb repulsion of the nuclei; the distances of the electron from nuclei A and B are r_{1A} and r_{1B} and the bond length R:

$$-\frac{\hbar^2}{2m}\nabla_1^2\Psi + \frac{e^2}{4\pi\varepsilon_o}\left(-\frac{1}{r_{1A}} - \frac{1}{r_{1B}} + \frac{1}{R}\right)\Psi = E\ \Psi$$

2. The Born-Oppenheimer approximation assumes that the electronic structure of the molecule adjusts instantaneously to the vibrational motion of the nuclei. The motion of the nuclei and the electrons are assumed to be independent.

3. The secular equations are solved by setting the determinant of the coefficients to zero:

$$\begin{vmatrix} H_{AA} - ES_{AA} & H_{AB} - ES_{AB} \\ H_{AB} - ES_{AB} & H_{BB} - ES_{BB} \end{vmatrix} = 0$$

4. Molecular orbitals are approximated as a linear combination of atomic orbitals. For H_2^+ with molecular orbital coefficients, c_A and c_B: $\Psi_{MO} = c_A\Psi_A + c_B\Psi_B$.

5. The secular equations are expressed in terms of atomic integrals $H_{AA} \equiv \int \Psi_A^* \mathcal{H}\Psi_A\ d\tau$, resonance integrals $H_{AB} \equiv \int \Psi_A^* \mathcal{H}\Psi_B\ d\tau$, atomic normalization $S_{AA} \equiv \int \Psi_A^*\Psi_A\ d\tau$, and overlap integrals $S_{AB} \equiv \int \Psi_A^*\Psi_B\ d\tau$.

6. The resonance integral is largely responsible for the energetic stabilization of the bond.

7. The normalized single electron bonding and anti-bonding orbitals for H_2^+ and H_2 are:

$$\Psi_+ = \frac{1}{\sqrt{2+2S}}\ (1s_A + 1s_B) \qquad\qquad \Psi_- = \frac{1}{\sqrt{2-2S}}\ (1s_A - 1s_B)$$

8. The ground state of H_2 is a product of one-electron molecular orbitals (the orbital approximation):

$$\Psi_{MO}(r_1,r_2) = \Psi_+(r_1)\ \Psi_+(r_2) = \frac{1}{2+2S}\ [1s_A(r_1) + 1s_B(r_1)]\ [1s_A(r_2) + 1s_B(r_2)]$$

9. The increase in effective nuclear charge for H_2 to $Z_{eff} = 1.197$ causes a contraction of the molecular orbital, which causes an increase in kinetic energy of the electrons.

10. In a minimum basis set calculation, the atomic orbitals are the valence orbitals on each atom.

11. Adding atomic basis orbitals with higher angular momentum than the valence orbitals gives an extended basis set. The added orbitals are polarization functions.

12. A method to adjust molecular wave functions for electron correlation is configuration interaction, CI. CI calculations allow the ground state to mix with excited states of the molecule.

13. The formation of a chemical bond increases electron kinetic energy, decreases electron-nuclear Coulomb potential energy, and increases Coulomb repulsions of the electrons.

14. Correlation and exchange interactions increase bond stability by decreasing electron-electron repulsion.

15. Strong bonds require good atomic overlap and energy matching.

16. The fraction ionic character of the bond between atoms A and B is calculated from the MO coefficients; the sums extend over all filled molecular orbitals on the given atom:

$$\text{fraction ionic} = \frac{\Sigma(\text{A coefficients})^2 - \Sigma(\text{B coefficients})^2}{\Sigma(\text{A coefficients})^2 + \Sigma(\text{B coefficients})^2}$$

17. The density matrix elements, p_{jk}, are the sums over all molecular orbitals i. The atom electron density for a are the sums over all atomic orbitals j on atom-a and molecular orbitals i:

$$p_{jk} = \sum_{i=1}^{m} n_i\, c_{ij}\, c_{ik} \qquad\qquad d_a = \sum_{j\text{ on }a} \sum_{i=1}^{m} n_i c_{ij}^2 = \sum_{j\text{ on }a} p_{jj}^2$$

18. The bond order between atom-a and -b is approximated by the Mulliken overlap population, P_{ab}, the sum over all atomic orbitals j on atom-a and atomic orbitals k on atom-b and the sum over all molecular orbitals i with occupancy n_i:

$$P_{ab} = \sum_{j\text{ on }a} \sum_{k\text{ on }b} \sum_{i=1}^{m} n_i\, 2c_{ij}\, c_{ik}\, S_{jk} = \sum_{j\text{ on }a} \sum_{k\text{ on }b} 2\, p_{jk}\, S_{jk}$$

19. Unoccupied orbitals are called virtual orbitals.

20. The electric dipole moment operator for the electrons is the sum is taken over the coordinates of each electron, $\vec{r}_i$:

$$\hat{\vec{\mu}} = -\sum_{i=1}^{n} e\, \hat{\vec{r}}_i$$

21. For a linear molecule along x-axis, the contribution to the dipole moment from the electrons:

$$<\mu_x> = -\sum_{i=1}^{n} e \int \Psi_{MO}^{*}\, x_i\, \Psi_{MO}\, d\tau \qquad \text{in C m.}$$

22. The dipole is usually given in debyes with: $1\text{ D} = 3.336\times10^{-30}$ C m.

23. The Pauling electronegativities of two elements, χ_A and χ_B, are the deviation of the experimental bond energy from the equal-sharing prediction, with the bond energies in eV:

$$(\chi_A - \chi_B)^2 = D_o(\text{A–B}) - [D_o(\text{A–A})\, D_o(\text{B–B})]^{1/2}$$

24. The Mulliken electronegativity, x_A, is the arithmetic average of the first ionization potential and the negative of the electron affinity for the valence state of the atom:
$x_A = [I_{1A} + (\text{-EA}_A)]/2$. The Pauling and Mulliken scales relate by $\chi_A = 0.336(x_A - 0.615)$.

25. The qualitative bond order, BO, is: BO = ½ (bonding electrons – anti-bonding electrons)

26. Paramagnetic substances are attracted into an inhomogeneous magnetic field. Diamagnetic substances are weakly repelled from an inhomogeneous magnetic field. The ground states of B_2 and O_2 are paramagnetic. Odd electron species are paramagnetic, e.g. CN, NO, and OF.

27. The p-orbital character of a molecular orbital is given by population analysis on the atom:

$$\% \text{ p character} = \frac{\Sigma\,(\text{p coefficients})^2}{(\text{s coefficient})^2 + \Sigma(\text{p coefficients})^2}$$

28. Orbitals that can overlap, will. In forming a molecular orbital, include all possible overlaps between atomic orbitals of similar energy.

29. The minimum of the electronic potential curve is at the equilibrium bond length r_e. The experimental bond length, r_o, is the vibrationally averaged bond length in the zero-point vibrational state. The bond dissociation energy, D_e, is the experimental bond dissociation energy, adjusted for zero point vibration: $D_o = D_e - \frac{1}{2}h\nu_o$. The bond force constant is the curvature of the electronic potential energy at the equilibrium bond length:

$$k = \left(\frac{\partial^2 V}{\partial r^2}\right)_{r=r_e}$$

30. Experimental bond strength measures for second-period diatomics show an excellent correlation with the qualitative bond order predicted from MO theory.

31. The Roothaan form of the Fock equations are derived under the Born-Oppenheimer and orbital approximations using the SCF-LCAO approach.

32. A one-electron molecular spin orbital, $\Psi_a\sigma(1)$, is a LCAO of N atomic orbitals, ϕ_i, with coefficients, c_{ia}, as variational parameters:

$$\Psi_a = \sum_{i=1}^{N} c_{ia}\, \phi_i \ \text{ and } \sigma(1) = \alpha(1) \text{ or } \beta(1).$$

33. The one-electron molecular orbital energies, ε_a, are determined as: $f_1\, \Psi_a(1)\sigma(1) = \varepsilon_a\, \Psi_a(1)\sigma(1)$. Parallel equations are written for MOs b, c, ….

34. The one-electron Fock operator for electron 1 is the sum over all $j\neq i$ filled orbitals:

$$f_1 = h_1 + \sum_{j=1}^{n/2} \{2J_j(1) - K_j(1)\} \qquad\qquad h_1 = -\frac{\hbar^2}{2m}\nabla_1^2 - \sum_{k=1}^{m}\frac{Z_k e^2}{4\pi\varepsilon_o r_{k1}}$$

The core Hamiltonian, h_1, is the sum of the kinetic energy of electron 1 and the electron-nuclear attraction of electron 1 with each of the m nuclei, k, with nuclear charge Z_k:

35. Electron-electron repulsion is evaluated by the coulomb and exchange operators. The coulomb operator between electron 1 in MO a and electron 2 in MO j is summed over all one-electron molecular orbitals:

$$J_j(1)\, \Psi_a(1) = \left(\int \Psi_j^*(2)\, \frac{e^2}{4\pi\varepsilon_o r_{12}}\, \Psi_j(2)\, d\tau_2\right) \Psi_a(1)$$

36. The exchange operator is an exact representation of the cross terms in the Slater determinant necessary to guarantee electron indistinguishability and is the source of "quantum avoidance":

$$K_j(1)\, \Psi_a(1) = \left(\int \Psi_j^*(2)\, \frac{e^2}{4\pi\varepsilon_o r_{12}}\, \Psi_a(2)\, d\tau_2\right) \Psi_j(1)$$

37. The Roothaan form of the Fock equations is an NxN matrix equation: $\underset{\approx}{F}\, \underset{\sim}{c_a} = \varepsilon_a\, \underset{\approx}{S}\, \underset{\sim}{c_a}$. The Fock matrix elements. F_{ji}, and the overlap matrix elements S_{ji} are:

$F_{ji} = \int \phi_j(1) f_1 \phi_i(1) d\tau_1$ and $S_{ji} = \int \phi_j(1)\phi_i(1)\, d\tau_1$.

38. DFT includes exchange and correlation directly. The electronic energy is the sum of the kinetic energy of the electrons, e-n attraction, e-e repulsion, and the exchange-correlation energy: $E = E_T + E_V + E_J + E_{xc}$.

39. In DFT, the one-electron Fock operator includes the exchange-correlation potential $V_j^{XC}(1)$:

$$f_1 = h_1 + \sum_{j=1}^{n/2} \{2J_j(1) - V_j^{XC}(1)\}$$

40. E_J, E_{XC}, and $V_j^{XC}(1)$ are functions of the electron density: $\rho(r) = 2 \sum_{i=1}^{n/2} |\Psi_i(r)|^2$.

41. Hybrid functionals (B3LYP) mix Hartree-Fock exchange with DFT exchange-correlation.

42. A valid set of molecular orbitals:
    1. use LCAO approach
    2. combine AOs with good overlap and similar energy (orbitals that can overlap, will)
    3. give number of AOs = number of MOs
    4. use MOs that have the same symmetry as the molecule.

43. The symmetry of molecular orbitals is characterized under rotation (σ, π, δ), inversion symmetry (g or u), and reflection (bonding or anti-bonding for diatomics). For polyatomics, the bonding and anti-bonding character is specified with respect to the overall number of pairwise bonding interactions. Orbitals are numbered sequentially within each symmetry class, starting with the core orbitals.

44. Walsh diagrams plot the molecular orbital energies as a function of bond angle for pairs of correlated orbitals. Orbital energies vary smoothly with bond angle. Orbitals of the same symmetry correlate. Orbital energies of the same symmetry do not cross (non-crossing rule). Orbitals with a node between the two outer atoms increase in energy upon bending.

45. Walsh's Rules: Valence electrons determine the correlated MO pairs that have the predominant influence. Up to 16 electrons give linear, 17-21 electrons give bent, and 22 electrons give linear AB_2 molecules.

46. Bonds form in the direction of maximum overlap. Hybridization combines atomic orbitals to give an orthonormal set of hybridized atomic orbitals, which are equivalent in size, energy, and shape. Hybrids are geometrically disposed to maximize overlap with adjacent atoms.

47. The overlap of the hybrid atomic orbitals on adjacent atoms creates bonding and anti-bonding pairs of localized molecular orbitals that form the σ-framework of the molecule.

48. Valence shell electron pair repulsion theory, VSEPR, predicts that non-bonding pairs of electrons have a larger extent than bonding pairs.

49. Hückel Molecular Orbital theory applies to the π-bonding network. The secular equations are constructed using the approximations:
    1. All atomic integrals, α, are equal.
    2. All resonance integrals for adjacent atoms, β, are equal ($\beta \cong$ -75 kJ mol^{-1}).
    3. All resonance integrals for non-adjacent atoms are zero.
    4. All overlap integrals in the secular equations are set to zero.

50. The π-bond order and π-electron density are sums over molecular orbitals for atoms j and k:

$$P_{jk}^{\pi} = \sum_{i=1}^{m} n_i\, c_{ij}\, c_{ik} \qquad\qquad d_j^{\pi} = \sum_{i=1}^{m} n_i c_{ij}^2$$

51. The π-delocalization energy is the difference between the total π-bond energy for the molecule and the equivalent number of localized double bonds, each at $E_{ethylene}^{\pi} = 2\,\alpha + 2\,\beta$.

52. Extended Hückel theory is applicable to σ- and π- orbitals. Atomic integrals, H_{ii}, are given by valence atomic orbital ionization energies, VOIEs. The resonance integral between atoms i and j is $H_{ij} = K S_{ij} (H_{ii} + H_{jj})/2$ with $K \cong 1.75$. With $\underset{\approx}{H}$, the matrix of Hamiltonian integrals, $\underset{\approx}{S}$, the overlap matrix, and $\underset{\sim}{c_i}$ the vector of molecular orbital coefficients: $\underset{\approx}{H}\,\underset{\sim}{c_i} = E_i\,\underset{\approx}{S}\,\underset{\sim}{c_i}$.

53. Electron excess molecules or ions are adducts of closed shell atoms, molecules, or ions (XeF_2, I_3^-, $[F–H–F]^-$).

Literature Cited:

1. R. S. Mulliken, "Electronic Population Analysis on LCAO-MO Molecular Wave Functions. I," *J. Chem. Phys.*, **1955**, *23(10)*, 1833-1840.

2. H. B. Gray, *Electrons and Chemical Bonding*, Benjamin/Cummings, Menlo Park, CA, 1964.

3. A. L. Allred, "Electronegativity values from thermochemical data," *J. Inorg. Nucl. Chem*., **1961**, *17*, 215-221.

4. G. C. Pimentel, R. D. Spratley, *Understanding Chemistry*, Holden-Day Inc., San Francisco, CA, 1971.

5. G. C. Pimentel, R. D. Spratley, *Chemical Bonding Clarified Through Quantum Mechanics*, Holden-Day, Inc., San Francisco, CA, 1969.

6. C. J. Cramer, *Essentials of Computational Chemistry, 2nd. Ed*., Wiley, Chichester, West Sussex,2006, pp. 126-128, 224-227.

7. W. Koch, M. C. Holthausen, *A Chemist's Guide to Density Functional Theory, 2nd Ed*., Wiley-VCH, Weinheim, DE, 2001.

8. A. D. Walsh, "The Electronic Orbitals, Shapes, and Spectra of Polyatomic Molecules, Part I. AH_2 Molecules," *J. Chem. Soc.*, **1953**, 2260-2265

9. A. D. Walsh, "The Electronic Orbitals, Shapes, and Spectra of Polyatomic Molecules, Part II. AB_2 and BAC Molecules," *J. Chem. Soc.*, **1953**, 2266-2289.

10. R. Hoffman, *Solids and Surfaces, A Chemists View of Bonding in Extended Structures*, VCH, New York, NY, 1988.

11. H. B. Gray, *Electrons and Chemical Bonding*, Benjamin/Cummings, Menlo Park, CA, 1964, Appendix.

12. R. L. DeKock, H. B. Gray, *Chemical Structure and Bonding*, Benjamin/Cummings, Menlo Park, CA, 1980, p. 227.

Further Reading:

M. W. Hanna, *Quantum Mechanics in Chemistry, 3rd. ed.,* Benjamin/Cummings, Menlo Park, CA, 1981.

M. Karplus, R. N. Porter, *Atoms and Molecules*, Benjamin/Cummings, Menlo Park, CA, 1970.

I. N. Levine, *Quantum Chemistry, 4th ed.* Prentice Hall, Englewood Cliffs, NJ, 1991.

J. P. Lowe, K. A. Peterson, Q*uantum Chemistry*, Elsevier Academic Press, Burlington, MA, 2006.

D. A. McQuarrie, *Quantum Chemistry*, University Science Books, Sausalito, CA, 2008.

R. L. DeKock, H. B. Gray, *Chemical Structure and Bonding*, Benjamin/Cummings, Menlo Park, CA, 1980.

W. J. Hehre, L. Radom, P. v.R. Schlyer, J. A. Pople, *Ab Initio Molecular Orbital Theory*, Wiley, New York, NY, 1986.

Chapter 26: Molecular Structure Problems

<u>1</u>. Draw the Lewis dot resonance structures for the carbonate ion, CO_3^{2-}. Are the electrons delocalized? Give the average bond order for the bonds. The procedure for the determination of Lewis dot structures is:

(1). Place the nuclei to establish the expected connectivity. In polyatomics, the first listed non-hydrogen atom is assumed to be the central atom, unless otherwise stated. Alternatively, the atom with the smallest electronegativity is often the central atom. (2). Determine the total number of valence electrons. (3). Draw single bonds between the bonded pairs of atoms. (4). Fill in the remaining electrons as lone pairs without exceeding an octet on each heavy atom, or a duet on H or He. (5). If any atoms do not have a completed octet, then move lone pairs to complete the octets by forming multiple bonds. (6). If several non-equivalent structures are possible, the predicted lowest energy structure is the structure that minimizes the total formal charges. (7). The bonding pattern that places the largest negative formal charges on the most electronegative atoms is the most important. (8). Use expanded octets on 3rd and 4th period elements only if necessary to accommodate the required total number of electrons. (9). Show the overall ionic charge in the final structures.

<u>2</u>. Draw the Lewis dot resonance structures for (a) ozone, (b) sulfur dioxide, and (c) nitrite ion, NO_2^-. Are the electrons delocalized? Give the average bond order for the bonds. The procedure for the determination of Lewis dot structures is summarized in the previous problem.

<u>3</u>. For the H_2^+ ion, show that for the bonding orbital $c_A = c_B$ using E_+ and for the anti-bonding orbitals $c_A = - c_B$ using E_- in the secular equations, Eq. 21.1.12.

<u>4</u>. Show that the atomic integral for the H_2^+ molecule, $H_{AA} \equiv \int \Psi_A^* \hat{\mathcal{H}} \Psi_A \, d\tau$, reduces to:

$$H_{AA} \cong E_A + \frac{e^2}{4\pi\varepsilon_o R}$$

at large internuclear separation, Eq. 26.1.6. Then argue that at large R the atomic integral is approximately equal to the atomic energy of the H-atom. The bond dissociation at large R gives $H_2 \rightarrow H + H^+$.

<u>5</u>. Determine the Pauling electronegativity of Br. The experimental bond dissociation energies are $D_o(H–H) = 432.0$ kJ mol^{-1}, $D_o(Br–Br) = 190.$ kJ mol^{-1}, and $D_o(H–Br) = 363.$ kJ mol^{-1}. The electronegativity of H is 2.2.

<u>6</u>. Determine the Pauling electronegativity of Ge. The experimental bond dissociation energies are $D_o(Ge-Ge) = 272.$ kJ mol^{-1}, $D_o(F-F) = 154.8$ kJ mol^{-1}, and $D_o(Ge-F) = 484.$ kJ mol^{-1}.[1,2] The electronegativity of F is 3.98, in current revised scales.

<u>7</u>. Sketch the qualitative molecular orbital diagram for BeH^+. Calculate the qualitative bond order. Is the bond completely covalent, partially ionic, or strongly ionic?

<u>8</u>. Sketch the qualitative molecular orbital diagram for linear H_3^+. The H_3^+ ion is symmetrical about the center H-atom. Show that the odd number of atomic orbitals results in a bonding, non-bonding, anti-bonding trio of molecular orbitals. Calculate the qualitative bond order. Is the ion stable?

<u>9</u>. Consider the bond between atoms A and B with bonding wave function:
$\Psi_1 = 0.800 \, \Psi_A + 0.360 \, \Psi_B$. (a). Calculate the % ionic character. (b). Choose the corresponding

molecular energy diagram from below. (c). Find the corresponding anti-bonding orbital. Assume the atomic orbitals are normalized and the overlap integral is S = 0.400.

(a).   (b).   (c).
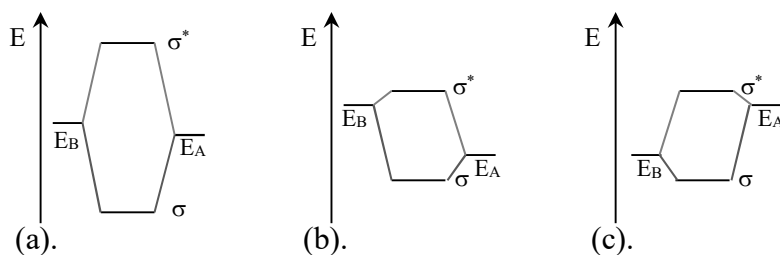
10. Calculate the bond order and atom charges for BH at the CNDO level at the experimental bond length, 1.236 Å. Calculate the charges and bond order using the molecular orbital coefficients and the overlap integrals (in effect, verifying the listed bond order in the CNDO printout). [Use the online CNDO applet on the textbook Web site.]

11. Using molecular orbital theory, decide if OF is more likely to form an OF^+ ion or an OF^- ion.

12. Using molecular orbital theory, which of CN, CN^+, or CN^- has the strongest bond?

13. What is the symmetry of the orbital formed from the side-on overlap of two d-orbitals as shown below (σ, π, or δ; bonding or anti-bonding; g or u). The lobes of both orbitals lie in the plane of the paper. The x-axis is the internuclear axis.
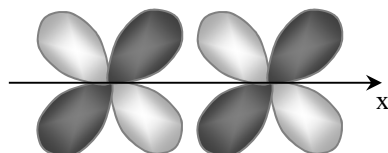
14. Calculate the bond order in linear BeH_2 in the CNDO approximation. Characterize the highest occupied molecular orbital (σ or π, bonding, non-bonding, or anti-bonding). The bond length is 1.330 Å. Calculate the Mulliken bond order using the molecular orbital coefficients and the overlap integrals (in effect, verifying the listed bond order in the CNDO printout).

15. Determine the bond order for the O-H bond in H_2O assuming a 90° bond angle and an O-H bond length of 0.96 Å, in the CNDO approximation. Calculate the bond order using the molecular orbital coefficients and the overlap integrals (in effect, verifying the listed bond order in the CNDO printout).

16. Calculate the % ionic character in the lowest energy molecular orbital, for the valence electrons, of one of the O-H bonds in H_2O assuming a 90° bond angle and an O-H bond length of 0.96 Å, in the CNDO approximation (the same geometry as the previous problem).

17. Characterize the highest occupied molecular orbital for H_2O as bonding, non-bonding, or anti-bonding. Is the orbital σ or π type, or is the orbital better characterized as purely atomic? Compare this result to the prediction from hybridization theory. You may use semi-empirical or HF/STO-3G methods.

18. Using geometrical considerations, find the Cartesian coordinates for the planar molecule BH_3. Place the B atom at the origin and use a bond length of 1.19 Å. Orient one of the H atoms along the x-axis. Obtain the overlap matrix and the molecular orbital coefficients using the

version of the "*cndo*" applet that has Cartesian coordinate input, which is on the text book Web site and on the companion CD. Example input files are shown at the bottom of the applet. The first line of the input file is the number of atoms, the second line is a comment, and the remaining lines are the atom and the x, y, z coordinates. (a). Give the molecular orbital energy diagram and indicate the electron occupancy. (b). Draw orbital 3. (c). Write orbital 3 in terms of the molecular orbital coefficients and the atomic orbitals: $2s_B$, $2p_{x,B}$, $2p_{y,B}$, $2p_{z,B}$, $1s_{H2}$, $1s_{H3}$, and $1s_{H4}$, where the H atoms are atoms 2, 3, and 4. (d). Characterize orbital 3 as bonding, non-bonding, or anti-bonding. (e). Characterize the LUMO as bonding, non-bonding, or anti-bonding. (f). Show the lowest energy electronic transition on the energy level diagram. (g) Referring to the H atom along the x-axis, which atomic orbital on the central B atom has better overlap with the H atom 1s-atomic orbital?

19. Consider the B-H bond using the CNDO level calculation for BH_3 in the previous problem. Focus on the Mulliken overlap population between the B atom and H atom 2, which is along the x-axis. Does the $2s_B$-$1s_{H,2}$ or the $2p_{x,B}$-$1s_{H,2}$ overlap make a stronger contribution to the bond strength?

20. (a). Compare the molecular orbital and hybridization models of methane. (b). Find the C-H bond order and the charge on the C-atom in methane. Obtain the molecular orbital coefficients, atom electron distribution and bond order matrices using the version of the "*cndo*" applet that has Cartesian coordinate input, which is on the text book Web site and on the companion CD. The atomic coordinates for methane with a C-H bond length of 1.084 Å are:

Atom	x	y	z
1 C	0.0	0.0	0.0
2 H	0.62565	0.62565	0.62565
3 H	-0.62565	-0.62565	0.62565
4 H	-0.62565	0.62565	-0.62565
5 H	0.62565	-0.62565	-0.62565
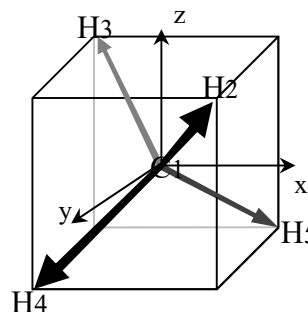
21. Acrolein is the unsaturated aldehyde: $H_2C=CH–CH=O$. (a). Characterize the HOMO and LUMO of acrolein (σ or π, bonding, non-bonding, or anti-bonding). (b). Draw the molecular orbital energy diagram for the π-orbitals, only. (c) Find the charge on the O-atom of acrolein and the C-O and C-C bond orders. Base your answers on a molecular orbital calculation at the CNDO level. [You need not do any calculations by hand, just interpret the output of the MO program.] The input file for the "*cndo*" Web applet is given below in xyz format. The molecule is oriented in the x-y plane with the O-atom at the origin and the C=O bond along the x-axis.

```
8
Acrolein
O        0        0      0
C      1.230       0      0
C      2.058    1.229     0
C      3.404    1.150     0
H      4.039    2.042     0
H      3.911    0.175     0
H      1.521    2.187     0
H      1.810   -0.961     0
```

22. Consider the molecular orbital for linear BH_2: $\Psi_{MO} = N(s_{H1} + p_{x,B2} - s_{H3})$
with N a normalization constant and the atom numbering H_1— B_2 — $H_3 \rightarrow_x$. The internuclear axis is the x-axis. (a). Determine the symmetry designation of the molecular orbital under the symmetry operations for a linear molecule (σ, π, g, u, and also overall bonding, non-bonding, anti-bonding). (b) Determine the symmetry designation of the molecular orbital under the symmetry operations appropriate to a bent molecule (a, b, 1, 2, and also overall bonding, non-bonding, anti-bonding, Figure 26.6.4).

23. Consider the molecular orbital for linear BF_2: $\Psi_{MO} = N(-p_{x,F1} + p_{x,B2} - p_{x,F3})$
with N a normalization constant and the atom numbering F_1— B_2 — $F_3 \rightarrow_x$. The internuclear axis is the x-axis. (a). Determine the symmetry designation of the molecular orbital under the symmetry operations for a linear molecule (σ, π, g, u, and also overall bonding, non-bonding, anti-bonding). (b) Determine the symmetry designation of the molecular orbital under the symmetry operations appropriate to a bent molecule (a, b, 1, 2, and also overall bonding, non-bonding, anti-bonding, Figure 26.6.4).

24. Sketch the qualitative molecular orbital diagram for I_3^-. The ion is linear. Assume the valence s-orbitals are sufficiently lower in energy than the valence 2-orbitals, so that the valence s-orbitals form an inner core set. Combine the valance p-orbitals to give the MO diagram. Characterize the orbitals as σ or π, g or u. Characterize the orbitals as overall bonding, non-bonding, or anti-bonding. Determine the electron filling and calculate the overall bond order. Characterize the bond order of each separate I–I bond. Halogens rarely form double bonds, especially as the atom radius increases. Does your MO diagram agree with this expectation. Determine the primary MOs that determine the bond order. Compare your MO diagram to the MO diagram for $[F–H–F]^-$; explain the stability of I_3^- in terms of the pattern of MO formation.

25. Bent's Rule states that an atom directs hybrids of greater p character toward more electronegative atoms.[1,2] Consider linear HCN. The C atom sp hybrid that overlaps with the N is expected to have higher p character than the C atom hybrid that overlaps with the H. The hybrid orbital on C that overlaps with the orbital on N is given by $\Psi_{sp,1} = 0.698\, s_C + 0.716\, p_{x,C}$, which is a $sp^{1.05}$ hybrid. Find the second hybrid orbital on carbon, $\Psi_{sp,2}$, which also forms from the s orbital and the p_x orbital. Is the second hybrid $s^{1.05}p$?

26. Give the hybridization, in the form sp^α, and show that the orbital is normalized for the hybrid orbital:

$$\Psi_{sp\alpha,a} = 0.563\, s + 0.826\, p_x$$

27. Calculate the bond angle in sp^3 hybridization.

28. An sp^2 hybrid orbital oriented along the y-axis is given below. Find the two remaining sp^2 hybrids in the x-y plane. [Hint: Represent the hybrids $\Psi_{sp2,i} = c_{s,i}\, s + c_{px,i}\, p_x + c_{py,i}\, p_y$. Solve for the ratio of the coefficients $r_{k,i} = c_{k,i}/c_{s,i}$ using orthogonality and then use normalization to find the final values.]

$$\Psi_{sp2,1} = \frac{1}{\sqrt{3}}\, s + \frac{\sqrt{2}}{\sqrt{3}}\, p_y$$

29. One model for Zn(CN)$_4$ is to use sd^3 hybridization. Use VSEPR rules to determine the shape of Zn(CN)$_4$. Which d-orbitals on Zn are used to form sd^3 hybrids.

30. (a). Use the enthalpies of vaporization and formation in Tables 8.1.1 and 8.4.2 for benzene and cyclohexene to calculate the value of the Hückel C(2p$_z$)–C(2p$_z$) resonance integral, β. (b). Repeat the calculation with 1,3-butadiene. Compare the two values for β.

31. Use Hückel molecular orbital theory to determine the molecular orbitals and energies for 1,3,5-hexatriene:

(a). Give the Hückel determinant in terms of x's and 1's:
(b). Determine the energies and the orbital coefficients using a matrix diagonalization program. The "eigen" applet to diagonalize a matrix is available on the text book Web site or companion CD. MatLab or Mathematica are also useful.
(c). Sketch the orbitals with the appropriate phase for each p$_z$ orbital.
(d). Give the number of nodes in each wave function. Classify each orbital as bonding or anti-bonding.
(e). Draw the energy level diagram. Give the electron filling.
(f). Calculate the π-bond order for each unique bond in the molecule (Eq. 26.8.6).
(g). Calculate the π-bond delocalization energy.
(h). Calculate the π-electron density on any two atoms of your choosing (Eq. 26.8.7).
(i). On the energy levels in part (e), indicate the lowest energy electronic transition with a vertical arrow. Label the HOMO and LUMO.

32. Answer the questions listed in Problem 31 for 3-vinyl-1,3-butadiene:
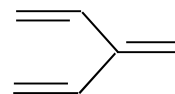
33. Heteroatoms are introduced into the HMO matrix using two parameters, h and k. The diagonal element is the Coulomb integral, which for carbon is α. The off-diagonal elements are the resonance integrals, which for directly bonded carbon atoms are β. The diagonal element for a heteroatom is changed to α + h β and the off-diagonal element for directly bonded atoms is changed to kβ. A table of h and k is given below.

Table P26.1: Hückel Parameters for Heteroatoms.

Atom	Bond Type	π electrons for atom	h	k
C	-C=C-	1	0	1
N	-C=N- (pyridine)	1	0.5	1.0
N	=C-N< (pyrrole)	2	1.5	0.8
N	-N=N- (azo)	1	1.0	1.0
O	-C=O (carbonyl)	1	1.0	1.0
O	=C-O- (furan)	2	2.0	0.8
F	=C-F	2	3.0	0.7
Cl	=C-Cl	2	2.0	0.4
Br	=C-Br	2	1.5	0.3
S	=C-S- (thiophene)	2	1.5	0.8

For example, acrolein, $C_A=C_B-C_C=O_D$, has four total π-electrons and the lower diagonal elements of the Hückel matrix in the form of Eq. 26.8.16 is:

0

1	0

0	1	0

0	0	1	**1**

For acrolein:
(a). Give the Hückel determinant in terms of x's and 1's:
(b). Determine the energies and the orbital coefficients using a matrix diagonalization program. The "eigen" applet to diagonalize a matrix is available on the text book Web site or companion CD. MatLab or Mathematica are also useful.
(c). Sketch the orbitals with the appropriate phase for each p_z orbital.
(d). Give the number of nodes in each wave function. Classify each orbital as bonding or anti-bonding.
(e). Draw the energy level diagram. Give the electron filling.
(f). Calculate the π-bond order for each unique bond in the molecule (Eq. 26.8.6).
(g). Calculate the π-bond delocalization energy.
(h). Calculate the π-electron density on any two atoms of your choosing (Eq. 26.8.7).
(i). On the energy levels in part (e), indicate the lowest energy electronic transition with a vertical arrow. Label the HOMO and LUMO.

34. Use Hückel molecular orbital theory and the parameters in Table P26.1 to determine the HOMO for vinyl fluoride, $CH_2=CH-F$. Draw the molecular orbital diagram and show the electron filling. Characterize the HOMO as σ or π, bonding, non-bonding, or anti-bonding. Does the HOMO have predominant character on any one particular atom?

35. Characterize the highest occupied molecular orbital in liner BeH_2. Use extended Hückel theory. Draw the molecular orbital energy diagram and sketch the molecular orbitals. Orient the molecule along the x-axis. Number the Be as atom 1 and the two hydrogens as 2 and 3.The bond length in BeH_2 is 1.330 Å giving the Be(2s)-H(1s) overlap integrals of 0.491 and the Be($2p_x$)-H($1s$)$_2$ overlap as 0.559. Notice the change in sign for the H($1s$)$_3$-Be($2p_x$) overlap:
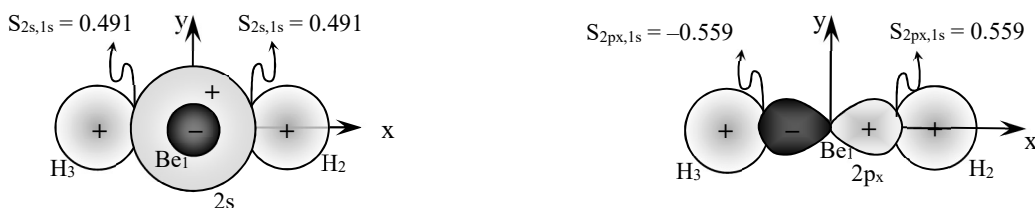
36. Calculate the Be-H bond order in BeH_2 using the results in the previous problem, at the extended Hückel level of approximation.

37. Use extended Hückel theory to find the molecular orbital energy diagram for water. Number the oxygen as atom 1 and the two hydrogens as 2 and 3. Orient the molecule in the x-y plane. The overlap integrals for a bond angle and 105° and bond lengths of 0.962 Å are shown below (the overlap between the two hydrogens is $S_{1s,1s} = 0.2242$):
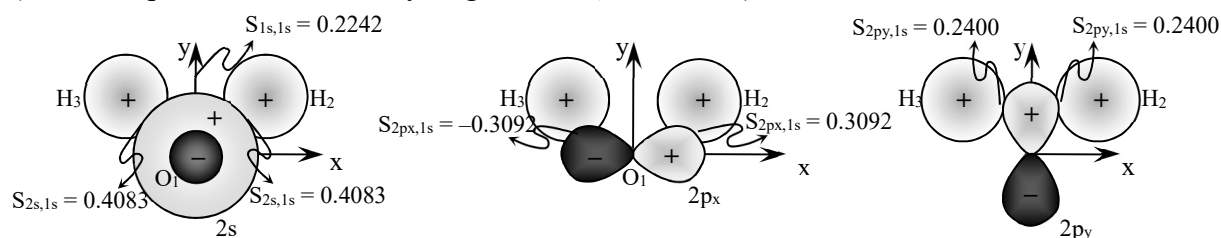
38. Calculate the O-H bond order in water from the extended Hückel calculation in the previous problem.

39. Calculate the charge on the C-atom in methane. Use the extended Hückel method. The atomic coordinates for methane with a C-H bond length of 1.084 Å are:

Atom	x	y	z
1 C	0.0	0.0	0.0
2 H	0.62565	0.62565	0.62565
3 H	-0.62565	-0.62565	0.62565
4 H	-0.62565	0.62565	-0.62565
5 H	0.62565	-0.62565	-0.62565
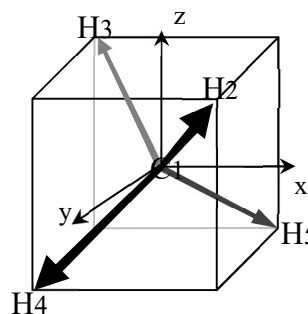
For this orientation, the overlap matrix is:

	1 C2s	1 C2p$_x$	1 C2p$_y$	1 C2p$_z$	2 H1s	3 H1s	4 H1s	5 H1s
1 C2s	1.0	0.0	0.0	0.0	0.5224	0.5224	0.5224	0.5224
1 C2p$_x$	0.0	1.0	0.0	0.0	0.2832	-0.2832	-0.2832	0.2832
1 C2p$_y$	0.0	0.0	1.0	0.0	0.2832	-0.2832	0.2832	-0.2832
1 C2p$_z$	0.0	0.0	0.0	1.0	0.2832	0.2832	-0.2832	-0.2832
2 H1s	0.5224	0.2832	0.2832	0.2832	1.0	0.1877	0.1877	0.1877
3 H1s	0.5224	-0.2832	-0.2832	0.2832	0.1877	1.0	0.1877	0.1877
4 H1s	0.5224	-0.2832	0.2832	-0.2832	0.1877	0.1877	1.0	0.1877
5 H1s	0.5224	0.2832	-0.2832	-0.2832	0.1877	0.1877	0.1877	1.0

40. Place the following electronic structure methods in order of typical energy accuracy: HF, CNDO, MNDO, AM1, PM3, CISD or CCSD, CISDT or CCSDT, CCSD(T), LSDA, B3LYP.

Literature Cited:

1. B. deB. Darwent, "Bond Dissociation Energies in Simple Molecules," *Nat. Stand. Ref. Data Ser.*, 1970, NSRDS-NBS 31.
2. K. S. Pitzer, *Quantum Chemistry*, Prentice-Hall, Englewood Cliffs, NJ, 1953. Table 8.4.
3. H. A. Bent, *Chem. Revs.*, **1961**, *61*, 275-311.
4. J. P. Foster, F. Weinhold, *J. Am. Chem. Soc.*, **1980**, *102*, 7211-7218.